Scuola Internazionale Superiore di Studi Avanzati - Trieste

An electrophysiological analysis of conformational changes occurring during the gating of CNG channels.

Thesis submitted for the degree of "Doctor Philosophiae"

CANDIDATE
Monica Mazzolini

SUPERVISOR
Prof. Vincent Torre

SISSA – Via Beirut 2-4 – 34014 TRIESTE – ITALY

Dedicata a colei che, più di ogni altra persona,
mi sa capire, mi sa ascoltare, mi sa amare.
Dedicata a colei che, più di ogni altra persona,
io amo.
Dedicata a mia madre.

DECLARATION

The work described in this thesis was carried out at the International School for Advanced Studies, Trieste, between October 1999 and September 2003. All work reported arise solely from my own experiments with the exception of the part regarding the homology modelling performed in collaboration with Marco Punta and Alejandro Giorgetti. Many thanks go to Katia Gamel, for preparing some mutant DNAs of the pore region.

The plasmids for expressing the wild type forms of the CNGA1 subunit of the bovine rod cyclic nucleotide gated channels were a kind gift of Prof W.N. Zagotta and of Prof. U.B. Kaupp.

Part of this thesis has been published in the article below:
Mazzolini M, Punta M and Torre V. "Movement of the C-helix during the gating of cyclic nucleotide gated channels". Biophysical Journal 83(6):3283-95

Monica Mazzolini
September 2003

TABLE OF CONTENTS

ABBREVIATIONS USED IN THE TEXT

CNG=cyclic nucleotide-gated
CNBD=cyclic nucleotide-binding domain
LG=ligand-gated
VG=voltage-gated
cGMP=cyclic 3', 5'-guanosine monophosphate
cAMP= cyclic 3', 5'-adenosine monophosphate
GDP=3', 5'-guanosine diphosphate
GTP=3',5'-guanosine triphosphate
GMP=3', 5'-guanosine monophosphate
ATP=adenosine triphosphate
dNTP=desoxyribonucleotide triphosphate
PDE=phosphodiesterase
RPE=retinal pigment epithelium
IP_3=inositol 1,4,5-triphosphate
PKA=protein kinaseA
PLC=phospholipaseC
DAG=diacylglycerol
GARP=glutamic-acid-rich protein
CAP=catabolite activator protein
CuP=copper phenantroline
PIP_2=phosphatidylinositol-4',5'-biphosphate
CaM1 & CaM2=Ca^{2+}-calmodulin binding sites 1 & 2
cDNA=complementary DNA
SCAM=substituted-cysteine accessibility method
PCR=polimerase chain reaction
SDS=sodium dodecylsulphate
PAGE=polyacrylamide gel electrophoresis
MTS=methane thiosulfonate
MTSEA=2-aminoethylmethane thiosulfonate
MTSES=sulfonatoethyl methanethiosulfonate
MTSET=2-trimethylammonioethylmethane thiosulfonate
TE=Tris-EDTA=tris-ethylenediamine tetraacetate
DEPC=diethil pyrocarbonate
HEPES=(N-2-hydroxyethyl)piperazine-N'-(2-ethanesulphonicacid)
TMAOH=tetramethylammonium hydroxide
HCN=hyperpolarization-activated cation channel
NO=nitric oxide

ABSTRACT

In my thesis I have addressed the problem of understanding the relation between the structure and function of CNG channels by combining electrophysiological experiments with molecular modeling. In particular I focussed my attention into two regions present in the A1 subunit: the putative C-helix of the CNBD and the pore region. I have used molecular biology to construct mutant channels and electrophysiology to analyse their properties. I have heterologously expressed mutant channels in *Xenopus laevis* oocites and studied their properties in excised-patches under voltage-clamp conditions. I have mutated one by one all residues in the C-helix and in the pore region and probed the effect of sulfhydryl reagents on mutant channels. My experiments indicate that when cGMP is bound to the CNBD, the stretch of residues from Leu583 to Asn610 is likely to form an alpha helix. In addition I have identified the residues, in which the C-helices are in close contact in the open state. Therefore the conformation of the CNBD of CNGA1 channels is different from that determined in HCN2 channels (Zagotta et al., 2003) and is likely to be a dimer of dimers as suggested (Scott et al., 2001 and Higgins et al., 2002). In the absence of cGMP, C-helices are likely to kink and bend at variable angles. My experiments also indicate that in CNG channels the S6 transmembrane segment does not have the large movement during gating as observed in K^+ channels (Jiang et al., 2002) and that the gating is primarily localised at the pore level. I suggest that the gating of CNG channels is caused by a fine movement producing a conformational rearrangement of the pore walls. The movement of the pore helix is likely to be initiated by a translation of the S6 domain mediated by hydrophobic interaction between the P-helix and the S6 domain.

INTRODUCTION

Ionic channels are membrane proteins that play a fundamental role in cell physiology and in signal transduction and transmission (Hille, 2001). Their functional properties have been extensively investigated by electrophysiological and biochemical assays and their aminoacid sequence has been determined by molecular biology and genetics. The recent determination of the three dimensional (3D) structure of the K^+ channel (Doyle et al., 1998) from the bacteria *Streptomyces lividans*, i.e. the KcsA channel, has opened a new era where it is possible to understand the relation between structure and function of ionic channels. In order to understand this relation it is necessary to: i. obtain the 3D structure and ii. relate functional properties to specific molecular mechanisms. This challenging aim requires the combination of electrophysiological, biochemical and biological tools combined with techniques of structural biology and theoretical tools from molecular modeling and computational chemistry. In my thesis I have attempted to address some of these issues in cyclic-nucleotide gated (CNG) channels.

CNG channels are expressed in neurons and also in non-neuronal tissue where their specific function is unknown. The main source for my present knowledge has been CNG channels from sensory neurons, photoreceptors and olfactory sensory neurons. These channels are cation selective and not very selective among monovalent alkali cations (Menini, 1990) compared to Na^+ and K^+ channels (Hille, 2001). Under physiological conditions CNG channels conduct mixed inward currents carried by Na^+ and Ca^{2+} ions (Dzeja et al., 1999). CNG channels are structurally related to the large family of voltage-gated channels (Kaupp et al., 1989) and are composed by four subunits (Zhong et al., 2002; Weitz et al., 2002; Zheng et al., 2002). Native CNG channels from photoreceptors and olfactory sensory neurons are composed by two types of subunits usually referred to as A1 and B1 subunits (Kaupp et al., 1989; Körschen et al., 1995). Homomeric CNG channels composed by only the A1 subunit give rise to functional channels with properties similar, but not identical, to those of native heteromeric CNG channels. Homomeric CNG channels composed by only B1 subunits are not functional. The A1 subunit of CNG channels from bovine rods is composed of 690 aminoacids (Kaupp et al., 1989), while the B1 subunit is composed of 1264 aminoacids and displays a long glutamic acid-rich domain (GARP), spanning from 1 to

590. It also has a calmodulin-binding region (from 667 to 708). Each subunit comprises 6 predicted transmembrane segments with both the N- and C- termini on the cytoplasmic side of the membrane (Henn et al., 1995). The N-terminus of the A1 subunit of CNG channels is composed by a segment of about 150 aminoacids that is highly charged. The pore region of the A1 and B1 subunits is formed by about 30 residues, located between helices S5 and S6. Each subunit harbors a cyclic nucleotide-binding (CNB) domain composed of about 125 aminoacids in the cytoplasmic C-terminal. The so-called C-linker, from residue 396 to 485, in the A1 subunit, links the last membrane-spanning segment S6 to the CNB domain. The B1 subunit has a similar domain organization, with the exception of the GARP, at the N- terminal region, and the CaM-binding domains. All CNG channels respond to some extent to both cAMP and cGMP. In rods and cones, CNG channels sharply discriminate between cGMP and cAMP, while channels in chemosensory cilia respond equally well to both ligands. The family of hyperpolarization gated and cyclic nucleotide regulated channels (HCN) is related to CNG channels (Robinson and Siegelbaum, 2002).

The determination of the structure of the complete CNG channel by X-ray crystallography poses severe difficulties, both at the level of protein expression and crystallization. Other methodologies must be found in order to gather its 3D structure. It is possible to obtain the structure of the entire CNG channel by electron microscopy (Higgins et al., 2002) at a resolution of 35 Å and to elucidate the 3D structure of specific domains of the CNG channel at a high resolution with different techniques such as NMR, X-ray crystallography and electron microscopy. Indeed the CNBD of HCN2 channels has been recently obtained by X-ray diffraction at a resolution of 2 Å (Zagotta et al., 2003). It is also possible to model other domains of the channel by exploiting the significant homology with other proteins whose 3D structure has been determined. For instance, the pore region of a CNG channel has a 40% homology with the recently structurally resolved KcsA channel (Doyle et al., 1998). Similarly, the CNB domain of CNG channels has a 22-27% homology with the CNB domains of two structurally resolved proteins; the catabolite activating protein (CAP) (Weber and Steitz, 1987) and the cAMP-dependent protein kinase PKA (Su et al., 1995).

Model-building on the basis of the known 3D structure of homologous proteins is at present the most reliable method to obtain structural information on proteins for which

no direct experimental data is available. At the basis of homology modelling lies the observation that 3D structures are better conserved during evolution than protein primary sequences. Model building by homology is a multi step process which can be summarized in the following steps; i. template recognition; ii. alignment; iii. backbone generation; iv. loops generation; v. side chain generation; vi. overall model optimization; vii. model verification with optional repeat of previous steps.

Therefore I have decided to tackle the problem of determining the 3D structure of CNG channels and of understanding the relation between its structure and function by combining electrophysiological experiments with molecular modelling. The work on molecular modeling has been performed in collaboration with Paolo Carloni, Alejandro Giorgetti and Marco Punta at SISSA.

The objective of my thesis is to study the relation between the structure and function of the CNG channels in particular of CNGA1 channels from bovine rods. In particular I focussed my attention into two regions: the putative C-helix of the CNBD and the pore region. I have used molecular biology to construct mutant channels and electrophysiology to analyse their properties. In particular I have heterologously expressed mutant channels in *Xenopus laevis* oocites and studied their properties in excised-patches under voltage-clamp conditions. I have mutated one by one all residues in the C-helix and in the pore region and probed the effect of sulfhydryl reagents on mutant channels.

Let me now summarise the motivations of my analysis and the obtained results for the two domains that I have analysed.

Cyclic nucleotide binding domain.

This part of the work has two major aims: firstly to probe the 3D structure of the CNBD of CNG channels and its homology with that of CAP and PKA protein (Weber and Steitz, 1987; Doyle et al., 1998), and secondly to determine possible conformational changes associated to the binding of cyclic nucleotides (Sun et al., 1996; Li and Lester, 1999; Matulef et al., 1999). Cysteines were introduced, one by one, in the stretch from Leu583 to Asn610 forming the putative C-helix of the CNBD. Currents activated by cGMP were recorded under voltage-clamp conditions from membrane patches, excised from oocytes and the effect of sulfhydryl-specific reagents (Cd^{2+}, CuP and MTSET)

was tested in the open and closed state of the channel. My experiments indicate that when cGMP is bound to the CNBD, the stretch of residues from Leu583 to Asn610 is likely to form an alpha helix. In addition I have identified the residues, in which the C-helices are in close contact in the open state. Therefore the conformation of the CNBD of CNGA1 channels is different from that determined in HCN2 channels (Zagotta et al., 2003) and is likely to be a dimer of dimers as suggested (Scott et al., 2001 and Higgins et al., 2002). In the absence of cGMP, C-helices are likely to kink and bend at variable angles.

The pore region and the S6 transmembrane domain.

In this part of my thesis I have studied, with the same methodology used for investigating CNBD, the structure and rearrangement of the CNGA1 channel pore during the gating. The aim of my work was to verify whether the gate of CNG channels is the pore itself as previously suggested (Karpen et al., 1993; Fodor et al., 1997; Bucossi et al, 1997; Becchetti et al., 1999) and to establish conformational rearrangements of the pore, P-helix and S6 domain during channel gating. In particular, I constructed mutant channels, containing one cysteine at all positions between Phe375 and His420 in the S6 region and in position Val348, Leu351, Thr359, Thr360 and Ile361 in the inner pore (see also Becchetti et al., 1999 and Liu and Siegelbaum, 2000). Two are the major conclusions of my experiments: firstly, in CNG channels the S6 transmembrane segment does not have the large movement during gating as observed in K^+ channels (Jiang et al., 2002); secondly, in CNG channels, the gating is primarily localised at the pore level. I suggest that the gating of CNG channels is caused by a fine movement producing a conformational rearrangement of the pore walls. The movement of the pore helix is likely to be initiated by a translation of the S6 domain mediated by hydrophobic interaction between the P-helix and the S6 domain.

PROPERTIES OF CNG CHANNELS

1-Shedding light on voltage-gated channels

Most ionic channels are members of two large subfamilies usually referred as ligand-gated (LG) and voltage-gated (VG) channels (Hille B., 2001). The membership of one class or the other depends on the transmembrane structure, the quaternary organisation and the functional characteristics.

Three important channels activated by voltage are the Na^+ channels, the Ca^{2+} channels and the K^+ channels.

1. Na^+ channels: these channels are responsible of the sodium current that underlies the rapid upstroke of the action potential in nerve and muscle fibres. They serve to let positive charge into the cell to mediate the rising phase of the action potential. These channels are present into the brain, in peripheral neurones, skeletal muscle and cardiac muscle. One of the most distinctive properties of the voltage-gated Na^+ channels is yours marked voltage sensitivity. At the resting potential the open probability of these channels is extremely low and very few channels are open. The depolarisation increases dramatically the probability of channel opening. The channel open probability is also time dependent. In response to depolarisation the channels open briefly after a short latency and then close to an inactivated state which persists until the membrane is hyperpolarized. This produces a macroscopic current that rises to a peak within about 1 millisecond and then declines. These channels are highly selective for Na^+ and have a single channel conductance of 10-30 pS in 100 mM extracellular Na^+. Voltage-gated Na^+ channels are usually composed of a principal subunit named α and one or more small β-subunits (Catterall et al., 1986). Functional activity is observed when the α-subunit is expressed in heterologous systems on its own, indicating that it possesses all the necessary structural elements for channel formation. The β-subunit enhances the current amplitude and modified its properties. The α-subunit of voltage-gated Na^+ channels is composed of around 2000 amino acids residues and the sequence contains four homologous repeats (from I to IV). Each of these repeats contains six transmembrane domains (called S1, S2, S3, S4, S5 and S6) linked by loops and two

citoplasmatic domains in position N- and C- terminal. Most important is the domain S4 because it contains 6-8 charged residues and its function is the voltage sensor. Another important region is the pore region between the S5 and S6 transmembrane domains. The β-subunit consists of a single transmembrane domain with an extracellular N terminus and an intracellular C terminus.

2. K^+ channels: these channels are found in all cells. They are subdivided in two families different from the structure: which posses six transmembrane domains and those that are formed from only two transmembrane domains. In this part of these of mine I discuss only the structure of two important potassium channels, the *Shaker* and the KcsA channels. The first kind of channel is identificated in the first time in the fruitfly *Drosophila melanogaster* (Papizan et al., 1987) and the second one from the bacterium *Streptomyces lividans* (Doyle et al., 1998). The α-subunit of the voltage-gated K^+ channel (Kv) corresponds to a single domain of the Na^{2+} channel and four subunits come together to form the K^+ channel pore. Each α-subunit consists on six transmembrane spanning segments (from S1 to S6), highly conserved and intracellular N and C terminal of variable length. The S4 segment shows considerable homology with that of the voltage-gated Na^{2+} channel, in particular it is amphipathic and has a positive charge at every third position. The linker between the S5 and S6 segment dips back down into the membrane and implicated to the formation of the pore region. This part is known SS1-SS2 in Na^{2+} channels and referred to as H5 region (pore loop) in K^+ channels. Electrophysiological studies first provided support for the idea that the Kv channel is composed of four α-subunits (MacKinnon, 1991); in 1994 Li and colleagues (Li et al., 1994) with the electron microscope obtain direct evidences that this channel is made up of four subunits. Kv channels may be homo-oligomers or hetero-holigomers. In 1994 a family of voltage-gated K^+ channel β-subunits has been identified (Retting et al., 1994). The β-subunits has a molecular mass of about 40 kDa and they are citoplasmatic and not span the membrane. In the 1998 was publicised the crystal structure of the KcsA (Doyle et al., 1998). The structure of this channel was solved at 3.2 Å resolution. KcsA has only two transmembrane domains connected by a pore loop. Within the pore region the sequence of this channel is nearly identical to that of Kv channels. Crystallographic analysis reveals

that the KcsA channel is a tetramer with four identical subunits arranged symmetrically around a central pore. Each subunit consists of two transmembrane α-helices (S1 and S2) which are linked by a stretch of about 30 amino acids that form a pore helix. The subunits are arranged in such a way that they form a structure similar to an inverted tepee. The poles of the tepee are formed by the four S2 helices. These lie close together at the inner side of the membrane but widen out towards the intracellular side, forming a funnel-shaped tent that is lined by the S2 helices at its stem and by the pore helices at its outer mouth. The pore helix is connected to the S2 helix by a stretch of amino acids that contains the GYG motif and form a narrow selectivity filter close to the extracellular side of the membrane. Below the selectivity filter lies a large cavity within the membrane, about 10 Å in diameter. The pore helices are arranged so that their helix dipole is focused on its cavity. Finally a water-filled tunnel (18 Å length) connects the central cavity to the intracellular solution. The overall length of the KcsA pore is 45 Å.

3. Ca^{2+} channels: these channels, like Na^{+} channels are voltage-gated and open when the internal voltage becomes more positive than the resting potential, and inactive, or close, spontaneously even through the voltage stimulus is maintained. They tend to open more slowly than Na^{+} channels. Ca^{2+} channels run the rising phase of the action potential in the axon terminals of neurons. Are present also in vertebrate smooth muscle and, with the Na^{+} channels, in cardiac muscle. Ca^{2+} channels participate in action potentials when you need to get Ca^{2+} into the cell to do something, such as make cardiac muscle contraction or release neurotransmitter at the axon terminal.

2-Molecular cloning of CNG channels

The physiological findings describing channels directly activated by cyclic nucleotides (Fesenko et al., 1985; Koch and Kaupp, 1985; Yau and Nakatani, 1985) were confirmed when molecular cloning of these channels became possible. The first CNG channel was identified through protein purification (Cook et al., 1987) and subsequent cloning of the gene from a cDNA library from bovine retina (Kaupp et al., 1989). This cDNA encoded for a 63 kDa polypeptide and was termed A1 subunit. Functional reconstitution of the purified channel into liposomes (Cook et al., 1987) as well as heterologous expression of the cloned cDNA (Kaupp et al., 1989) confirmed that the purified protein and the related cDNA correspond to a functional cGMP-gated channel.

Heterologous expression of the A1 subunit of the bovine rod CNG channel results in channel activity largely resembling the one of the native channel. However, the native rod channels display a rapid flickering behaviour indicating very brief open and closed times (Haynes et al., 1986; Zimmerman and Baylor, 1986; Matthews and Watanabe, 1988; Quandt et al., 1991; Torre et al., 1992) contrary to the expression of the cloned A1 subunit that gives rise to distinct rectangular currents (Kaupp et al., 1989; Nizzari et al., 1993). An additional difference between the native and the cloned bovine rod CNG channel lies in their distinct sensitivity to *l-cis*-diltiazem. Indeed, the native channel is more sensitive to this ion channel blocker (Stern et al., 1986; Quandt et al., 1991; Haynes, 1992). These differences suggested that A1 subunits require additional factors or subunits in order to form the native channel. The first 'second' subunit of a CNG channel was reported by Chen and co-workers who cloned the B1 subunit of the human rod CNG channel (Chen et al., 1993). This subunit appeared to exist in two different forms of respectively 70 and 102 kDa but none of these proteins was found in retinal rod channel preparations. Two years later, a polypeptide of 240 kDa was identified as the authentic B1 subunit and was shown to have a bipartite structure (Korschen et al., 1995). Although the B1 subunit does not lead to functional CNG channels when expressed on its own, when co-expressed with the corresponding A1 subunit (Dhallan et al., 1992; Korschen et al., 1995), it introduced rapid flickering to the channel openings reminiscent of the ones observed in the native channel (Torre et al., 1992; Sesti et al., 1994). In addition, the heteromeric channel was shown to be highly sensitive to *l-cis*-diltiazem, similarly to the native channel (McLatchie and Matthews, 1992; Chen et al.,

1993; Korschen et al., 1995). Coexpression of the B1 subunit also led to a reduced sensitivity to blockage by external divalent cations (Korschen et al., 1995) similar to the level reported for the native channel and different from the block observed for the A1 homomeric channels (Root and MacKinnon, 1993; Eismann et al., 1994). This result is explained by the presence of a glycine residue in the B1 subunit at a position corresponding to the glutamate 363 in the bovine rod A1 subunit which was reported to be involved in divalent cations block (Root and MacKinnon, 1993; Eismann et al., 1994). The currents carried by the native and hetero-oligomeric channels were also diminished by Ca^{2+}/Calmodulin (Korschen et al., 1995); this feature was not observed for the homomeric channels formed with A1 subunits only (Chen et al., 1994).

The cyclic-nucleotide-gated channels were found also in the olfactory epithelium. The first subunit, discovered in 1990, is named A2 subunit, (Dhallan et al., 1990; Ludwig et al., 1990); in 1994 a second subunit was found to be expressed in the olfactory epithelium (Bradley et al., 1994; Liman and Buck, 1994). This second subunit, designated A4 had a shorter N-terminus as the one of the rod B1 subunit and is phylogenetically more related to the A2 subunits than to the rod B1 subunit (Kaupp, 1995). Coexpressing this second subunit of the olfactory channel with the corresponding A2 subunit conferred increased sensitivity to cAMP. Nevertheless, this sensitivity to cAMP was still two folds lower than the one observed for native channels. Recently, a third subunit was cloned from the rat olfactory epithelium (Sautter et al., 1998). This subunit represents a splice form of the B1 subunit of the rod CNG channel. Coexpression of this olfactory subunit together with the A2 subunit and the A4 subunit produced channels displaying a sensitivity for cAMP similar to the native channels (Bonigk et al., 1999). Moreover, in situ hybridisation and RNase protection assays confirmed the presence of all three subunits mRNAs in the olfactory epithelium and subsequent immunoprecipitation experiments made on preparations of solubilized olfactory cilia suggested that all three subunits co-assemble in the cilia to form the native channels. Macroscopic currents as well as single-channel analysis were finally performed on patches excised from rat olfactory neurons and confirmed that the best match with respect to functional characteristics of the native channels were obtained when all three subunits were present (Bonigk et al., 1999).

In cone photoreceptors, the A3 subunit (Bonigk et al., 1993) and the B3 subunit (Gerstner et al., 2000) were described.

It is now clear that ion channels directly activated by cyclic nucleotides are not unique to neurons involved in visual and olfactory transduction: after being cloned from olfactory epithelium (Dhallan et al., Ludwig et al., 1990, Goulding et al., 1992) and cone photoreceptors (Bonigk et al., 1993), they were also identified in aorta (Biel et al., 1993), kidney (Biel et al., 1994), testis (Weyand, 1994), keratinocytes (Oda et al., 1997) and taste buds (Misaka et al., 1997). CNG channels have also been cloned from invertebrates like *L. polyphemus* (Chen et al., 1999), *D. melanogaster* (Baumann et al., 1994) and *C. elegans* (Coburn and Bargmann, 1996; Komatsu et al., 1999).

3-Role of CNG channels in phototransduction

The electrical signal generated by the absorption of light originates in rod and cone photoreceptor cells. These cells are organised in two principal parts: the outer segment and the inner segment. The outer segment is the site where the phototransduction takes place. Its structure consists of a stack of membranous disks containing the visual pigment rhodopsin; in a rod cell, the discs are enclosed by the surface membrane, whereas they consist of foldings of the surface membrane in a cone (Fig.1A). A rhodopsin molecule is made of a chromophore, the retinal, and a protein component, the opsin. The outer segment also houses the cGMP-gated channels and the Na^+/Ca^{2+}-K^+ exchangers. The inner segment contains the nucleus as well as mitochondria and the endoplasmic reticulum. In addition to these cellular organelles, the inner segment includes Na^+/K^+ pumps in its membrane. The photoreceptor cells, with the synaptic terminals, are connected to bipolar and horizontal cells. The synaptic endings house glutamate containing vesicles. Although it was thought that cGMP-gated channels were exclusively present in the outer segment, it is now clear that they are also found in the inner segment as well as in the synaptic terminals of cones but not of rods (Watanabe and Matthews, 1988; Rieke and Schwartz, 1994; Savchenko et al., 1997).

In darkness, the cGMP-gated channels in the outer segment are open and allow a steady "dark-current" to enter the photoreceptor cells (Hagins et al., 1970; Baylor et al., 1979): Ca^{2+} and Na^+ ions are entering the cells through the cGMP-gated channels and Ca^{2+} ions are leaving the outer segment via the Na^+/Ca^{2+}-K^+ exchangers. As a consequence, intracellular Ca^{2+} concentration in darkness is around 550 nM (Gray-Keller and Detwiler, 1994). The cell in dark is kept slightly depolarised with a membrane potential of -40 mV and glutamate is continuously released from the synaptic endings. The absorption of a photon by a rhodopsin molecule causes the conversion of the retinal chromophore from its 11-*cis* stereoisomer to its all-*trans* form (Yoshizawa and Wald, 1963; Baylor, 1996). The resulting photoisomerization to all-*trans* retinal triggers the conversion of rhodopsin to the active metarhodopsin state (Emeis et al., 1982). This form of rhodopsin exchanges the GDP which is bound to the α subunit of a G protein, called transducin, for GTP. The GDP $\rightarrow$ GTP exchange leads to the transfer of the GTP-Tα to one of the inhibitory γ subunit of the phosphodiesterase (PDE), an enzyme,

which is then able to hydrolyse cGMP to GMP. This enzymatic reaction causes the closure of the cGMP-gated channels and thus causes a decrease in the intracellular Ca^{2+} concentration (Yau and Nakatani, 1984). In saturating light (Fig.1B), the intracellular Ca^{2+} concentration declines to a minimum value of about 50 nM (Gray-Keller and Detwiler, 1994). The membrane is hyperpolarized and the rate of glutamate release is reduced. In order for a bleached rhodopsin molecule to be able to absorb an other photon, rhodopsin must be regenerated. The chromophore of rhodopsin is separates from the opsin component and is converted to retinol; also the chromophore is regenerated. It is transported by an interphotoreceptor retinol-binding protein (IRBP) to the retinal pigment epithelium (RPE) where the retinol after various enzymatic steps is finally converted into 11-*cis* retinal. The chromophore is transported back to the photoreceptor where it associates with the dephosphorylated form of opsin to give the functional rhodopsin. The transducin molecule regenerates also thanks to an endogenous GTPase activity of the α subunit which subsequently permits the reunion of the α subunit to the $\beta\gamma$ complex. Without the GTP-α transducin, the PDE inactivates and the guanylate cyclase can transform GTP into cGMP and restore the cGMP concentration present in the dark (see Yau and Baylor, 1989; Fain et al, 1996).

To fulfil their function, the photoreceptor cells have to be able to register small changes in light intensity. For this goal it is important to prevent the closure of all cGMP-gated channels when moderate changes of the background light occur. This role is played by Ca^{2+} ions, which are involved, in a fairly complex mechanism of feedback (Koutalos and Yau, 1996; Baylor, 1996). First, guanylate cyclase is stimulated as Ca^{2+} level decrease (Lolley and Racz, 1982; Koch and Stryer, 1988). The Ca^{2+} sensitivity of the guanylate cyclase is relayed by two small Ca^{2+}-binding proteins termed GCAP1 and GCAP2 (Koch, 1992, Palczewski et al., 2000). Second, at low Ca^{2+} concentration, the shut-off of rhodopsin by phosphorylation is favoured by recoverin (another Ca^{2+}-binding protein) which prevents inhibition of phosphorylation (see Gray-Keller et al., 1993). This action may have an influence on the different steps occurring downstream in the light-triggered cascade (Lagnado and Baylor, 1994). Finally the cGMP-gated channel itself is a target for Ca^{2+}-dependent feedback through the action of calmodulin (for review see Molday, 1996). Indeed, activated by Ca^{2+}, calmodulin binds to the N-

terminal part of the cGMP-gated channel B1 subunit (Weitz et al., 1998; Grunwald et al., 1999) and the apparent affinity of the CNG channel for its ligand decreases. Thus when intracellular Ca^{2+} concentration decreases in the presence of light, some of the cGMP-gated channels tend to reopen. The contribution of this feedback process to the overall light adaptation is thought to be rather small (Nakatani et al., 1995).

A

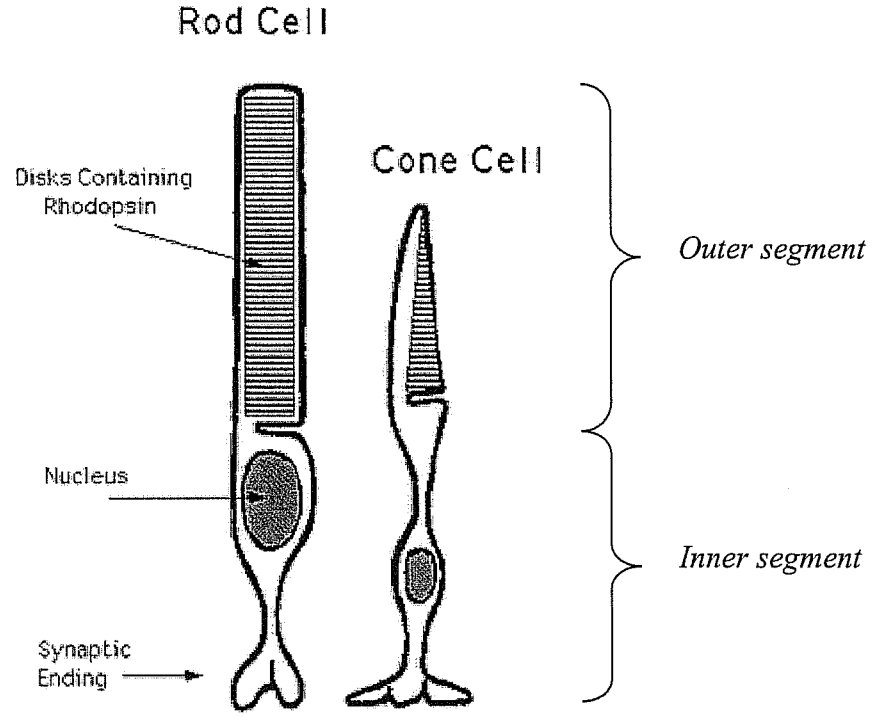

B

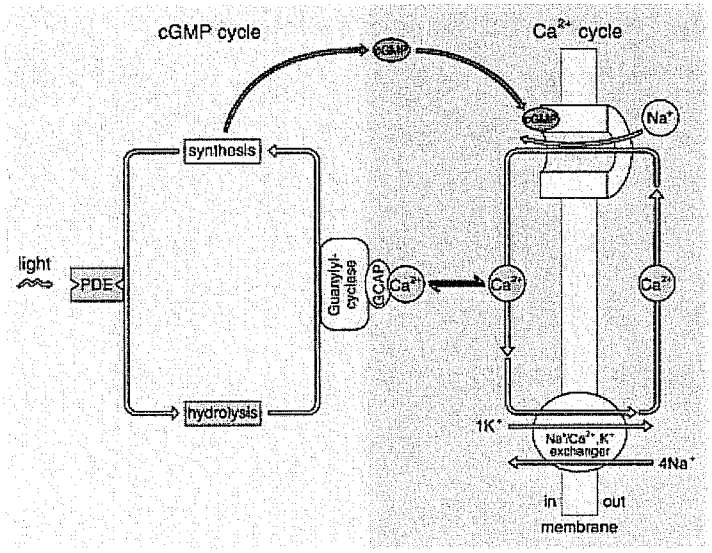

Fig.1: *Phototransduction process* ***A:*** *Schematic diagram of photoreceptor cells.* ***B:*** *scheme of vertebrate phototransduction. Phosphodiesterase (PDE), guanylyl cyclase-activating protein (GCAP). (Kaupp and Seifert, 2002).*

4-Role of CNG channels in olfactory transduction

The olfactory epithellium is made of three different cell types: supporting cells, basal cells and olfactory receptor cells. The supporting cells are involved in the so-called secretion transduction, a mechanism stimulated by odorants and that generates a field potential before the large response occurring in the olfactory receptors. The supporting cells are also involved in the oxidation of odorant molecules in order to render them less membrane permeable. The basal cells are dividing cells that upon differentiation lead to the receptor cells. Finally, the olfactory receptor cells function is to transduce odorant stimulus into membrane depolarisation. Olfactory receptor cells are bipolar neurons having a single dendrite extending to the apical surface of the olfactory epithelium. The tip of the dendrite is the olfactory knob from which numerous (10-30) cilia extend into the mucus that covers the olfactory epithelium. The cell body contains the nucleus and a single axon projects to the olfactory bulb (Buck and Axel, 1991; Gold, 1999).

Olfactory transduction (Fig.2) in vertebrates occurs in the olfactory cilia, which extend into a thin layer of mucus covering the olfactory epithelium and that, is exposed to the environment i.e. to the odorant molecules. It is generally thought that olfactory transduction occurs via two different second-messenger pathways (Sklar et al., 1986; for review see Ache and Zhainazarov, 1995). The cyclic 3', 5'-adenosine monophosphate (cAMP) transduction pathway and the inositol 1, 4, 5-trisphosphate (IP_3) pathway (Fig.2). According to the cAMP-second messenger model (Buck and Axel, 1991), a subset of odorants activates a subset of receptor proteins which are coupled to a G-protein (G_{olf}; a G_s-like G protein) which is itself coupled to adenylate cyclase. The activation of the adenylate cyclase leads to a rise in cAMP concentration and to the subsequent activation of CNG channels. Through the open CNG channels flows a current of Na^+ and Ca^{2+} ions. The entry of Ca^{2+} in the olfactory cells results in the activation of a Ca^{2+}-dependent chloride current. This Cl^- current amplifies the primary odour-induced cations current. Mechanisms of odorant adaptation and inactivation in the olfactory receptor cells were first studied *in vitro* and several possible mechanisms were proposed: phosphorylation of the odour-receptor by protein kinase A (PKA) (Boekhoff and Breer, 1992; Boekhoff et al., 1992), activation of a phosphodiesterase to reduce the cAMP concentration (Borisy, 1992), ion channel regulation (Kramer and

Siegelbaum, 1992; Chen and Yau, 1994; Lynch and Lindemann, 1994; Balasubramanian et al., 1996). The nature of the olfactory adaptation was investigated later in intact olfactory cells of the new (Kurahashi and Menini, 1997) and the principal mechanism of adaptation was identified as being a regulation of the cAMP-gated channels by a Ca^{2+}-feedback via Ca^{2+}-calmodulin. According to the IP_3 hypothesis (Boekhoff et al., 1990; Breer and Boekhoff, 1991), a different subset of odorant molecules would activate a different subset of receptors that couple to phospholipase C (PLC) via a different G-protein (Gq-like G protein); PLC then cleaves the membrane phospholipid phosphatidyl inositol leading to diacylglycerol (DAG) and IP_3. IP_3 which is water soluble would then activate IP_3-gated Ca^{2+} channels in the ciliary membrane antecedens subsequently mediate Ca^{2+} influx and membrane depolarisation. A recent review (Gold, 1999) favours the cAMP-triggered cascade and proposes that the cAMP-cascade is the only transduction mechanism in olfactory cells. Gold criticises the sensitivity of the biochemical assays and cilia preparations used for the IP3 pathway. A study made by the group of Gold (Lowe et al., 1989) showed that differences observed by Sklar et al. (1986) in the magnitude of cyclase activity was simply reflecting the number of cells activated by each odour. In addition, knockout mice have been bred for both the cAMP-gated channels (Brunet et al., 1996) and for G_{olf} (Belluscio et al., 1998). Knockout mice for the CNG channel showed that both the cAMP and IP3 responses were abolished suggesting that olfactory transduction in any case depend on the activation of the cAMP-gated channel. In the new born G_{olf} knockout mice, G_s was able to substitute the lacking G_{olf} but G_s expression declines after birth and by 3 weeks of age, the responses induced by both cAMP and IP_3 were only 2.5% of the wild-type responses, arguing for the cAMP-cascade as major transduction pathway. It has been also proposed that gaseous second messengers such as carbon monoxide (CO; Zufall and Leinders-Zufall, 1997) and nitric oxide (NO; Broillet and Firestein, 1997) produce cGMP and prolong the responses to odorants triggered by cAMP. However the data obtained for CO were obtained for the salamander; regarding the NO pathway, the way of activation of NO synthase is still unclear (Gold, 1999). In brief, the mechanism of olfactory transduction and its modulation are still a matter of debate.

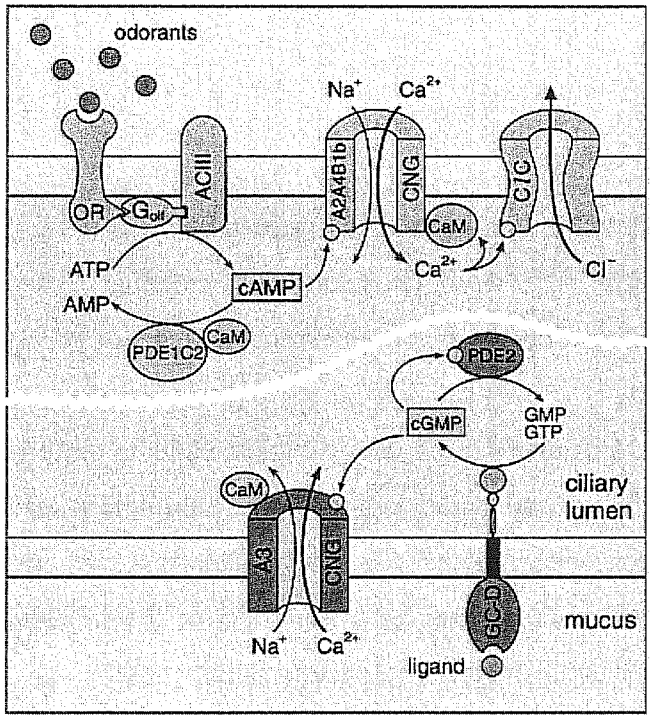

Fig.2: Scheme of olfactory transduction. Odorant receptor (OR), G protein (G_{olf}), calmodulin (CaM), Cl⁻ channels (ClC), CaM-dependent phosphodiesterase (PDE1C2), cGMP-regulated phosphodiesterase (PDE2), guanylyl cylcase type D (GC-D),Ca2+-dependent denylyl cyclase type III (ACIII)(Kaupp and Seifert, 2002).

5-The CNG gene family

Based on sequence comparison, CNG channel genes can be subdivided in different subfamilies (Kaupp and Siefert, 2002). In particular, in mammals two gene families can be distinguished; the first subfamily consists of four members, named (see the new nomenclature, from Bradley et al., 2001) CNGA1, CNGA2, CNGA3, CNGA4. These represent the principal subunits that, except CNGA4, form functional channels on their own and are responsible for several key properties of CNG channels. The second subfamily comprises two members, designated CNGB1 and CNGB3. Genes encoding CNG channel subunits have been also identified from invertebrates such as *C. elegans, D. melanogaster, and L. polyphemus*. Six different genes have been cloned from *C. elegans* (tax-2 and tax-4 and from ce3 to ce6). Four genes encoding CNG channel

subunits have been cloned from *D. melanogaster*, named dmA, dmB, dm3 and dm4 (Kaupp and Seifert, 2002).

6-CNG channels and disease

Frances M. Ashcroft writes in her book: "in the last few years a new word has entered the medical and scientific vocabulary. This word, channelopathy, describes those human and animal diseases that result from defects in ion channel function" (F.M. Ashcroft "Ion channels and disease" 2000).

The *retinitis pigmentosa* (RP) is an inherited disease in which patients suffer from a progressive degeneration of both rod and cone photoreceptors ultimately leading to blindness. Mutations in the genes encoding the A1 subunit cause a rare autosomal recessive form of RP, another form is caused by a mutation in the CNGB1 gene encoding the B1 subunit of the rod CNG channel (Kaupp and Seifert, 2002).

Mutations of the CNGA3 and CNGB3 of gene cone photoreceptors cause colour blindness (named *achromatopsia*). This disease is a rare autosomal recessive disorder characterised by the total loss of color discrimination by photophobia, nystagmus and reduced visual acuity (Kaupp and Seifert, 2002).

7-Functional domains of the A1 subunit

The CNG channels are opened by the direct binding of cyclic nucleotides, cGMP (Fesenko et al., 1985) and cAMP (Nakamuta and Gold, 1987). Although their activity shows very little voltage dependence, CNG channels belong to the superfamily of voltage-gated ion channels. Like the voltage-gated K^+ channels, CNG channels are heterotetramers composed by two or three different types of subunits. Each subunit is composed of six transmembrane domains (Henn et al., 1995; Zagotta and Siegelbaum, 1996; Kaupp and Seifert, 2002).

In this thesis I focus my attention to the A1 subunit of the CNG channel present in bovine rods, and I use the new nomenclature (Bradley et al., 2001) (see Table 1).

SUBUNITS	REPORTED NAMES
CNGA1	Rod CNG channel CNG1, CNGα1, RCNC1
CNGA2	Olfactory CNG channel CNG2, CNGα3, OCNC1
CNGA3	Cone CNG channel CNG3, CNGα2, CCNC1
CNGA4	Second/modulatory subunit of olfactory CNG channel CNG5, CNGB2, CNGα4, OCNC2
CNGB1	Second/modulatory subunit of rod CNG channel CNG4, CNGβ1
CNGB3	Second/modulatory subunit of cone CNG channel CNG6, CNGβ3

Table 1: *Adopted nomenclature for cyclic nucleotide-gated ion channel subunits (modofied from Bradley et al., 2001).*

7.1-TRANSMEMBRANE TOPOLOGY

The A1 subunit (Fig.3), a polypeptide of 63 kDa, composed of 690 amino acids, consists of six transmembrane domains, named S1-S6, located between the NH_2- and COOH- terminals (both present at the cytoplasmic side). The pore region of about 20-30 amino acids (from Y347 to V368) is located between S5 and S6. The S4 segment in CNG channels is similar to the voltage-sensor motif found in the S4 segment of voltage-gated K^+, Na^+ and Ca^{2+} channels (Kaupp and Seifert, 2002).

The B1 subunit (Fig.3) shows many differences compared to the A1 subunit, but I will dwell on this point later (Kaupp and Seifert, 2002).

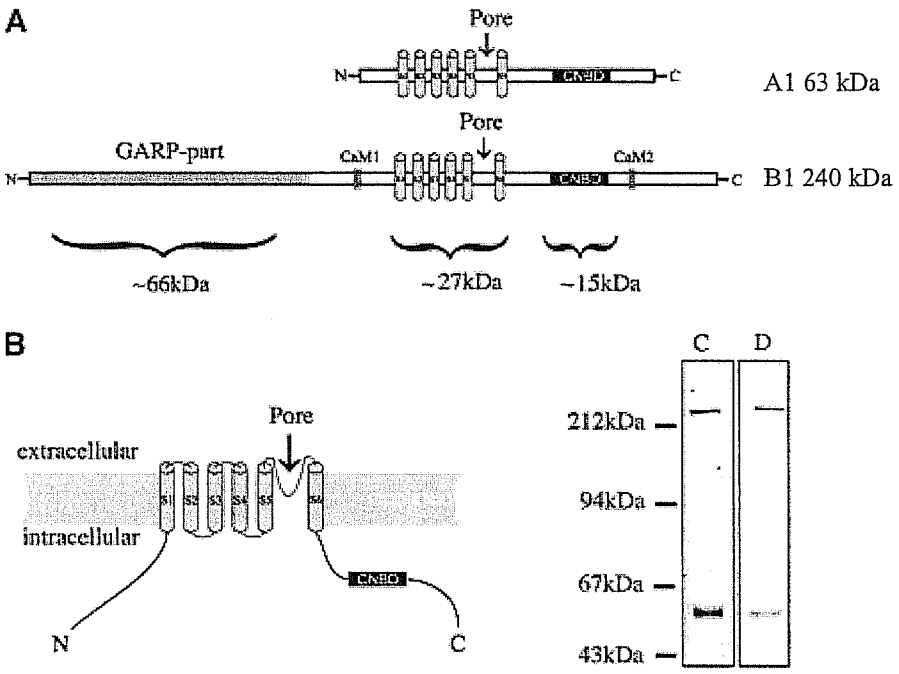

*Fig.3: Schematic representation of subunits present in the rod CNG channel). **A:** the differences between A1 and B1-subunits; **B:** the proposed topology of CNGA1 subunit in the membrane; **C** and **D:** Coomassie Blue staining and western blotting, respectively, used to study the purified CNG channel (modified from Higgins et al., 2002).*

7.2-VOLTAGE-SENSOR MOTIF

The fourth transmembrane segment in VG channels is characterised by repeated positively charged residues (R or K) at every third position interspersed with mainly hydrophobic amino acids. Similarly to VG channels, CNG channels bear between the third and the fifth transmembrane domains a segment that is reminiscent of the S4 segment of VG channels. Indeed, the fourth transmembrane domain of CNG channels also contains a repetitive arrangement of positively charged residues, but the net charge of the motif, is reduced by the presence of negative amino acids. The S4 segment is considered to be the voltage sensor in VG channels and undergoes a conformational change that propagates through the protein (Guy and Conti, 1990; Durell and Guy, 1992). This model has been confirmed by site-directed mutagenesis (Yang and Horn, 1995; Aggarwal and Mac Kinnon, 1996; Yang et al., 1996; Yusaf et al., 1996). In CNG

channels, the fourth transmembrane segment resembles a voltage sensor, and this similarity with VG channels served as a link for the classification of CNG channels (North, 1995). Even if the net charge of the motif is reduced by the presence of additional negatively charged residues, the presence of such an S4 segment is unexpected in channels that don't respond to voltage, while being activated by ligand binding, and could represent a residual portion of a common ancestor of VG and CNG channels. Tang and Papazian showed that the S4 motif of the rat olfactory CNG channel when transferred to the *Drosophila* mutant ether-â-gogo (eag) the VG-channel sequence was able to retain significant sensitivity to voltage changes (Tang and Papazian, 1997). These authors also proposed that the S3-S4 loop of the rat olfactory CNG channel increases the stability of the open conformation of the eag channel converting it into a voltage-independent channel. Maybe, in CNG channels the S4 segment is not longer functional due to the presence of some adjacent portions of the protein. To date, no voltage-sensitive chimeras of CNG channels have been reported.

7.3-PORE REGION

A second motif shared by CNG- and VG- channels is the pore-forming region (P region). This region links the extracellular ends of the fifth and the sixth membrane-spanning regions. According to Sun and co-workers (1996) who applied scanning cysteine analysis method (SCAM) (Karlin and Akabas, 1998), the P region of the CNG tetramer would organise such as extending towards the central axis of the pore, forming the blades of an iris-like structure (Sun et al., 1996). In 1998, the crystal structure of a related K^+ channel was finally obtained and described the pore organisation like an inverted teepee or cone made of the P loops of the four subunits that form the channel (Doyle et al., 1998). The pore region consists of a stretch of about 20 amino acids and exhibits approximately 30% sequence identity between CNG- and VG- channels. In the pore region of all Shaker-like K^+ channels and of several other K^+ selective ion channels two residues, a tyrosine and a glycine (the YG motif), are always present. The YG motif is absent in CNG channels and VG Ca^{2+} and Na^{2+} channels. Interestingly, when these conserved residues are deleted from the Shaker pore region, the channel is converted into a non-selective ion channel (Heginbotham et al., 1994) suggesting that the YG

motif belongs to the selectivity filter. Any YG motif in the pore of the CNG channels has been reported.

7.4-INNER HELIX (S6)

The S6 transmembrane domain, from S371 to S399 residues, of the bovine rod CNG channels (CNGA1), shares sequence similarity with the S6 segment of KcsA and *Shaker* channels (Flynn and Zagotta, 2001; Flynn et al., 2001; Jiang et al., 2002 Johnson and Zagotta, 2001). Using sequence alignment between CNGA1 and KcsA (Doyle et al., 1998) Zagotta and co-workers constructed a homology model to represent the putative pore structure of CNG channels. The model is very similar to KcsA, with the S6 entering the membrane at an angle to forms a helix bundle on the intracellular side. As in KcsA, this inverted teepee structure forms the inner vestibule of the channel. A conformational change occurs in the CNGA1 during channel opening.

7.5- THE TERMINAL ENDS

Two different regions, the N- and C- terminals, of the CNG channels, are present in the cytoplasm. These parts are different in the A1 and in the B1 subunit (see Fig.3). In particular the B1 subunit has two binding sites for calcium-calmodulin (Hsu and Molday, 1993; Grunwald et al., 1998; Weitz et al., 1998) and a GARP region (Korschen et al., 1995), that are lacking in the A1 subunit.

7.5.1-The N-terminal portion

150 amino acid residues compose the N-terminal region present in the A1 subunit of the rod CNG channel. An interaction between this portion and the C-linker has been demonstrated using electrophysiological and biochemical methods (Gordon et al., 1997; Rosenbaum and Gordon, 2002). In particular it was shown that a disulphide bound between a cysteine residue at position 35 of the N-terminal region and a cysteine residue at position 481 of the C-linker region can be induced by oxidising conditions. These data suggest that these two regions are in close proximity in the tertiary structure.

The N-terminal region is different in the A- and in the B- subunits of the retinal CNG channel, in particular in the B1 subunit a domain is found named GARP protein that is composed of 571 residues (Korschen et al., 1995).

7.5.2-The C-terminal portion

7.5.2.1-C-linker

The C-linker is a segment about 90 amino acids long (from residues N400 to G484), that connect the S6 transmembrane domain and the CNBD (cyclic nucleotide-binding domain). This region is highly conserved among CNG channels. Some of its residues were shown to play an important role in coupling ligand binding to channel gating (Zong et al., 1998; Paoletti et al., 1999). Moreover, the histidine residues in position 420 of the A1 subunit of the bovine rod CNG channel is a binding site for Ni^{2+} and some other divalent cations (Zn^{2+}, Cd^{2+}, Co^{2+}, Mn^{2+}), which potentiate CNG current, suggesting that the His420 is involved in gating (Gordon and Zagotta, 1995). The C-linker is also involved in a direct interaction between the N- a C-terminal domains of CNG channels through a cysteine residue in position 481 of the A1 subunit of the bovine rod CNG channel (Gordon et al., 1997).

A hypothesis on the structural organisation has been proposed only for the first segment of the domain (up to His420) (Johnson and Zagotta, 2001). In particular, histidine-scanning experiments suggest that this region may be folded into a α-helix. Even the recent low resolution (35 Å) electron microscopy structure (Higgins et al., 2002) does not allow for the identification of the C-linker with a particular region of the electronic surface.

7.5.2.2-Cyclic nucleotide-binding domain

The observation that phototransduction in retinal rod photoreceptors involves a cation conductance directly activated by intracellular cGMP (Fesenko et al., 1985; Yau and Nakatani, 1985) suggested the existence of a binding site for cyclic-nucleotide on retinal ionic channels. Indeed, such a site was later identified in the C-terminal cytoplasmic portion of the A1 sequence (Kaupp et al., 1989) and the A2 sequence of the olfactory CNG channels (Dhallan et al., 1990; Ludwig et al., 1990). The cyclic-nucleotide binding site of CNG channels consists of a stretch of about 120 residues (from G484 to N610) that exhibits significant sequence similarity to the CNBD of PKA (Proteine kinase A) and the catabolite gene activator protein of *Escherichia coli* (CAP). Crystal structures of CAP and PKA were solved (McKay and Steitz, 1981; Weber and Steitz, 1987; Su et al., 1995) and, because most of the residues forming the nucleotide-binding

pocket of CAP are conserved in the cyclic-nucleotide binding site of CNG channels, the tertiary structure might be similar. The cAMP-binding site of CAP comprises three α-helices (A, B and C) and eight β-strands (β1-β8).

7.6-QUATERNARY STRUCTURE

In 2002 Kaupp and co-workers presented a low resolution three-dimensional structure of CNG from rod. They used electron microscopy, at low-resolution (35 Å), to reconstruct the structure of the native bovine rod channel (comprising both CNGA1 and CNGB1) (Fig.4) (Higgins et al., 2002). At this low resolution, the electron density of channel is clearly separated into three distinct domains (see Fig.4 panels D and E). The larger domain has a width of about 100 Å, a thickness of 50 Å and four corners and it is similar in size to the putative membrane-spanning domain of the *Shaker* potassium channel (Solokova et al., 2001) and has a diameter similar to that of the voltage-gated sodium channel (Sato et al., 2001). Attached to the cytosolic side of the transmembrane domain there are two smaller domains. The idea is that they are the cytoplasmic parts of the channel, including four cyclic nucleotide-binding domains and the ordered parts of four N-terminal regions. It therefore appears as though the four ligand-binding domains fold into two dimers, and these two dimers 'hang' below the transmembrane part of the channel. This model is in agreement with the structure of the cyclic nucleotide-binding domain homologue, CAP (Weber and Steitz, 1987), and a low-resolution structure of a chimera of the CNG channel ligand-binding domain with the DNA-binding domains of CAP (Scott et al., 2001). These structures show a dimer of cyclic nucleotide-binding domains to have dimensions of 30x45x50 Å (Weber and Steitz, 1987). Therefore, the volume of one of the small domains of the channel is similar to that of a dimer in the cyclic nucleotide-binding domains of CAP. The structure also suggests that the four cyclic nucleotide-binding domains, present in each channel, form two distinct domains, suggesting that the four subunits in the CNG channel is arranged as a pair of dimers.

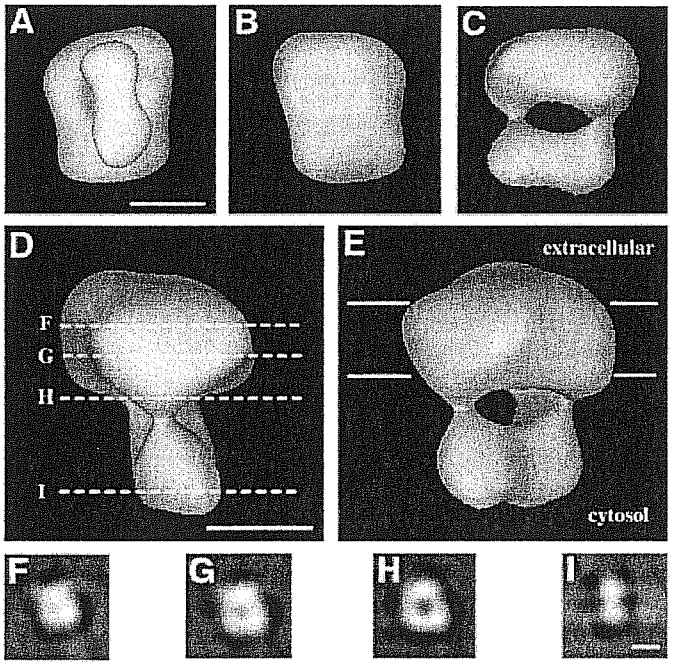

Fig.4: Surface representation of the CNG channels. (A-E) Five different views of the molecule. (F-I) sections through the electrn density alng the lines indicate in (D). The scale bars are 50 Å in length (Higgins et al., 2002).

7.7-B1 SUBUNIT

Native CNG channels are oligomeric proteins composed of different subunits, named A and B subunits, that are present at different stoichiometry in different channels. Briefly, I will discuss the differences between the second subunits present in rod photoreceptor and in olfactory neuron, but I will focus to the first one.

The properties of the A1 subunit, which can form functional channels by itself, are modified by co-expression with B1 subunit, and in this case the properties of channel are very similar to native channel (Korschen et al., 1995; Biel et al., 1999; Kaupp and Seifert, 2002). There are different second subunits that differ from each other in the length and the sequence of the cytoplasmic N-terminus. "Long" isoform, expressed in rod photoreceptor (CNGB1, 240 kDa) (Korschen et al., 1995; Ardell et al., 1996; Colville et Molday, 1996) and also in pineal gland (Sautter et al., 1997), is characterised by an extended N-terminal that is negatively charged due to the presence of a large number of glutamate residues. This part is named GARP-part (glutamic acid-rich

protein) is composed by 571 amino acid residues and the physiological function of this region is not known. In the "short" B subunit, the GARP-part is replaced by various sequences depending on the respective isoform; this short isoform is present in olfactory epithelium (CNGA4) (Sautter et al., 1998) and in bovine testis (Wiesner et al., 1998; Biel et al., 1999). Six transmembrane domains (S1-S6), a pore region, a S4 voltage sensor motif and a cyclic nucleotide-binding domain compose the core region of B1 subunit. Moreover, in this "second" subunit two distinct binding sites for Ca^{2+}/CaM are localised in the cytoplasmic N-terminus preceding the first transmembrane segment and in the C-terminus downstream of the CNBD. This subunit is a modulatory subunit (see: "Molecular cloning and diversity of subunits" and "Effect of subunit composition").

7.8-SUBUNIT STOICHIOMETRY OF CNG CHANNEL

The native CNG channels consists of two different types of subunits, the A- and the B-subunits but the subunit composition and the stoichiometry are different in the different type of cells. The native CNG channel in rods comprises three A1 and one B1 subunit (Kaupp and Seifert, 2002). The CNG channel of cones is composed of three A3 and one B3 (Kaupp and Seifert, 2002; Zheng et al., 2002) and the olfactory channel consists of three different subunits: A2, A4 and B1b subunit (Kaupp and Seifert, 2002) (Fig.5).

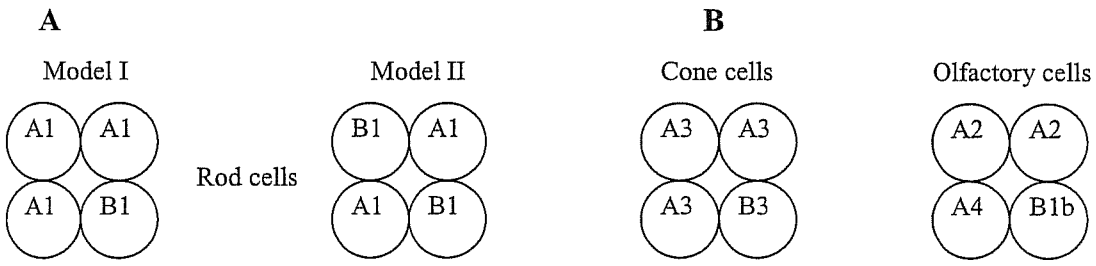

Fig.5: Subunits stoichiometry proposed for different CNG channels. ***A:*** *the new model (I) proposed by Kaupp and collaborators and the old model (II) proposed by He et al., 2000;* ***B:*** *cones and olfactory neurons (Kaupp and Seifert, 2002).*

8-Functional properties of CNG channels

8.1-FUNCTIONAL PROPERTIES OF THE PORE REGION

8.1.1-IONIC PERMEATION

The pore-forming region is known to be the major determinant of ion permeation in VG- (Heginbotham et al., 1994; Yang et al., 1993) as well as in CNG- channels (Goulding et al., 1993). Despite the sequence homologies displayed by the pores of VG-K^+ channels and CNG channels, ions surprisingly do not permeate in the same manner in both groups of channels. Indeed, while VG-K^+ channels, like VG-Na^+ channels, are highly selective, CNG channels do not discriminate well between the different monovalent alkali cations (Picco and Menini, 1993). This peculiarity of CNG channels was early demonstrated both in intact retinal rods (Capovilla et al., 1983; Nakatani and Yau, 1988, Menini et al., 1988) as well as in excised patches (Fesenko et al., 1985; Nunn, 1987; Furman and Tanaka, 1990; Menini, 1990; Colamartino et al., 1991). Nevertheless, a small difference in the permeability for monovalent alkali cations is observed between the native CNG channel and the A1 subunit: contrary to the native channel, the A1 subunit is more selective for Na^+ than for Li^+ (Kaupp et al., 1989). Surprisingly, CNG channels share many permeation properties with VG-Ca^{2+} channels, despite different amino acid sequences in their pore regions. Indeed, both channels are permeable to Ca^{2+} and monovalent cations (Yau and Nakatani, 1985). But in addition to permeating through the pore of both channels, Ca^{2+} also blocks the flow of current carried by monovalent ions (for photoreceptors, see Yau and Baylor, 1989; Zimmerman and Baylor, 1992; for olfactory receptors, see Zufall et al., 1994; for Ca^{2+} channels, see Almers and McCleskey, 1984; Hess and Tsien, 1984). In CNG channels, Ca^{2+} permeation depends on the cyclic nucleotide concentration: Ca^{2+} ions either permeate or block the channel (Colamartino et al., 1991). Similarly to Ca^{2+} channels, CNG channels are also sensitive to external proton concentration in that a subconductance state due to a blocking effect is observed when the pH is decreased (for CNG channels, see Goulding et al., 1992; Zufall and Firestein, 1993). Ionic selectivity of CNG channels to

non physiological cations has also been investigated in order to understand the permeability rules at the molecular level and to give an estimate of the pore size (Picco and Menini, 1993). The study of permeation of ammonium and guanidinium derivatives indicates that the pore of CNG channels is permeable to at least thirteen organic cations. Whereas Na^+ and K^+ VG channels exclude all methylated cations, the cGMP-gated channel is permeable to many cations containing a methyl group. Following this study of ionic permeation an estimate of the size of the pore was given: the cross section of the narrowest part of the pore must be at least as large as 0.38 x 0.5 nm. This estimated size suggests that the pore of CNG channels is bigger than the ones of Na^+ and K^+ channels but smaller than the one of the Ca^{2+} channel of skeletal muscle. This conclusion is in accordance with the estimation obtained by Laio and Torre after a study of statistical mechanics (Laio and Torre, 1999). In this study, the physical origins of ionic selectivity were investigated and it was concluded that the selectivity for monovalent cations depends on geometrical properties of the inner core of the channel without any critical contribution from charged or polar groups that would interact electrostatically with the permeant ions. This hypothesis may explain the differences in ionic selectivity between channels having similar pore residues and *vice-versa* the similarities in ionic selectivity between channels having different pore residues.

8.1.2-THE FUNCTIONAL ROLE OF A CONSERVED GLUTAMATE

The pore region of CNG channels is the site of ion permeat, in particular, some residues might be more important than others in controlling the flow of ions. Indeed, a conserved glutamate which is found at position 363 in the CNGA1 sequence appeared to be involved in the block by external Mg^{2+}, Ca^{2+} (Root and MacKinnon, 1993; Eismann et al., 1994) and protons (Root and MacKinnon, 1993). Since substitution of E363 by a neutral amino acid reduced external divalent cations block but maintained the channel sensitivity to internal blockade, it was suggested that this glutamate was localised inside the pore, close to the external surface. The B1 subunit bears a glycine residue at the position corresponding to the glutamate 363. Interestingly, coexpression of A1 and B1 subunits led to a reduced sensitivity to external divalent cations (Korschen et al., 1995) analogue to the level reported for the native channel. This result is consistent with the role played by E363 in divalent cations block. Indeed, it has been proposed that in

homotetrameric channels the four glutamate residues form the high affinity Ca^{2+} binding site. Various homomeric CNG channels differ in their sensitivity to external Ca^{2+} ions (Frings et al, 1995). Since the glutamate residue is conserved in all CNG channels A1 subunits known so far, additional residues or factors must participate in the binding of divalent cations and account for the different sensitivity to Ca^{2+} blockade. Indeed, it was recently shown that the S5-P-S6 region defines a particular dielectric environment that sets the state of protonation of the glutamate residues and consequently determines the affinity of the Ca^{2+} binding site inside the pore (Seifert et al., 1999). This glutamate was also shown to be responsible for the multi-ion nature of the pore of CNG channels (Sesti et al., 1995). Sesti and co-workers tested the anomalous mole fraction effect with mixtures of Li^{+} and Cs^{+}. This effect is characteristic of a pore containing multi ion-binding sites and was observed for the native channel as well as for the homomeric channels. At the contrary, the anomalous mole fraction was not observed when the glutamate 363 was replaced by a neutral amino acid and was only reduced when it was mutated into an aspartate. These results suggest that the coordination of several negative residues is necessary to form the molecular structure that can bind one or two monovalent cations. This structural organisation is reminiscent from the coordination of four glutamate residues in the four different repeats of Ca^{2+} channels that constitutes a binding site for one or two small cations (Armstrong and Neyton, 1992). Another interesting observation regarding E363 of the CNGA1 was made regarding channel gating (Bucossi et al., 1996). By mutating E363 into an alanine, a serine or an asparagine, a current decline reminiscent of the desensitisation of LG channels was observed for the CNG channel suggesting that glutamate 363 was involved in gating properties in addition to be part of the selectivity filter. In the same study, it was demonstrated that, contrary to the wild type channel, the mutant E363S was permeable to dimethylammonium. The fact that replacing the glutamate by a smaller residue led larger organic cations to permeate suggested that E363 was located close to the narrowest part of the pore.

8.2-FUNCTION OF THE CYCLIC-NUCLEOTIDE BINDING SITE

The ligand sensitivity of the cyclic-nucleotide binding sites depends on the channel considered. Nevertheless, all CNG channels are more sensitive for cGMP than for cAMP. The constant for half activation, $K_{1/2}$ for the native and for the cloned bovine rod is similar: 10-50 μM for cGMP and 1.2-1.5 mM for cAMP. For the cone photoreceptor, $K_{1/2}$ is around 34-70 μM for cGMP and 1 mM for cAMP. For the olfactory CNG channels, the $K_{1/2}$ values for both cyclic nucleotides are in general closer: for the cloned bovine olfactory receptor, $K_{1/2}$ is 1.4 μM for cGMP and 54 μM for cAMP; for the native rat olfactory receptor, $K_{1/2}$ is 1 μM for cGMP and 2.5 μM for cAMP; for the native salamander photoreceptor $K_{1/2}$ is 4 μM for cGMP and 20 μM for cAMP (for review, see Eisman et al., 1993). Although the olfactory CNG channel is slightly more sensitive for cGMP than for cAMP, its physiological ligand is cAMP.

The binding site is formed by eight-stranded antiparallel β-rolls flanked by a short amino-terminal α-helix (A helix) and two C-terminal α-helices (B and C helices). Based on sequence comparison between the different cyclic-nucleotide binding protein, a model of binding was proposed (Kumar and Weber, 1992). Some residues were identified as key residues in the interaction with the cyclic-nucleotides. A set of highly conserved glycines in the β-rolls is important for the proper folding of the binding pocket. Using a photoaffinity radioactive analogue of the cGMP able to label specifically both subunits of the bovine rod CNG channel, Brown and co-workers localised more precisely the cGMP binding site and identified the residues lining the binding pocket (Brown et al., 1995). Indeed, the specific labelling of the rod A1 subunit was localised to a 66 amino acid region (Tyr 515-Met 580) entirely contained into the 120 amino acids previously supposed to form the binding site for cyclic-nucleotides. Moreover, within this fragment, residues Val 524, 525 and Ala 526 were found to contain label and thus to line the binding pocket. The specific labelling was also confirmed repeating these experiments on the B1 subunit of the bovine rod. Conserved residues of the β7 strand were also subjected to investigation. Molecular modelling on cGMP-dependent protein kinase suggested that the hydroxyl group of the threonine residues of the β7 strand formed a hydrogen bond with the amino group attached to the C2 of cGMP (Weber et al., 1989). Based on the fact that this amino group is absent

from the cAMP molecule, this residue might have accounted for ligand discrimination. Mutation of the first alanine of the β7 roll into a threonine in the cAMP dependent kinase indeed increased the binding of cGMP but this mutation had little effects on the cAMP binding (Shabb et al., 1990). This alanine/threonine hypothesis was subsequently studied by Altenhofen and coworkers who concluded that the hydroxyl group of Thr 560 (rod) and Thr 537 (olf) form an hydrogen bond with cGMP but not cAMP (Altenhofen et al., 1991). However this threonine could not account for the molecular basis of ligand discrimination between the retinal and olfactory channels since all CNG channels contain a threonine at this position. Moreover the hydrogen bond can only be formed when the cGMP is in a *syn* conformation whereas for the CAP the binding is known to occur in the *anti* conformation (see the review of Zagotta and Siegelbaum, 1996). Based on the observation that the C-helix of the CAP (Thr 127- Ser 128) makes two hydrogen bonds with the C6-amino group of cAMP (Weber and Steitz, 1987), the group of Siegelbaum performed a study of chimeras between the BROD and the catfish olfactory channel and concluded that the C-helix is both necessary and sufficient to account for ligand specificity (Goulding et al., 1994). By comparing the sequences of the CAP and the CNGA1 C-helices, the residue D604 of the CNGA1, which corresponds to T127 in the CAP sequence, was mutated (Varnum et al., 1995). The nucleotide selectivity of the CNGA1 (cGMP > cIMP >> cAMP) was significantly altered when the aspartate was mutated into a glutamine (corresponding residue in the fish olfactory channel) (cGMP >> cAMP > cIMP). Substitution of D604 by a methionine completely inverted the initial selectivity sequence (cAMP >> cIMP > cGMP). Varnum and co-workers concluded that these changes were due to an alteration in the relative ability of the bound agonist to trigger the allosteric conformational changes necessary to the channel opening. In addition, they proposed that D604 forms two hydrogen bonds with N1 and N2 of the guanine ring in anti configuration. Recently, the functional role of aromatic residues in the ligand-binding domain of CNG channels was analysed (Li and Lester, 1999). By replacing Tyr 565 of the rat olfactory CNG channel into an alanine, a 10-fold increase in sensitivity to both cAMP and cGMP. This tyrosine lies in the hinge between helices B and C and is thought to facilitate gating transitions that occur after ligand binding.

8.3-GATING PROPERTIES

8.3.1-PROPERTIES OF THE MACROSCOPIC CURRENTS

The macroscopic properties of CNG channels are usually studied using the patch-clamp technique, excising membrane patches either from photoreceptors or from *Xenopus* oocytes or cultured cells expressing the heterologous channel of interest. When an inside-out patch excised from the membrane of the system expressing CNG channels, is exposed to micromolar concentrations of cyclic-nucleotide, many channels are activated and macroscopic currents are recorded. Fig.6 shows the macroscopic current obtained from an inside-out patch excised from the outer segment membrane of a photoreceptor, at +60 mV and in the presence of different cGMP concentrations. The current observed is dependent on the cGMP concentration: at saturating concentrations of cGMP (100 μM) currents as large as 1-2 nA can be obtained whereas very small currents (some pA) are measured at low cGMP concentration. As a consequence, the relationship between the current and the cGMP concentration can be described as:

$$I = I_{max} [g^n / (g^n + K^n)]$$

where Imax is the maximal current activated by cGMP, g is the cGMP concentration, K the cGMP concentration activating half of the maximal current and n the Hill coefficient. Experimentally, n is between 1.7 and 3.5 (Zimmerman and Baylor, 1986; Yau and Baylor, 1989) and K has a value of 10 μM or 50 μM (for CNG channels of salamander photoreceptors; see Zimmerman and Baylor, 1986; Colamartino et al., 1991; for CNG channels of bovine rods; see Luehring et al., 1990). CNG channel activation also presents evidence for a slight voltage-dependence: hyperpolarisation appears to increase the rate constant of channel closing (Karpen et al., 1988). According to Sesti and co-workers (1994), analysis of single channel activity at positive and negative voltages indicates that the outward rectification observed in the presence of low cGMP concentration is primarily due to an increase in the open probability at positive voltages. Contrary to the cGMP-activated channel involved in phototransduction that responds instantaneously to the variation in cGMP levels, the cAMP-gated channel involved in olfactory transduction displays much slower activation kinetics (Zufall et al., 1993). These differences certainly account for the different requirement of the two modes of sensory transduction, in the sense that the olfactory system must discriminate between

thousands of odours without lost in sensitivity even if this feature is filled at the expense of time. Similarly to the CNG channel from photoreceptors, the ones from olfactory receptors physiologically respond to the binding of an agonist, cAMP. Surprisingly, for the cloned channel, the half saturating concentration value (at +40 mV) is higher in the case of cAMP (38-68 μM) than for cGMP (1.2-2.4 μM) (Dhallan et al., 1990); for the native channel, Nakamura and Gold (1987) found a bimodal value (K = 2 and 40 mM for cAMP). The Hill coefficient is around 1.9, similar to the one of the cGMP-activated channel from photoreceptor (Dhallan et al., 1990). Similarly to the CNG channels involved in phototransduction, the currents activated by cAMP in olfactory receptors also present a very small outward rectification (Dhallan et al., 1990; Goulding et al., 1992).

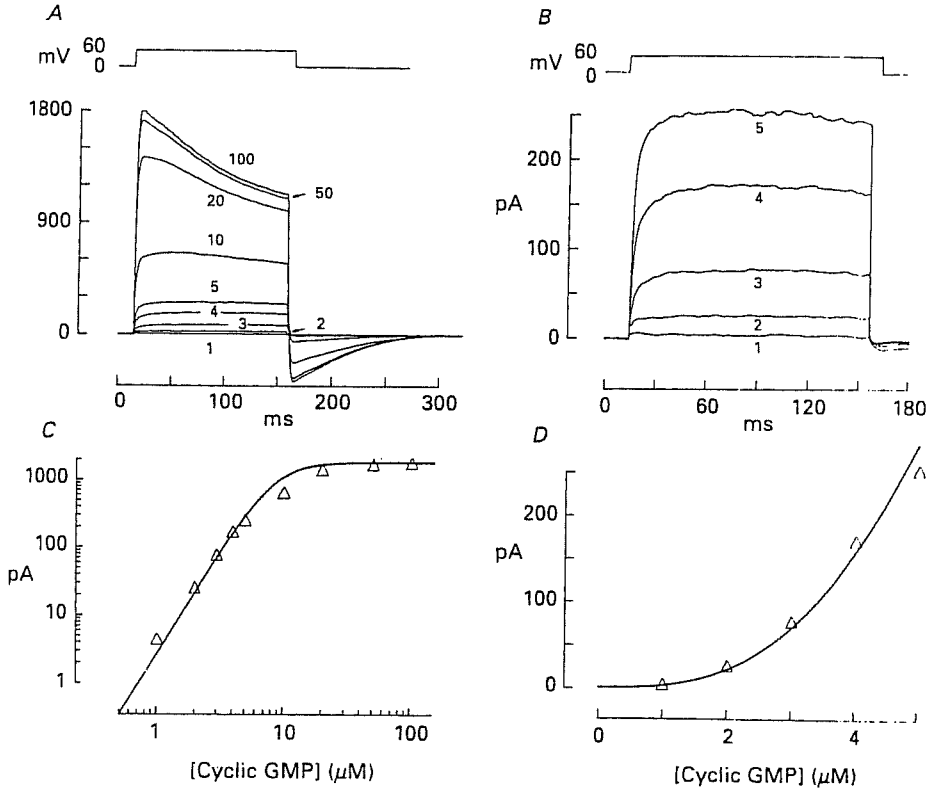

Fig.6: *Stoichiometry of the activation of the macroscopic CNG current in inside-out membrane patches from salamander rod outer segment. Voltage steps were from 0 to +60 mV. In A and B cGMP stoichiometry of the activation of the Na^+ current.* ***A:*** *current recording activated by 1, 2,3,4, 5, 10, 20, 50 and 100 μM cGMP;* ***B:*** *current recording activated by 1, 2, 3, 4, and 5 100 μM cGMP.* ***C*** *and* ***D:*** *relation between activated current and cyclic GMP concentration (Colamartino et al., 1991).*

8.3.2-SINGLE CHANNEL PROPERTIES

The first attempts to record cGMP-induced single channel current were unsuccessful (Fesenko et al., 1985; Nakamura and Gold, 1987). Noise measurements revealed a very small single channel conductance of less than 0.1 pS that was inconsistent with an aqueous pore but fitted more to the conduction observed in case of membrane carriers (Fesenko et al., 1985). Another explanation for a so small unitary current was that the effective conductance of the channel pore was reduced because of a blockade. Indeed, the first measurements of single-channels were obtained in excised rod membrane

patches using solutions free in divalent cations (Zimmerman and Baylor, 1986; Haynes et al., 1986; Matthews and Watanabe, 1987, 1988). The reduction in single-channel conductance by divalent cations was proposed to be physiologically important in reducing the signal-to-noise ratio of sensory transduction (Yau and Baylor, 1989). A great variability in the mean open time ranging from 0.1 to 1 msec and a single-channel conductance between 20 and 60 pS were obtained (Yau and Baylor, 1989; Torre et al., 1992; Zufall et al., 1994; Sesti et al., 1994). The typical traces for single-channel recordings from excised patches of rod outer segments reveal a continuous flickering between the closed and the open states (Fig.7). Theoretical analysis of the experimental amplitude histograms gives an estimate of the mean open time of maximally 35 μsec (Torre and Menini, 1994). The density of cGMP-activated channels in the membrane of the rod outer segment is high (126 μm^{-2}, Karpen et al., 1992) and single-channels openings can only be obtained using very small concentrations of cGMP. However, cGMP-gated channels are not so dense in the inner segment simplifying single-channel recordings (Matthews and Watanabe, 1988). Inner segment recordings also exhibited in majority the flickering behaviour. Surprisingly, in some rare recordings the application of cGMP induced well defined openings without flickering behaviour (Torre et al., 1992; Sesti et al., 1994). The properties of these single-channel recordings in terms of conductance (25-30 pS) and open probability (half activation of this channel occurred at about 18 μM cGMP) were reminiscent from the ones observed when expressing the A1 subunit of the CNG channel (Kaupp et al., 1989). Depending on the nature of the preparations, the properties of CNG channels were quite different. It has been just mentioned that the A1 subunit of the CNG channels displays a single open state with a conductance around 28 pS (Kaupp et al., 1989). In contrast, the A2 subunit of the CNG channels from catfish olfactory sensory neurons were found to be characterised by three different open states with respective conductances of 25, 50 and 80 pS (Goulding et al., 1992; Root and MacKinnon, 1994). The A4 subunit of the CNG channel from rat olfactory neurons has a conductance of about 40 pS and is characterised by the absence of subconductance states (Li and Lester, 1999). Complessively, the sum of the collected data are consistent with the existence of different conducting levels in the CNG channel, leading to the appearance of well resolved open states in homomeric channels and to flickering behaviour in heteromeric channels (Bucossi et al., 1997).

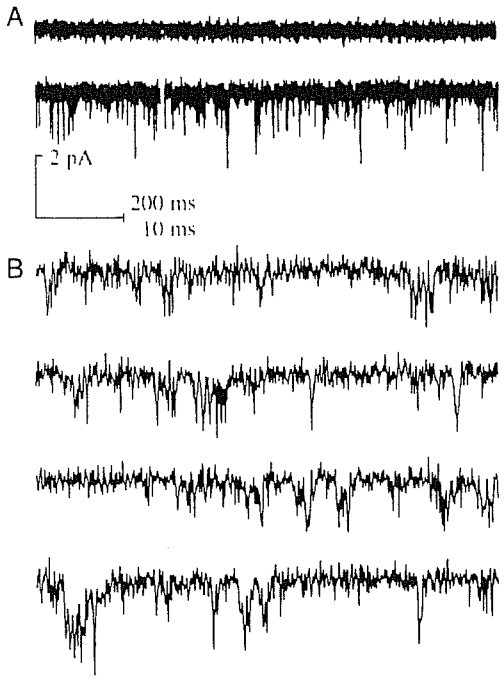

*Fig.7: **A:** Single channel currents recorded with 0 (top) and 2 (bottom) μM cGMP. **B:** Single channel currents recorded with 2 μM cGMP at –60 mV and filtered at 4 kHz (Torre and Menini, 1994).*

8.4-COUPLING OF LIGAND BINDING TO CHANNEL GATING: ROLE OF THE C-LINKER

The molecular mechanisms underlying the coupling of ligand binding to channel opening have been recently investigated. One of the first insights were given by Gordon and Zagotta, who identified a histidine residue in the C-linker of the bovine rod CNG channel responsible for potentiation by internal Ni^{2+} ions (a phenomenon previously described by Ildefonse et al., 1992) by stabilisation of the open conformation (Gordon and Zagotta, 1995a). Another histidine was found by the same researchers in the rat olfactory CNG channel but this histidine accounted for channel inhibition by binding preferentially to the closed states, stabilising them and thus reducing the efficiency of channel activation (Gordon and Zagotta, 1995b). A conserved cysteine residue in the C-linker L2 region was then identified as a site of potentiation through the modification of sulfhydryl-reactive chemical (Broillet and Firestein, 1996; Brown et al., 1998). Based on their results, Brown et al. suggested that the C-linker undergoes a movement during

channel activation which is essential for coupling ligand binding to channel gating. More recently, Zong et al. investigated chimeric channels between the cone photoreceptor and the olfactory receptor and identified three amino acids in the C-linker that account for the differences in cAMP efficacy and are major determinants in channel gating (Zong et al., 1998). Three other residues in the C-linker L2 region were found to be involved in gating processes after another study of chimeras. Indeed, the group of Siegelbaum conferred the very high cAMP efficacy of a *Caernobitis elegans* sensory neuron channel (TAX-4) to the CNG channel which is usually poorly activated by cAMP (Paoletti et al., 1999). The exchange of the two different C-linker L2 regions did not alter the spontaneous open probability of the channel, despite a large effect on gating. This result inferred the possibility of a gate-like function for the C-linker but suggested a possible role for the C-linker in determining the differences in agonist interaction between the closed and the open states. Indeed, they found that the C-linker favours the stability of the ligand-binding to the open state, stabilising the interactions between the ligand and its binding site. This stabilisation occurring in the same way for both cGMP and cAMP, the C-linker must interact with the cyclic nucleotide in a part of the molecule which is common to both cGMP and cAMP. They proposed that the C-linker would act as a rigid arm that couples a change in the structure of the core of the channels to a movement of the ligand-binding site, which favours the binding of the cyclic-nucleotide in the open conformation, intersubunits interactions and consequently stabilises the open state. The cyclic nucleotide-binding site itself has been proposed to play an important role in coupling ligand-binding to channel allosteric conformational change.

8.5-KINETIC MODELS OF GATING

The gating kinetics of CNG channels were studied by Karpen and co-workers (1988). As previously mentioned, they showed the cGMP-dependence of channel activation, the saturation of the opening rate at high cGMP levels and mentioned also the slight voltage sensitivity of CNG channels whose opening can be increased by depolarisation. From their results, they proposed a model with three ligand-binding steps followed by a closed to open transition that is favoured by depolarisation and occurs when the channel is fully liganded. This model accounts for the nearly linear current-voltage (I/V) relation

observed at saturating concentration of cGMP, i.e. when almost all channels are open even at negative voltages. At low concentration of cGMP, the open probability is low so that the role of voltage changes in the C4 to O equilibrium is major for increasing the open probability.

8.6-ALLOSTERIC MODELS

Spontaneous openings of CNG channels in the absence of ligand have been reported (Picones and Korenbrot, 1995b). Taking this observation into account, an allosteric model has been proposed by Stryer (1987). In this model, the affinity of cGMP is higher for the open conformation than for the closed one, the change of conformation is concerted between the different subunits, the binding of the ligand to each subunit is independent from the other bound subunits and the greater the number of cGMP molecules that bind, the more stable the conformational change. By constructing chimeras between the bovine rod and the rat olfactory channels, Goulding and co-workers identified two distinct domains, the N-S2 domain of the N-terminal region and the C-helix of the C-terminal domain, which are important for channel opening. They propose that the N-S2 region is a portion of intersubunit contact. These contacts are enhanced during channel activation, these modifications lead to changes in subunit orientation, that, combined to a movement of the C-helix leads to channel opening (Goulding et al., 1994). This interpretation is based on a simple tetrameric allosteric model that, similarly to the model proposed by Stryer, supposes that the ligand prefers the open conformation. The N-terminal region of the olfactory channels seems to be of particular importance (Chen and Yau, 1994; Gordon and Zagotta, 1995b). This feature has been exploited by Sunderman and Zagotta, who analysed the kinetic behaviour of single CNGA1 channel in which mutations in the binding domain (D604, see Varnum et al., 1995) have been introduced and/or the rat olfactory N-terminal domain substituted to the original one of the CNGA1 (Sunderman and Zagotta, 1999). They refined the previously proposed model (Gordon and Zagotta, 1995b; Varnum et al., 1995) in which the cyclic nucleotide is supposed to bind to the closed state through interactions with the β-roll of the binding site, this binding leads to a movement of the β-roll relative to the C helix and to a subsequent strenghtening of the cGMP binding through hydrogen bonds with D604. The formation of the hydrogen bonds has been shown to be important for

the allosteric transition leading to channel opening whereas the closure of the channels requires their dissolution. The stabilisation exerted by the N-terminal portion occurs just before the allosteric transition and then after for stabilising the interactions between the aspartate residue of binding domain and the ligand. The same authors studied in details the mechanisms of allosteric transition performing single-channels analysis of the CNGA1 subunit expressed in *Xenopus* oocytes (Sunderman and Zagotta, 1999). They determined that two closed and one open states are required to explain the gating at saturating ligand-concentration. Two kinds of models were then possible: C <--> C <--> O or C <--> O <--> C. The first hypothetical model could describe the activation of a channel composed of two functional dimers which would have to enter both in the activated conformation to allow the channel to open (concerted transition). A scheme similar to this C <--> C <--> O model was previously proposed by Liu et al. (1998). For the second possible model, a single concerted allosteric conformational change could underlie the C <--> O transition, while the O <--> C being cyclic nucleotide independent would depend on an open-channel block or closing of a secondary gate (multiple conformational changes). While the real mechanism is undoubtedly more complex than two closed and one open state, they favoured the second model. Sunderman and Zagotta also studied the effect of Ni^{2+} and concluded that Ni^{2+} induces and stabilises the allosteric transition of liganded channels. This hypothesis also implies that the conformational changes occurring spontaneously are based on a different mechanism that does not involve the movement of H420. This is in accordance with the recent findings of Paoletti et al. (1999) that showed that alterations in the C-linker do not affect spontaneous openings. Opening mechanisms have been recently studied by Ruiz and Karpen (1999) who performed analysis of single channels locked in each liganded state. Usually, studies of kinetics have always been impaired by the fact that the ligand binds and unbinds continuously from the binding site. In 1997, Ruiz and Karpen overcame these problems by using a photoaffinity cGMP analogue that binds covalently to CNG channels. From this study, these researchers found that CNG channels can be locked in four liganded states and that in each state, channels opened to two or three different conductance states. Now, Ruiz and Karpen refined their studies and concluded that the channels exhibit at least nine different states for each doubly, triply and fully liganded channel. This observation supposes that the channels exhibit

the same series of conformational changes at each possible liganded state. Such complex behaviour can not be explained with simple concerted or sequential allosteric models. A general allosteric model is proposed in this study: channels with zero and one activated subunits are closed, channels with two adjacent subunits activated lead to an open state (O1), channels with diagonally activated subunits are closed, channels with three or four activated subunits are open (states O2 and O3). In the four liganded channels, additional states are required: an additional conformational change can be added for a change in the interaction between two liganded subunits that are adjacent. There are some evidence for such a conformational change that occurs between pairs of subunits: Gordon and Zagotta (1995) showed that the open state is stabilised by such intersubunits interactions through Ni^{2+} coordination; Varnum and Zagotta (1996) showed that activation properties were different for adjacent subunits than for diagonally opposed ones; Liu et al. (1998) also proposed a mechanism based on interaction between adjacent subunits.

8.7-MODULATION OF CNG CHANNELS

For review see Kaupp and Seifert, 2002

8.7.1-MODULATION BY Ca^{2+}-CALMODULIN

Two Ca^{2+}/calmodulin binding sites (CaM1 and CaM2) are located in the N- and C-terminal domains of the B1 subunit of rod CNG channel, respectively. Only the CaM1 site is necessary for channel modulation, whereas the function of the CaM2 site is unknown yet. The rod A1 subunit it self does not bind CaM and a channel consisting of only A1 subunits is not modulated by calmodulin, in contrast to the olfactory channel (Weitz et al., 1998). CaM binding domains are composed of about 20 residues and are characterised by aromatic residues at positions 1 and 14 of the motif and additional hydrophobic residues at position 5 and 8. Several positively charged residues are interspersed between the hydrophobic residues. Modulation of CNG channels by Ca^{2+}-calmodulin was first reported for the rod photoreceptor by Hsu and Molday (1993). In this study, the effect of Ca^{2+}/calmodulin was investigated using in particular a calcium ion flux assay with a calcium-sensitive dye. The results of this work allowed concluding that Ca^{2+}/calmodulin increases the apparent Michaelis constant of the channel for

cGMP. This effect leads to a decrease from two- to six- fold in the rate of cations influx, including Ca^{2+}, through CNG channels activated by low cGMP concentrations. The Ca^{2+}/calmodulin effect can be incorporated into the process of phototransduction. In the dark, cGMP-activated channels are open and the cytoplasmic Ca^{2+} concentration is maintained at relatively high levels (around 0.3 μM). In this situation, the guanylate cyclase is at its basal level, the cGMP-gated channels are in a low affinity state for cGMP binding and Ca^{2+}/calmodulin is bound to the channel. In the presence of light, cGMP-gated channels are closed, cytoplasmic Ca^{2+} level decreases, guanylate cyclase is activated, Ca^{2+}/calmodulin dissociates from the channel that consequently switches to its high affinity state for cGMP. This causes the reopening of cGMP-activated channels in the presence of low cGMP facilitating the photorecovery of the system. An action of Ca^{2+}/calmodulin was also described for CNG channels of olfactory receptors using the cloned rat olfactory channel expressed in cell lines (Chen and Yau, 1994). In this study, Ca^{2+} was shown to reduce the apparent affinity of the channel for cAMP by up to 20-fold in the presence of Ca^{2+}/calmodulin. This action involves a direct interaction between the calmodulin and the 63 kDa channel protein as expression of the cloned olfactory CNG channel is enough to observe Ca^{2+}/calmodulin modulation. The group of Yau went on studying the modulation of CNG channels by Ca^{2+}/calmodulin and succeeded in the identification of the Ca^{2+}/calmodulin binding site on the A2 subunit of the olfactory CNG channel (Liu et al., 1994). They used chimeras between the rat olfactory channel and the human rod channel N-terminal parts. The cDNAs encoding for these chimeras were then transfected into HEK293 cells and tested for Ca^{2+}/calmodulin sensitivity. These experiments showed that the N-terminal portion of the olfactory channel contains a putative Ca^{2+}/calmodulin binding domain that is a peptidic sequence characterised by two aromatic or long chain residues (aromatic residues at position 1 and 14; other hydrophobic residues at position 5 and 8) separated by 12 amino acids which are often positively charged. In the case of the rat olfactory channel, this calmodulin binding sequence is located from residues Arg62 to Arg87 on the A2 subunit and constitutes the only Ca^{2+}/calmodulin binding domain. In order to quantify the interaction of the Ca^{2+}/calmodulin and its binding site, they performed the

synthesis of a peptide made of the residues comprised between Arg62 and Arg87 and performed experiments of gel-shift assays and fluorescence. They concluded in a one-to-one stoichiometry with a dissociation constant of 3.4 nM. Experiments using cAMP indicated that Ca^{2+}/calmodulin in addition to change ligand affinity affects channel gating in that the current activated by high cAMP concentration is reduced in the presence of calmodulin. In addition the Ca^{2+}/calmodulin mediated feedback, another mechanism of CNG channel inhibition in olfactory neurons that involves high intracellular Ca^{2+} concentration and an unknown Ca^{2+} binding protein has been suggested (Kramer and Siegelbaum, 1992; Gordon et al., 1995).

8.7.2-MODULATION BY PHOSPHORYLATION/DEPHOSPHORYLATION

The response of cGMP-gated channel to the binding of cGMP is influenced by dephosphorylation. Just after excision of patches from the membrane of frog rod outer segments, Gordon and co-workers observed a spontaneous increase in apparent agonist affinity. The conversion of the cGMP-activated channel from a low cGMP affinity state to a state of higher sensitivity was blocked by serine/threonine phosphatase inhibitor suggesting that an endogenous phosphatase was involved. Two different phosphatases may play a role: an increase in apparent cGMP affinity was observed when phosphatase type 1 was added whereas a decrease in ligand affinity appeared in the presence of phosphatase type 2A. This dual action suggested that two sites of phosphorylation might regulate agonist affinity during phototransduction mechanism (Gordon et al., 1992). CNG channels have been also shown to be modulated by protein kinases (Molokanova et al., 1997; Muller et al., 1998). Recently a site for tyrosine phosphorylation was identified on the C-terminal portion of the A1 subunit of the cGMP-gated channel (Molokanova et al., 1999). Because only CNG channels from photoreceptors display this modulation *via* phosphorylation, studies of chimeras between the A1 subunits of the bovine rod and the rat olfactory channels allowed localising the phosphorylation site on a specific tyrosine residue (Y498). Y498 is located in the C-linker, i.e. a region shown to be important in coupling ligand-binding to channel gating, and is highly conserved in proteins bearing a binding site for cyclic nucleotides. When this tyrosine is removed from the CNGA1 channel, modulation is reduced by 75%; the residual modulation suggests the existence of additional phosphorylation sites. Considering that deletion of

the C-terminal part of the channel totally abolishes the modulation by phosphorylation, the supplementary phosphorylation sites must be located on this cytoplasmic region. Molokanova and coworkers suggest a model for the mechanism of tyrosine phosphorylation/dephosphorylation: in presence of cGMP, the binding of the phosphatase leads to dephosphorylation and promotes channel opening by increasing the affinity for cGMP; at the contrary, when the channel is closed, the tyrosine kinase binds to the channel, phosphorylates it and stabilises the closed conformation by reducing the affinity for cGMP. Hence, modulation by changes in tyrosine phosphorylation is activity-dependent and is interpreted as a positive feedback, maybe present to counterbalance the Ca^{2+}-dependent negative feedback. In a recent work, the effect of genistein, a competitive inhibitor of the ATP binding site on protein kinases, was studied on inside out patches excised from the membrane of *Xenopus* oocytes expressing the A1 subunit of the CNG channel (Molokanova et al., 1999; Molokanova et al., 2000; Molokanova and Kramer, 2001). Cytoplasmic application of genistein prevents changes in cGMP sensitivity that are attributed to tyrosine phosphorylation, slows activation kinetics and reduces the maximal current through CNG channels at saturating cGMP concentrations. These effect are ATP-independent and occur indirectly via the binding of genistein to the protein tyrosine kinase. This interaction between genistein and the kinase induces a non catalytic interaction between the enzyme and the CNG channel. The consequence is an allosteric inhibition of channel gating. This study allows confirming that protein kinase catalysis the phosphorylation of the cGMP-gated channel but in addition suggest a second effect of tyrosine kinase on the regulation of channel gating.

8.7.3-OTHER TYPES OF MODULATORS

Gaseous Messengers

In addition to its activation by cyclic nucleotides, the native olfactory CNG channel can be independently activated by NO in the form of nitrosonium (NO^{+}). This ion can interact with sulfhydryl groups. Consistent with this idea, the effect of NO was mimicked by SH-modifying reagents (Broillet and Firestein, 1996). The chemical reaction that leads to the formation of nitrosothiol has been shown to occur *in vivo* (Lander, 1997) thus, this chemical modification may play a role in modulating CNG

channels activity in olfactory transduction. Indeed, it has been demonstrated that the native olfactory CNG channel is activated by such a mechanism (Broillet and Firestein, 1996). The target site for S-nitrosylation is a cysteine residue present in the C-linker and conserved in the A1 and B1 subunits. The report by Berghard et al. (1996) of B1 subunits but not A1 subunits in the vomeronasal organ (results of *in situ* hybridisations) suggested the possibility of homomeric channels constituted by B1b subunits only. Broillet and Firestein (1997) tested this hypothesis and concluded that such channels exist, are not activated by cyclic-nucleotides but by NO, present common features with Ca^{2+}-activated channels and may play an important role *in vivo*. Indeed, an important role for NO was described in cone photoreceptors (Savchenko et al., 1997). CNG channels are numerous in cones synaptic terminals and endogenous NO was shown to modulate synapses between cones and horizontal cells in lizard retina by triggering neurotransmitter release. NO has been described as a retrograde messenger in brain (O'Dell et al., 1991; Schuman and Madison, 1994) and the discovery of CNG channels in hippocampus (Kingston et al., 1996; Bradley et al., 1997) and elsewhere in the central nervous system (Finn et al., 1996) raises the possibility of a mechanism involving in the brain the action of both NO and cGMP on CNG channels in order to modulate synaptic transmission. Another gaseous messenger, carbon monoxide (CO), was shown to act as a modulator of CNG channels action. Like NO, CO was shown to activate soluble guanylate cyclase (Brune and Ullrich, 1987; Furchgott and Jothianandan, 1991; Kharitonov et al., 1995), and was proposed to act on synaptic strength in hippocampus (Stevens and Wang, 1993; Zhuo et al., 1993). In addition a long-lasting form of odour adaptation dependent on a CO/cGMP messenger system was described (Zufall and Leinders-Zufall, 1997) but the way CO is acting is not discussed in this paper.

Diacylglycerol

Diacylglycerol (DAG) analogous have been found to allosterically interfere with the rod cGMP-activated channel opening by reducing the apparent affinity of the channel for its ligand and by lowering the maximum current amplitude (Gordon et al., 1995). The action of DAG has been shown to be phosphorylation-independent. The olfactory CNG channel is not inhibited.

ATP and GTP

The light response is affected by both ATP and GTP *in vivo*. In rods, ATP has been shown to increase the response of cGMP-gated channels whereas GTP can abolish the action of ATP (Filatov et al., 1989). The action of ATP in cones was shown to change in function of pH variation (ATP enhances the response of cGMP-gated channels at low pH and decreases their response at high pH). The mechanism of modulation by ATP/GTP seems to consist in a change in apparent agonist affinity of CNG channels (Watanabe and Shen, 1997).

Nickel

It has been shown that Ni^{2+} enhances, at low concentrations, bovine rod CNG channel responses but inhibits the olfactory CNG channel through the binding of two different histidines present respectively in the rod CNG channel (H420) and in the olfactory CNG channel (H396) (Gordon and Zagotta, 1995). These histidine residues are located in the C-linker, a region found to play a role in coupling of ligand binding to channel gating. Ni^{2+} binding affects the conformational changes that lead to stabilisation of the open state in the cGMP-activated channel whereas it stabilises the closed state in the olfactory channel. At position 420 an histidine is effectively present in the A1 subunits of the bovine and human rod CNG channels (Kaupp et al., 1989; Dhallan et al., 1992) but an asparagine is present in the sequences of both mouse and rat homologues (Pittler et al., 1992; Barnstable and Wei, 1995) so that any physiological relevance of the interaction of Ni^{2+} with histidines is controversial.

Divalent Cations

Under physiological conditions, with photoreceptor membrane potential around -45 mV, rod CNG channels are always blocked by external divalent cations (Mg^{2+}, Co^{2+}, Cd^{2+}, Ca^{2+}). Blockade by divalent cations occurs on both external and internal sites which are located in the pore of CNG channels. In particular, a highly conserved glutamate residue has been identified as the binding site for external divalent cations in rod, cone and olfactory CNG channels (Root and MacKinnon, 1993; Eismann et al., 1994; Kramer and Siegelbaum, 1992; Kleene, 1995; Frings et al., 1995; Biel et al.,

1995; Haynes, 1995). It is thought that the carboxyl group is important to form a high affinity binding site.

External Protons

A mechanism similar to the one that regulates the block by divalent cations involves external protons. In the catfish olfactory neurons, pH titration combined with mutagenesis studies of Glu 333 (the conserved glutamate involved in the block by divalent cations) have suggested that this pore residue is also involved in protons binding and subsequent channel block (Tanaka, 1993; Root and MacKinnon, 1994). In some cases, protons have been shown to activate CNG channels: protonation of D604 in the rod CNG channel may enhance the interaction between the binding site and the cyclic-nucleotide triggering the allosteric changes that lead to channel opening (Varnum et al., 1995; Gordon et al., 1996).

Pseudechetoxin

Recently, a peptide blocker that can be used as a pharmacological tool has been extracted from the venom of the australian king brown snake and purified (Brown et al., 1999). This protein (PsTX, 24 kDa) blocks the cGMP dependent current when it was applied to the extracellular face of membrane if the patches contain the A2 subunit of the rat olfactory CNG channel. Block was independent of voltage and required only a single molecule of toxin. PsTx also blocked CNG channels containing the bovine rod A1 subunit with high affinity, but it was less effective on the heteromeric version of the rod channel.

Tetracaine

Tetracaine is a local anaesthetic which has been shown to block the bovine rod but not the rat olfactory CNG channel (Fodor et al., 1997). Studies of chimeras failed in identifying a specific sequence of interaction with tetracaine. The mechanism of this blockade is state-dependent because tetracaine binds more tightly to the closed channel. A single tetracaine molecule is enough to observe the block. In addition, this block has been shown to be voltage-dependent. A model for tetracaine block has been proposed: interactions between tetracaine and the inner mouth of the pore could lead to tighter

binding to closed channels and stabilisation of the closed conformation. An increase in the width of the pore when the channel opens could lead to the disruption of these interactions. Alternatively, repulsion of the pore blocker by cations permeating through the open channel pore has been envisaged.

Dequalinium

This is an organic divalent cation (Rosenbaum et al., 2003), in particular, it is a bis-quinolinium blocker. This compound is a high affinity bocker of CNGA1 channels and exhibits the following characteristics: the block occurs is a state-indipendent fashion; it is voltage dependent and at a single channel level the appearance of long closed state are observed with no change in unitary conductance. Moreover, dequalinium exhibits higher affinity for block from the intracellular side of CNGA1 channels compared with the outside.

Calcium Channels Blockers

L-*cis*-diltiazem, the inactive isomer of a calcium channel blocker was the first blocker of CNG channels to be discovered (Koch and Kaupp, 1985). In the rod channel, the efficiency of this block depends on the B1 subunit (Chen et al., 1993). It blocks the CNG channels of rods, cones and olfactory neurons in a voltage-dependent fashon (Haynes, 1992; Mclathee, 1992 and Picones and Korenbrot, 1992). Pimozide blocks the rod cGMP-gated channel (Nicol, 1993) whereas D-600 and nifedipine act on the olfactory CNG channels (Frings et al., 1992; Zufall and Firestein, 1993)

Nicotine

Nicotine has been reported to stabilise the closed conformation of the rod CNG channel (McGeoch et al., 1995).

Polyamines

Polyamines have been shown to block the pore of inward rectifier K^+ channels as well as some glutamate-gated channels. They have thus been tested also on CNG channels and in particular on the retinal cGMP-gated channel which was shown to be blocked by polyamines from both sides of the membrane. Because polyamines are constituents of

both intra- and extra-cellular media, they may play a physiological role of modulation of CNG channels, for example as suppressor of the noise in the phototransduction process (Lu and Ding, 1999).

MATERIAL AND METHODS

In order to study the relationship between structure and function of the CNBD (Cyclic Nucleotide Binding Domain), the P region and S6 transmembrane domain of CNG (Cyclic Nucleotide Gated) channels, I have used techniques of molecular biology, electrophysiology and homology modelling. The corresponding protocols are given in the next sections. In particular I constructed several mutants of the CNGA1 ion channel from bovine rods. All the constructed mutants are listed in the section 1.1 of this chapter.

1-The mutations

1.1-THE C-HELIX OF CNG CHANNELS

The technique of substituted-cysteine accessibility method (SCAM) was applied to the putative C-helix of the CNBD, present into the A1 subunit of the CNG from bovine rods (CNGA1), in order to determine its structure and its movements. Cysteines were introduced, one by one, in the stretch from Leu583 to Asn610 forming the putative C-helix (Fig.8).

For the SCAM analysis the following series of mutants were designed:

N610C, L607C, L606C, G605C, D604C, K603C, M602C, L601C, I600C, Q599C, K598C, G597C, K596C, E595C, E594C, L593C, M592C, G591C, K590C, A589C, D588C, P587C, Y586C, E585C, T584C and L583C.

1.2-THE S6 OF CNG CHANNELS AND THE PORE REGION

The SCAM method was used also to study the movement of the S6 transmembrane domain and the pore region during the gating of channel. In particular, cysteines were introduced in the stretch from position Phe375 to His406 and His420, and in positions Val348, Leu351,

Thr359, Thr360, Ile361 (named also: Val4, Leu7, Thr15, Thr16, Ile17 as in Becchetti et al., 1999 and Liu and Siegelbaum, 2000), respectively (Fig.8).

S6 transmembrane domain:

F375C, V376C, V377C, A378C, D379C, F380C, L381C, I382C, G383C, V384C, L385C, I386C, F387C, A388C, T389C, I390C, V391C, G392C, N393C, I394C, G395C, S396C, M397C, I398C, S399C, N400C, M401C, N402C, A403C, A404C, R405C, A406C, K416C, Q417C and H420C.

P-region:

V4C, L7C, T15C, T16C and I17C.

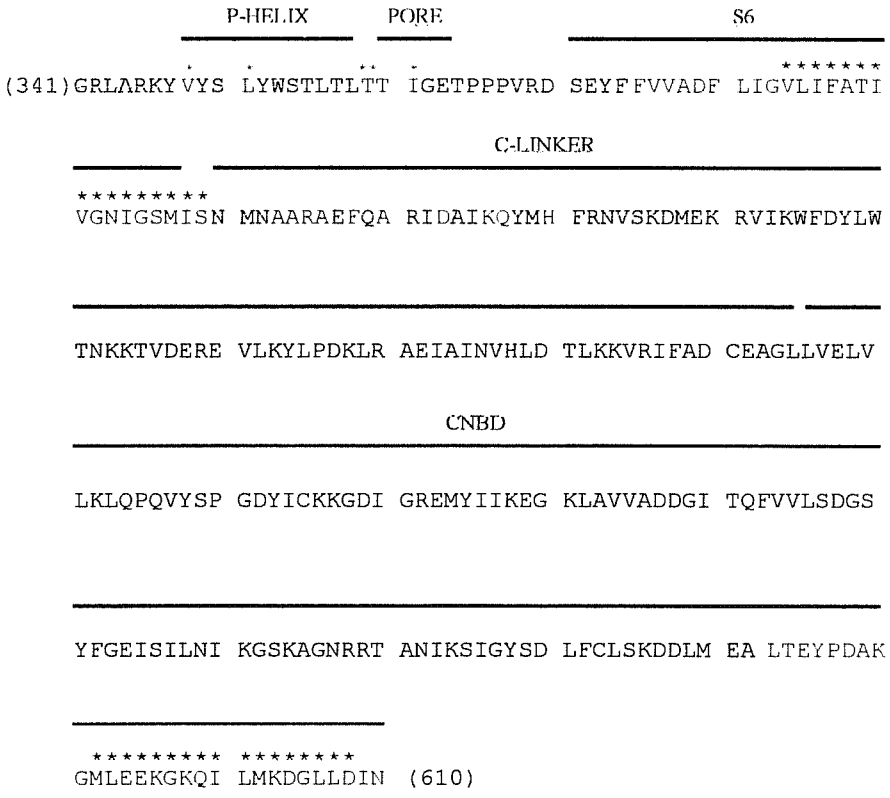

Fig.8: *Partial amino-acidic sequence of CNGA1. In red are mark the mutated aminoacid residues. The blue stars show the aminoacidic residues studied also from other groups.*

2-Molecular biology

2.1-DNA MATERIAL

The cDNA encoding for the A1 subunit of the bovine rod cyclic nucleotide gated channel (CNGA1) (Kaupp et al., 1989) was provided by the laboratory of Prof. W.N. Zagotta and by the laboratory of Prof. U.B. Kaupp, cloned into pGEM-3Z (Pharmacia, Uppsala, Sweden) modified vector named pGEM-HE. The pGEM-HecG (stands for pGEM-HE containing the cGMP-gated A1 subunit) plasmid was initially transformed into E. Coli DH5αF' competent cells following a classical $CaCl_2$ method (Sambrook et al., 1989). Medium scale of DNA preparation was obtained using the Plasmid Midi Kit (Quiagen GmbH, Hilden, Germany).

2.2-SITE-DIRECTED MUTAGENESIS

All the mutants were designed using the QuickChange™ Site-Directed Mutagenesis Method (Stratagene, La Jolla, CA). With this procedure, mutations can be obtained in a shorter time than with the classical method and with a mutagenesis efficiency of 33% (the analysis of 3 putative clones only always allowed to identify a real positive clone). The efficiency of mutagenesis calculated for the pWhitscript™ positive control provided in the kit was of 62%.

The basic procedure is summarised in Fig.9. The QuickChange™ Site-Directed Mutagenesis Method uses the Pfu DNA polymerase, wich replicates both strands of the supercoiled plasmid DNA template with a higher fidelity than the Taq polymerase (estimated error rates are 1.3×10^{-6} and 8×10^{-6} respectively) and avoids the linerization step required with the classical method. The two primers are designed to be complementary to each strand of the vector (thus overlapping) and to both contain the desired mutation; they should have a length of 25-45 pb, a minimum GC content of 40% and a recommended melting temperature of 78°C (although good results with T_m just above 73°C have also been experienced). A PCR reaction is performed to extend the primers, and the result is a circular mutated plasmid containing nicks. The parental DNA template, which doesn't

contain the mutation, is dam methylated, like most DNAs extracted from E. Coli strains, and can be recognised and digested by DpnI, contrarily to the newly synthesised DNA (DpnI is an endonuclease which targets the methylated or hemimethylated sequence 5'-$G^{m6}ATC$-3'). The nicked, mutated DNA vector is then transformed by heat-shock into Epicurian Coli XL1-Blue supercompetent cells, which repair the nicks.

The reaction mix for the QuickChange was prepared using 50 ng of the pGEM-HE plasmid containing the cDNA of the CNG channel and following the instructions of the manufacturer.

All the pipetting steps were done using small 10 µl ART pipet tips with filter, which are guaranteed sterile and Rnase/Dnase free by the manufacture (Molecular Bio-Products Inc., San Diego, CA). Thin-Wall tubes (Stratagene) were used for each reaction sample. The cyclic reactions were performed by a PTC-100 thermo-cycler (MJ Research) using the following parameters: 95°C, 30 s (denaturation step) followed by either 12 cycles (for single point mutaions) or 16 cycles (for 2-3 bases change) at 95°C 30 s; 55°C 1 min; 68°C 10min (2 min/kb plasmid length). After the cycling the reactions were cooled on ice and then treated with DpnI to digest the parental DNA. DpnI-treated samples were transformed into stratagene XL-1 Bue supercompetent cells using a classical $CaCl_2$ method with 42°C heat shock of 45 s. The transformation reactions were plated on LB+ampicillin Petri dishes. For each putative mutant, 4 colonies were picked up from the plates and grown for making DNA minipreps, which were obtained using the Quiagen PLASMID Mini Kit (Quiagen).

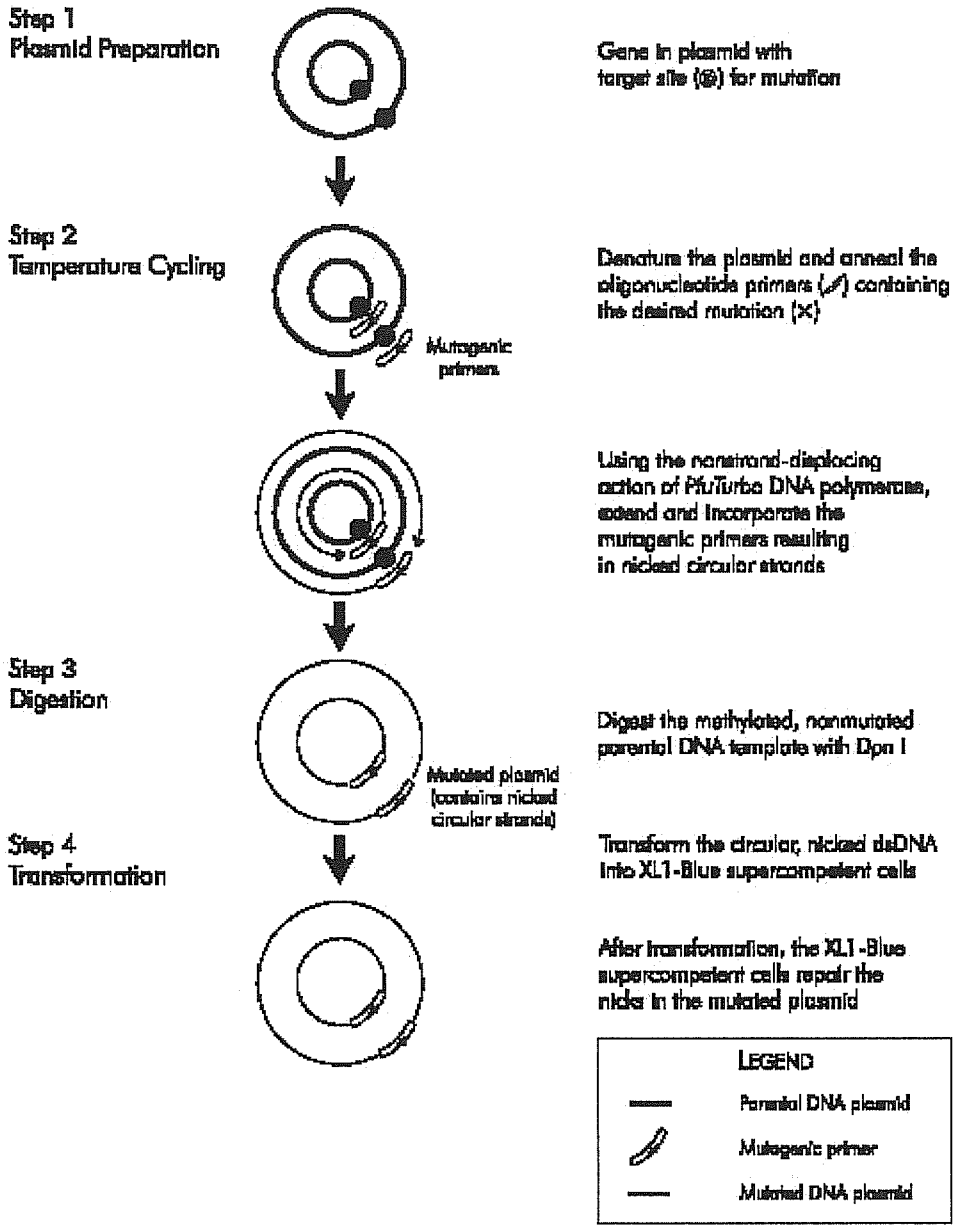

Fig.9: *QuickChange™ Site-Directed Mutagenesis Method (Stratagene, La Jolla, CA): overview of the experimental protocol.*

2.3-MUTATION ANALYSIS

The putative mutant DNAs obtained through the QuickChange™ Site-Directed Mutagenesis Method were analyse with automatic DNA sequencing (LI-COR, 4000L type; LI-COR, Lincoln, NE). In this way I sequenced completely all of the mutants produced, thus giving more relevance to my studies by gaining confidence in the real nature of the mutants and their electrophysiological characterisation. 1 μg of each clone was sequenced using the SequiTerm EXCEL II Long-Read DNA sequencing Kit-LC (Epicentre Technologies, Madison, WI) with 1 pmol of primer, as follows.

To sequence the A1 subunit of the bovine rod cyclic nucleotide-gated channel, the primers needed were:

T7	5' TAA TAC GAC TCA CTA TAC GG 3'
CNG-147	5' GAG GAA GAG AAG AAG GAA GTC 3'
CNG-313	5' GCG TGT GTG TAC TTC TCT ATT TCC 3'
CNG-481	5' TGT GAA GCT GGT CTG TTG GTG 3'
CNG-reverse	5' ATT CGG GTG TTC TTG AGG C 3'

2.4-RNA SYNTHESIS

The RNA of wild type (wt) and mutant channels was syntetized starting from 5-10 μg of DNA, and than injected in the cytoplasm of *Xenopus laevis* oocytes.

DNA preparing with midipreps was linearized by NheI (New England Bolabs), extracted, precipitated, washed and finally resuspended in 50 μl DEPC-treated ddH_20. All of steps following this one were carried out in Rnase-free conditions.

The DNA was then transcribed in vitro using the T7 RNA polymerase and the mCAP RNA Capping Kit (Stratagene). The remaining not transcribed DNA was digested by DNaseI, and the RNA was extracted with a kit for to purified the RNA (Stratagene, RNA purification kit). RNAs were finally resuspended in the DEPC-treated dH_20, and divided into aliquots suitable for microinjection (the finally concentration of each RNA was about 1 μg/μl).

3-Electophysiology

The electrophysiological experiments used in this thesis consisted in measuring the currents activated by cGMP in wt and mutant CNG channels. The channels were expressed in *Xenopus laevis* oocytes and the current recorded with excised patches in inside-out configuration.

3.1-CHEMICALS

The MTS compounds were purchased from Toronto Research chemicals (Ontario, Canada). All the other chemicals were purchased from Sigma (St. Louis, MO, USA).

3.2-ISOLATION AND PREPARATION OF *XENOPUS LAEVIS* OOCYTES

Xenopus laevis frogs were anaesthetised by immersion in a 0.2% aqueous solution of tricaine (methanesulphonate salt of 3-aminobenzoic acid ethyl esther) for about half an hour. The anaesthetised animal was put on its back on box of ice and a small incision of about 1 cm was performed with a scalpel laterally on the abdomen. Once the skin and the underneath abdominal muscles were cut through, the ovarian lobes became visible. The follicles (oocytes and follicle cells) were surgically removed from the ovary and placed in Barth's solution (in mM: 88 NaCl, 1 KCl, 0.82 $MgCl_2$, 0.33 $Ca(NO_3)_2$, 0.41 $CaCl_2$, 2.4 $NaHCO_3$, 5 TRIS-HCl, buffered to pH 7.4 with NaOH). Follicles were then separated in small groups containing about ten oocytes and incubated for 1 hour at 19°C in Barth's solution without calcium but supplemented with 1 mg/ml of collagenase. After the collagenase treatment, oocytes were washed extensively with Barth's solution and the residual follicle cells were removed manually with the forceps. At this step the healthiest defolliculated oocytes presenting two clearly delineated hemispheres were selected, and incubated in Barth's solution supplemented with gentamicine (50 μg/ml), during injection and incubation, until patch-clamp experiments were performed.

Injection needles of about 10 μm of tip diameter were made from borosilicate glass capillaries (World Precision Instrument, Sarasota, FL, USA) by using a horizontal puller (BB-CH-PC, Mecanex S.A., Geneva, Switzerland). Oocytes were injected under a

binocular microscope at low magnification (Olympus, Japan) using a manual microinjector (CellTram Air, Eppendorf, Germany). About 100-200 nl of capped RNA (at approximately 1 μg/μl in DEPC-treated dH_2O) were injected in each oocyte. Cells were then incubated at 19°C for 2-6 days. Just prior to patch-clamping, the vitelline membrane was removed from the oocytes under visual control in a hyperosmotic medium. During the experiments, oocytes were maintained in Ringer solution (in mM: 110 NaCl, 2.5 KCl, 1 $CaCl_2$, 10 HEPES-NaOH, buffered to ph 7.4 with NaOH).

3.3-RECORDING APPARATUS

cGMP-gated current from excised inside-out patches (Hamil et al., 1981) were recorded with a patch-clamp amplifier (Axopatch 200B, Axon Instruments Inc., Foster City, CA, USA) 1-5 days after RNA injection, at room temperature (20-22°C). The perfusion system was a s previously described (Sesti et al., 1995) and allowed complete solution changing within 1 s. Borosilicate glass pipettes had resistances of 3-5 MΩ in symmetrical standard solution. The current traces obtained in the inside-out patch-clamp configuration, soon after patch excision, used for obtaining steady-state current-voltage relations, were the difference between currents in the presence and in the absence of 1 mM cGMP. The patch potential was stepped up from 0 to +60 mV and from 0 to –60mV. Current were low-pass filtered at 1 kHz and acquired on-line (at 5 kHz). Macroscopic current were digitised from PCM/VCR or DAT tape (Sony PCM-601ES and Panasonic NV-F70 HQ respectively) at 50 Hz. pClamp hardware and software (Axon Instruments), Origin software (Microcal Software, Inc.) and SigmaPlot software (Jandel Scientific) were used for the data acquisition and analysis.

3.4-ANALYSIS OF CYSTEINE MUTANTS PROPERTIES

Macroscopic currents were analysed with pClamp8, Origin and SigmaPlot software. The effect of MTS compounds on wt and mutated CNG channels was calculated from current-voltage relations. The steady-state current amplitude at a given potential and in presence of MTS reagents (I_{MTS}) was normalised to the current in the absence of MTS (I_0) at the same potential.

For cGMP dose response experiments, the theoretical curve was a Hill equation of the form:

$$I/I_{MAX} = \{1 + (K_d /cGMP])^n\}^{-1}$$

Where I_{MAX} is the current produced by 1 mM cGMP, n is the Hill coefficient, K_d the concentration of cGMP which yields 50% of the maximal current.

Data points are usually given as mean values ± standard error (SE) of the mean (all point were obtained from at least four or five patches excised from at least two different oocytes).

3.5-SOLUTIONS

The patch pipette was filled with (in mM): 110 NaCl, 10 HEPES, 0.2 EDTA ("standard solution" buffered at pH 7.4 with tetramethylammonium hydroxide TMAOH). The cytoplasmic face of the excised patches was perfused with the same solution, supplemented or not with 1 mM cGMP and different reagents.

3.6-APPLICATION OF SULPHYDRYL-SPECIFIC REAGENTS

Sulfhydryl-specific reagents are useful tools for studying the proximity of specific regions in ion channels. Here, to study the conformational changes between the open and closed state of CNG channels, we analysed the effects of sulfhydryl-specific reagents on mutant channel activity (Cd^{2+}, MTSET, MTSEA, MTSES and CuP) in the presence and in the absence of saturating concentration of cGMP. In the presence of 1 mM cGMP the open probability is close to 1 (Bucossi et al., 1997) meaning that the channels are most frequently in the liganded and open state. Therefore, sulfhydryl-specific reagents were applied in the presence and in the absence of 1 mM cGMP. The Cd^{2+} effect was tested by perfusing the intracellular side of the patch with a standard solution devoid of EDTA (to avoid partial Cd^{2+} chelation; Gordon and Zagotta, 1995) supplemented with 1 mM cGMP and/or 100 μM $CdCl_2$ for 5 min. The only effect of the EDTA withdrawal is the activation of a background offset current due to the well-known presence of Ca^{2+}-dependent Cl^- channels in *Xenopus* oocytes (Miledi and Parker, 1984). This current, however, reached the steady state soon after the change of solution, as reported also in previous work (Becchetti and Roncaglia, 2000), therefore, no Cl^- channel blockers were used during these

experiments. Different concentrations of CuP (1μM and 1 mM) were applied in presence and in the absence of cyclic nucleotide and the patches were exposed for different times. The effect of MTS compounds was tested at a concentration of 2.5 mM and 10 mM, in standard solution with EDTA and also without EDTA, as previously described (Becchetti et al., 1999). To study the effect of the probe in the closed state, patches were exposed to the appropriate reagent for 5 min, in the absence of cGMP. After washout, cGMP was applied to measure the residual current. To study the effect in the open state, sulfhydryl-specific reagents were applied in the presence of 1 mM cGMP. All effects of sulfhydryl reagents on channel activity described in this study were obtained after washing-out reagents and in the presence of a steady cGMP-gated current, for at least 10 min. All currents were measured at the steady state, i.e. after the effect of sulfhydryl reagents had developed fully.

4-Homology modelling

The observation that proteins evolving from a common ancestor, maintaining similar core 3D structures, is an important base for the comparative modelling. In other words, the core structures of two homologous (evolutionary related) proteins are expected to be similar. Comparative modelling is then used to construct structural models of proteins (targets) that are homologous to other proteins whose 3D structure is known (templates).

Marco Punta and Alejandro Giorgetti perform this part of the project in SISSA. under the supervision of Prof. Vincent Torre.

When, one or more templates have been detected a comparative structural model of the target can be constructed. The accuracy of this model will depend on many factors, from the choice of the most appropriate template to the sequence alignment procedures adopted. The modelling procedure consists of four principal steps: template recognition, target-template sequence alignment, model building and model evaluation. In particular:

1) the first step in comparative modelling is the identification of protein structures related to the target sequence, proteins that may be regarded as possible templates. The templates are selected from protein sequence databases (Barker et al., 1998), GenBank

(Benson et al., 1998) or TrEMBL/SWISS-PROT (Bairoch and Apweiler, 1999). Several methods may be of help in selecting a template from database and the simplest criterion for the detection of homology between two proteins is the pairwise sequence identity (SI). When SI is greater than 30% the homology between two proteins are ensured. The most widely used programs for the sequence comparison include FASTA (Perason, 1998) and BLAST (Altschul et al., 1990).

2) the second step is the target/template sequence alignment in which the target sequence is aligned to all the potential template structures. The quality of the alignment is the single most important factor determining the accuracy of the 3D model. In the end the alignment procedure may provide with more than one possible alignment and the decision of the most appropriate one is often taken by directly evaluating the corresponding model on the basis of its structural properties and of the available experimental data.
3) there are two different possibilities for building the model, in the first case the model is assembled from a small number of rigid bodies obtained from the aligned protein structures. The protein is dissected into conserved region, variable loops that connect them and side-chains that decorates the backbone. In the second procedure, the target model is derived by minimising the violations of homology-derived restraints and stereo chemical restraints. The former is generally obtained by assuming that the distances, as well as other features, between the residues of the target are similar to those of the aligned template residues (topological equivalence of residues). The latter is obtained from a molecular mechanics force field and includes restraints on bond lengths, bond angles and non-bonded atom-atom contacts, for example. To build the models of the CNG channel domains Marco Punta and Alejandro Giorgetti. used MODELLER (Sali and Blundell, 1993) a program that implements modelling by satisfaction of spatial restrains.
4) the last step is the model evaluation; the main criteria for assessing the accuracy of a comparative model are the stereochemistry, the stability in terms of a potential energy function and the comparison with the available experimental data.

5-Effect of sulfhydryl reagents

In this section I summarise the characteristics of the reagents that were used to probe the CNBD, the pore region and S6 structure.

CADMIUM: this divalent cation (diameter of about 1 Å) is usually tetracoordinated and binds preferentially to cysteines, histidines and negatively charged residues. The distance between the Cα atoms of two cysteines binding to the same Cd^{2+} ion ranges between 4 and 9 Å (Kovetz et al., 1997; Ermler et al., 1998; Maroney, 1999).

COPPER PHENANTHROLINE: CuP is an oxidizing agent that favours disulfide bridge formation between neighbouring cysteines. The distance between the Cα of two cysteines forming a disulfide bond is between 4 and 6.5 Å (Srinvasan et al., 1990). Given the thermal fluctuations of the protein, the maximum distance between the Cα of two cysteines able to form a disulfide bond or to coordinate one Cd^{2+} ion can be estimated around 10 Å (Johnson and Zagotta, 2001; Careaga and Falke, 1992; Krovetz at al., 1997; Elmer et al., 1998). Thus, Cd^{2+} and CuP can be use to have a correct evaluation on the residue relative distance.

MTS COMPOUNDS: they are thiol specific reagents like MTSET, MTSEA and MTSES (trimethylammonium methanethiosulfonate, ethylammonium methanethiosulfonate and sulfonatoethyl methanethiosulfonate, respectively). In particular, in my experiments, I use the MTSET reagent to study the accessibility of residues that I have mutated to cysteines. This compound is a cylinder with a diameter of 5.8 Å and a height of 10 Å (Akabas et al., 1992) not able to cross the lipid bilayer and it is positively charged (Becchetti et al, 1999). In some cases I use also MTSEA and MTSES: the first one is a positively charged compound, able to cross the lipid bilayer (Becchetti et al, 1999), with a diameter of 4.8 Å and a Height of 10 Å (Akabas et al., 1992); the second one is a negatively charged compound with a diameter of 4.8 Å and a Height of 10 Å (Akabas et al., 1992).

These reagents react very rapidly and specifically with cysteine, in particular with the group SH- present in this amino acid and it form a covalent bond with only one thiol group.

RESULTS

In this chapter of my thesis, I describe the results obtained with the electrophysiological experiments regarding three different regions of CNGA1 channels. In particular, the C-helix of the cyclic nucleotide-binding domain, the S6 segment and the pore region. This chapter is subdivided in to two sections: the first dedicated to the CNBD and the second to the pore and the S6 region; before describe my experiments, I will present an introduction to previous results and structural suggestions concerning these channel regions.

1-Cyclic nucleotide binding domain

1.1-CYCLC NUCLEOTIDE BINDING DOMAIN: AN OVERVIEW

The CNB domain of the CNGA1 subunit shares about 20% sequence identity with other cyclic nucleotide (CN) binding proteins and in particular with two proteins for which a crystal structure is available: the catabolite gene activator protein (CAP) (Weber and Steitz, 1987; Passner et al., 2000) and the cAMP-dependent protein kinase (PKA) (Su et al., 1995). CAP is a homodimer, while PKA is a heterodimer, both having two CNB domains. The topography of CNB domain in CAP and PKA is common and consists of a short N-terminal alpha helix, referred to as the A helix, which precedes an eight-stranded antiparallel beta roll and is followed by two alpha helices, referred to as B and C-helix, respectively. Both proteins were crystallized in a complex with cAMP and the solution of their structure revealed that they bind cyclic nucleotides differently: cAMP is in *anti*-conformation in CAP whereas it is in *syn*-conformation in PKA. Contacts with ribofuranose are maintained in the two proteins but are different the interactions with purine ring: CAP binds purine through hydrogen bonds between the adenine atoms and polar residues on the C-helix, whereas PKA binds purine through interactions with hydrophobic and aromatic residues. Recently, a low-resolution (7 Å) structure of a A1/CAP chimera in complex with cAMP (in *anti*-conformation) has been obtained (Scott et al., 2001). The fusion protein conteined the CNB domain of the CNG channel and the DNA-binding domain of CAP. This structure suggests that the CNB domain of

CNG channels is composed of two dimers, and, each one of them has a folding very similar to that of CAP, in which the two C-helices are at the interface between the two monomers. This configuration, however, may be introduced in the chimera by the presence of the CAP DNA binding domain. For this reason, it is crucial to obtain direct evidence both for the existence of a helical structure in the C terminal part of the CNB domain of CNG channels (analogous to the C-helix of CAP) and for the dimeric folding of the whole domain.

In an important paper, Matulef and Zagotta, (2002) present work similar to that I present in my thesis and they conclude that although they cannot rule out the possibility that the binding domain of CNG channels come together as a 2-fold symmetric "dimer of dimers", the simplest explanation of their result is that the binding domain exhibits 4-fold symmetry.

Several electrophysiological experiments have shown that residues in the CNB domain move, following binding of cGMP in the binding pocket (Sun et al., 1996; Scott and Tanaka, 1998; Tibbs et al., 1998; Zong et al., 1998; Li and Lester, 1999; Matulef et al., 1999; Paoletti et al., 1999). These experiments, based on cysteine scanning mutagenesis, have shown that residues such as Gly597 and Cys505 have a different accessibility in the presence or in the absence of a saturating concentration of cGMP.

Many experimental observations were recently incorporated in a detailed molecular model (Punta et al., 2003) of the C-linker and of the CNB domain, based on homology modeling. In this model, the CNB domain is assumed to be a dimer, with a 3D structure similar to that of CAP. In the CNB domain model, there are two C terminal alpha helices, B and C

1.2-TEMPLATE AND SEQUENCE ALIGNMENT

CAP appears to be a suitable template for the modelling of the binding domain present in CNGA1. Indeed, a low resolution crystal structure of the chimera formed by the CNBD of CNGA1 and CAP DNA-binding domain suggests that this construct forms a dimer and that its folding is similar to that of CAP (Scott et al., 2001). Furthermore, the CAP structure has been successfully used to rationalise site-directed mutagenesis experiments in CNBD of CNGA1 (Gordon et al., 1996). In contrast, no available

experiments suggest that PKA is appropriate for modelling of the CNBD of CNGA1. Thus, only CAP is considered for modelling in this thesis.

The CNBD present in CAP is composed of an N-terminal α helix (A helix), followed by an eight-stranded anti parallel β roll and two more α helices (B and C helix) (Fig.10).

The alignment between CNGA1 and CAP is shown in Fig.11A. The alignment spans residues 495 to 588, comprising the CAP's β roll and B helix. The overall sequence identity is 20%; in particular, residues involved in the binding of cyclic nucleotides are highly conserved: CAP residues binding cAMP ribofuranose (G71, E72, R82 and S83) are either identical (G543, E544 and R559) or conserved (T560 for S83) in the CNBD of CNGA1. Two of these residues (R559 and T560) are known to bind cGMP in CNGA1 (Altenhofen et al., 1991; Varnum et al., 1995; Tibbs et al., 1998).

The predicted secondary structure elements (Rost and Sander, 1993) of the CNBD of CNGA1 agree fairly well with those of CAP (Fig.11B). In addition, the gaps of CNGA1 CNBD correctly fall into loop regions of the template (Fig.11B). These results justify the use of the CAP structure for comparative modelling of the CNBD of CNGA1.

To obtain a good alignment between the C-helix present in the binding domain of CAP and the C-helix located in the CNBD of CNGA1 is necessary to align the residues important for ligand affinity. These are D604 in CNGA1 (Varnum et al., 1995; Sundermann and Zagotta, 1999; Goulding et al., 1994; Gordon et al., 1996; Scott and Tanaka, 1998; Shapiro and Zagotta, 2000) and T127, S128 in CAP (Moore et al., 1996; Chang et al., 1998; Leu et al., 1999). The alignment of D604 to T127 (Fig.11C alignment I) or to S128 (Fig.11C alignment II) differ for the insertion of a one residue gap in the hinge region between the B and the C helix.

In order to discriminate between the two alignments Marco Punta under the supervision of Prof. Vincent Torre constructed a model and a simulation in the presence of cGMP. The model is approved by the site-directed mutagenesis, which has established the key role of R559, T560 and D604 for cGMP binding (Altenhofen et al., 1991; Varnum et al, 1995, Tibbs et al., 1998). In both complexes the ribofuranose moiety binds to the first two residues consistently with the experimental results, but the ligand interacts with D604 only in alignment I. Thus, only alignment I is consistent with the available experimental data and it is the only one considered in this thesis.

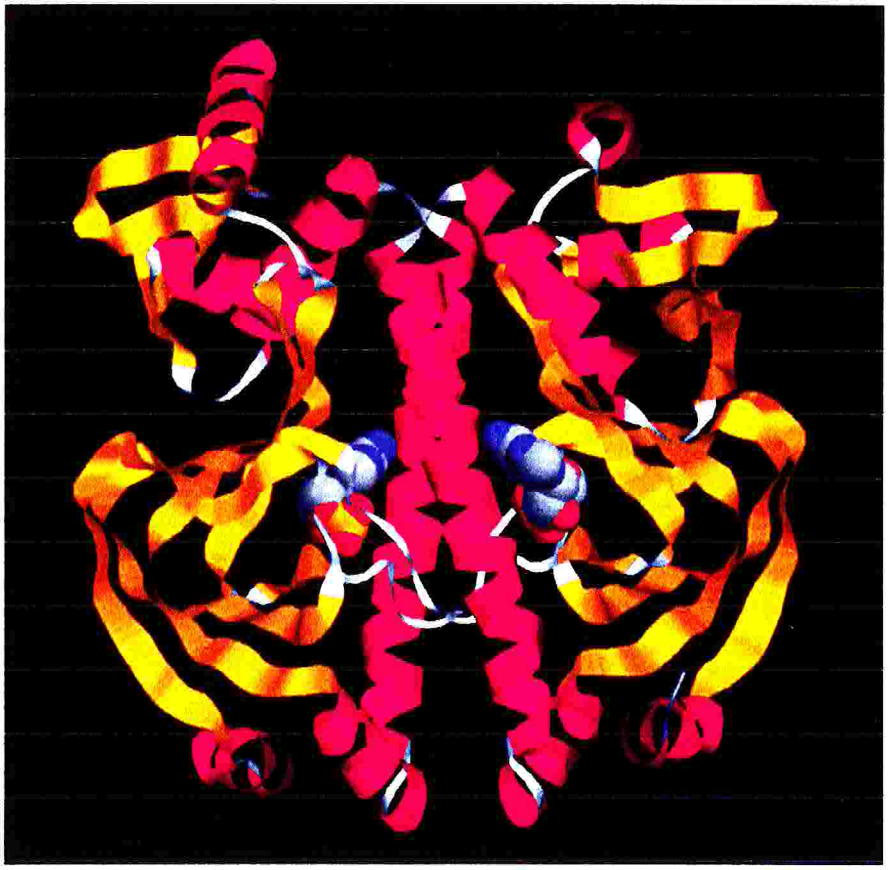

Fig.10: *CAP structure: in red the three alpha helices (A, B and C); in yellow the eight-stranded anti parallel beta roll; in blue the cAMP molecules (Kaupp and Seifert, 2002).*

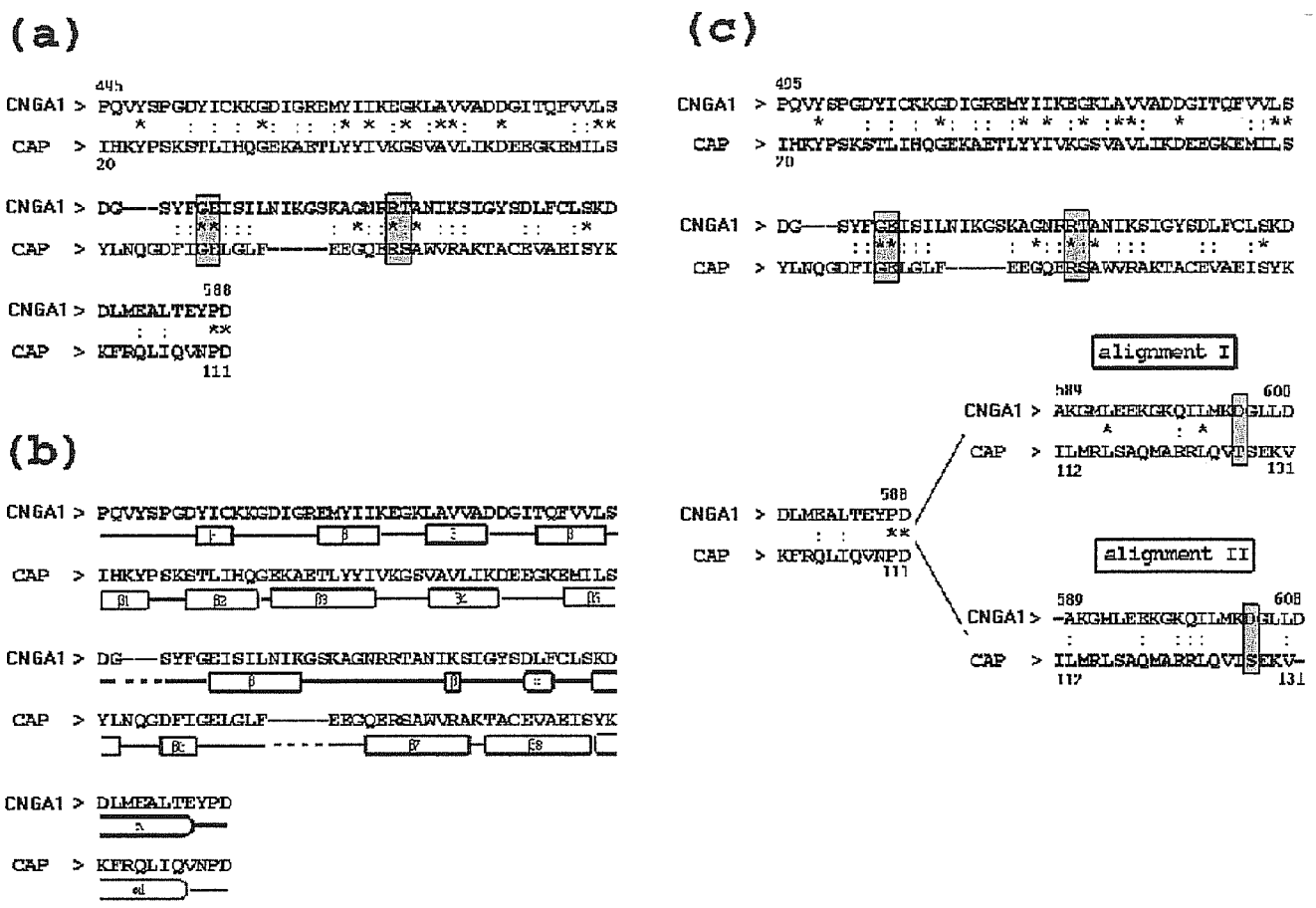

Fig.11: *CNGA1/CAP CNBD sequence alignment.* ***A:*** *alignment from residues 495 to 588 of CNGA1. Stars and colons mark identities and conservative substitutions, respectively. Shared boxes indicate the residues of CAP that bind to the ribofuranose moiety of cAMP.* ***B:*** *secondary structure elements either from X-ray structure of CAP (Weber and Steiz, 1987). Squared boxes represent β strands and round boxes represent α helices.* ***C:*** *Alignment including residues from 589 to 608. D604 (CNGA1) is paired either to T127 of CAP (I) or to S128 (II) (modified from Punta et al., 2003).*

1.3-EXPERIMENTAL RESULTS

All residues from Leu583 to Leu607 and Asn610 of the CNGA1 channel (Kaupp et al., 1989) were mutated, using as template the wt CNGA1 channel, one by one into a cysteine while the effect of sulfhydryl reagents such as MTSET, Cd^{2+} and CuP, was investigated. The construct that I use has all seven endogenous cysteines and it is not the cysteine free CNGA1 channel used by Zagotta and his collaborators (Matulef et al., 1999). The presence of these cysteines makes the channel under investigation close to the real CNG channel.

These mutant channels will be referred to as cysteine mutants, and the sensitivity of a given residue (such as Leu607) to sulfhydryl reagents implies the sensitivity of the

corresponding cysteine mutant (i.e., L607C). All results referred to in this thesis were obtained in at least five different patches excised from at least two different oocytes.

When a similar procedure was used to explore the pore topology of CNGA1 channels, MTSET and Cd^{2+} had very similar effects (Becchetti et al., 1999; Becchetti and Roncaglia, 2000), the only difference being that Cd^{2+} and not MTSET blocked mutant channel T360C. This difference was attributed to the larger dimension of MTSET, making some residues less accessible to MTSET. As will be shown in the present these, MTSET and Cd^{2+} act very differently on cysteine mutants in the CNB domain. Such a different blocking effect of MTSET and Cd^{2+} on cysteine mutants in the CNB domain cannot be uniquely ascribed to their different dimensions, but to their specific blocking mechanism and to the fact that cysteines introduced in the CNB domain are not necessarily in close contact like those introduced in the pore region. In fact, one molecule of MTSET forms a covalent bond with the thiol group of a single cysteine (Akabas et al., 1992; Karlin and Akabas, 1998), while one Cd^{2+} ion usually binds to two or even more cysteines (Benitah et al., 1996; Holmgren et al., 1998; Loussouarn et al., 2000). If the same effect produced by Cd^{2+} can be induced by applying the oxidizing agent CuP, known to enhance the formation of disulfide bonds between neighbouring cysteines (Glusker, 1991; Hastruph et al., 2001). The current modification caused by Cd^{2+} is very likely due to its binding to two cysteines in close contact.

The present analysis indicates that residues from Leu583 to Asn610 can be grouped in four distinct regions according to their Cd^{2+} and CuP sensitivity: residues in the C-terminal end (from Lys603 to Leu607) and in the N-terminal end (from Pro587 to Met592) are reduced by Cd^{2+} and CuP in the closed state but not in the open state; residues in the middle (from Leu593 to Met602) are reduced by Cd^{2+} both in the open and closed states, and residues downstream (from Leu583 to Pro587) are never blocked neither in the open nor in the closed state by Cd^{2+} and CuP.

Effect of sulfhydryl reagents and wt current

The wt - i.e., the CNGA1 - channel is not irreversibly reduced by 100 μM Cd^{2+} neither in the closed nor in the open state (using saturating concentration of cGMP) (Becchetti and Roncaglia, 2000). Similarly, the addition of 1 μM or 1 mM CuP to the bathing medium did not lead to any permanent decrease of the cGMP-gated current (data not

shown). This data is similar to that observed by Zagotta and collagorators using the cys-free CNG channel: in the open state with saturating concentration of cGMP they do not observe any modification of current amplitude; in subsaturating concentration of cGMP treatment with CuP drammatically increased the current and this potentiation was seen as a shift of the dose-response curve toward lower concentrations of cyclic-nucleotide (Gordon et al., 1997 and Matulef and Zagotta, 2002). As already shown (Sun et al., 1996; Becchetti et al., 1999; Becchetti and Roncaglia, 2000) MTSET does not reduce the wt in the open state, but in the closed state a decrease by about 20% of the cGMP-gated current is observed (fig.12). Therefore, current reduction by, Cd^{2+}, CuP and to some extent also by MTSET, can be attributed to an action on the exogenous introduced cysteines.

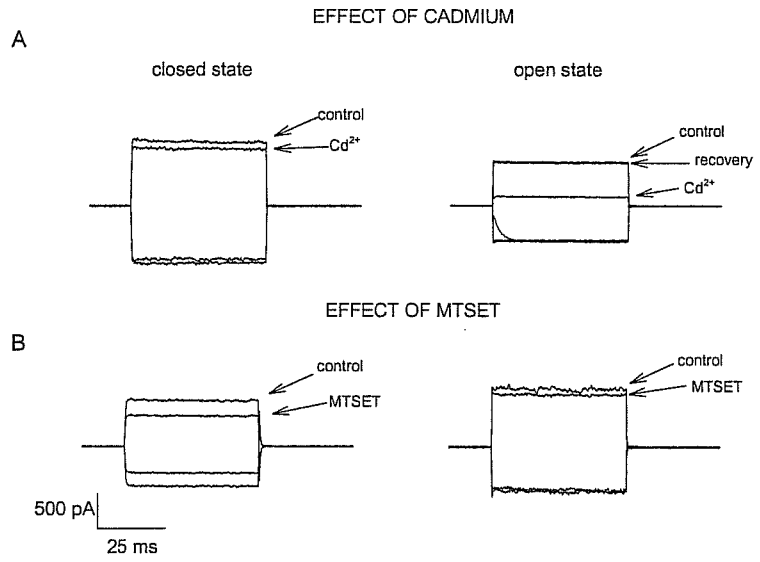

Fig.12: *The effect of 100 μM Cd^{2+} and 2.5mM MTSET on wt channel in the presence and in the absence of 1 mM cGMP. **A**: effect of 100 μM Cd^{2+} in the cGMP-gared current in the close (left) and in the open state (right). **B**: effect of 2.5 mM MTSET in the absence of cGMP (left) and in the presence of 1 mM cGMP (right). Voltage steps from 0 to +/- 60 mV. Each trace is the average of 10 individual trials. The cGMP-gated current was obtained as the difference of the current in the presence and in the absence of 1 mM cGMP. Control indicates the control current, Cd^{2+} the current after exposure for 5 min to 100 μM Cd^{2+}, MTSET the current after exposure for 5 min to 2.5 mM MTSET.*

Residues from Lys603 to Asn610

A cGMP-gated current was recorded in all cysteine mutants from Lys603 to Leu607 with the exception of mutant channel D604C. As shown in Figs.13 A and C in the case of mutant channels L607C and L606C, the application of Cd^{2+} and MTSET reduced the current to a different extent in the closed state, but not in the open state (see panels B and D).

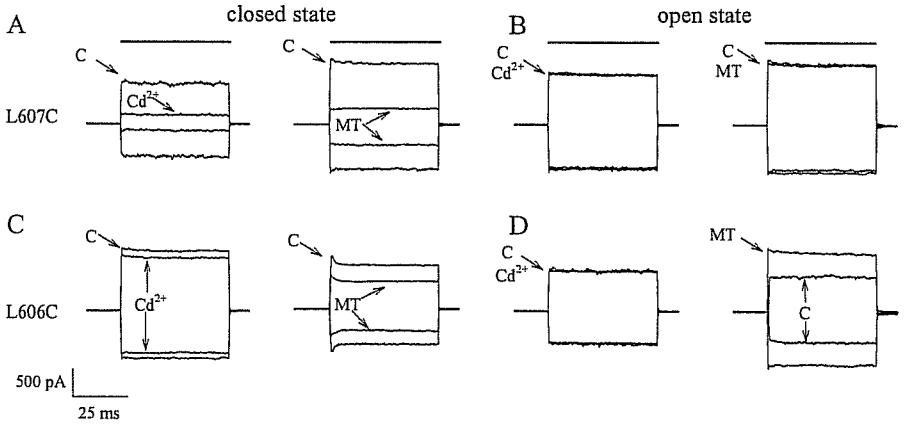

Fig.13: *The effect of Cd^{2+} and MTSET on mutant channels L607C and L606C in the presence and absence of cGMP.* ***A****: irreversible reduction of the cGMP-gated current caused by 100 μM Cd^{2+} (left) and 2.5 mM MTSET (right) added for 5 min in the absence of cGMP in mutant channel L607C.* ***B****: as in A, but with sulfhydryl reagents added in the presence of 1 mM cGMP.* ***C****: as in A, but for mutant channel L606C.* ***D****: as in C, but in the presence of 1 mM cGMP. In A, B, C and D voltage steps from 0 to +/- 60 mV. Each trace is the average of 10 individual trials. The cGMP-gated current was obtained as the difference of the current in the presence and in the absence of 1 mM cGMP. The solid horizontal lines over current traces indicate the time of the voltage command. C indicates the control current, Cd^{2+} the current after exposure for 5 min to 100 μM Cd^{2+}, MT the current after exposure for 5 min to 2.5 mM MTSET.*

The data of Fig.14 show that in the closed state the current of mutant channels L607C and G605C were powerfully decreased, by 83±2.4% and 88±3% respectively, but the current of mutant channels L606C and K603C were decrease only by 18.6±2.9 and 19.3±2.3% respectively. None of these mutant channels were permanently blocked by Cd^{2+} in the open state, as shown in Figs. 13 B, D and 14.

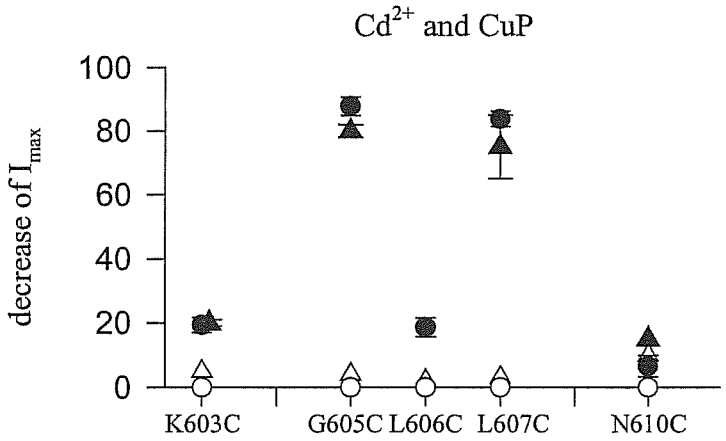

Fig.14: Percentage of 100 μM Cd^{2+} and 1□ μM CuP irreversible current reduction in the absence of cGMP (closed circles for Cd^{2+} and closed triangles for CuP) and in the presence of 1 mM cGMP (open circles for Cd^{2+} and open triangles for CuP) for cysteine mutants from Lys603 to Leu607. Error bars indicate the standard deviation. Each point was obtained from at least four patches excised from at least two different injected oocytes.

MTSET applied in the closed state decreased the current in mutant channel L607C by 77.5±2.5% and by about 30±7% and 23%±2% in mutant channels G605C and L606C respectively, but slightly potentiated mutant channel K603C. When MTSET was applied in the open state no current decrease was observed, like in the wt channel, but in the case of mutant channels L606C and K603C a potentiation of about 30% was observed (Fig.15). Similar results were obtained when the smaller sulfhydryl reagent MTSEA was used (data not shown).

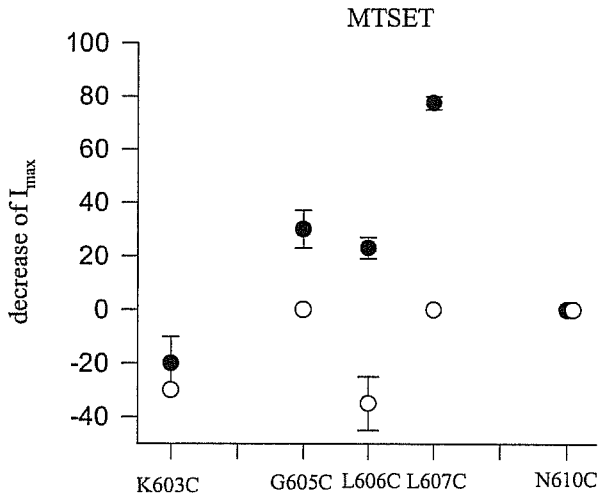

***Fig.15**: Percentage of 2.5mM MTSET irreversible current reduction in the absence of cGMP (closed circles) and in the presence of 1 mM cGMP (open circles) for cysteine mutants from Lys603 to Leu607. Error bars indicate the standard deviation. Each point was obtained from at least four patches excised from at least two different injected oocytes.*

The addition of 1 μM CuP to the bathing medium in the presence of 1 mM cGMP for 2 min had only a weak effect on the cGMP gated current in mutant channels G605C and K603C: the induced irreversible current reduction was at most 10% (see Fig.14). In the absence of cGMP, exposure to 1 μM CuP for 2 min decrease the cGMP gated current in mutant channels G605C by 80±4% and L607C by 75±25%. The decrease induced by the exposure of 1 μM CuP for 2 min was very similar to that caused by the exposure of 1 mM CuP for just 10 s (see Fig.18 in the case of mutant channel I600C). Also Asn610 was mutated into a cysteine and the mutant channel N610C was not reduced by any of the test sulfhydryl reagents neither in the open nor in the closed state.

Residues from Leu593 to Met602

Cysteine mutants from Leu593 to Met602 had a different sensitivity to Cd^{2+}: the current was decreased also in the open state. As shown in Fig.16 mutant channels L601C (A and B) and I600C (C and D) are powerfully reduced by 100 μM Cd^{2+} both in the closed (A and C) and in the open state (B and D).

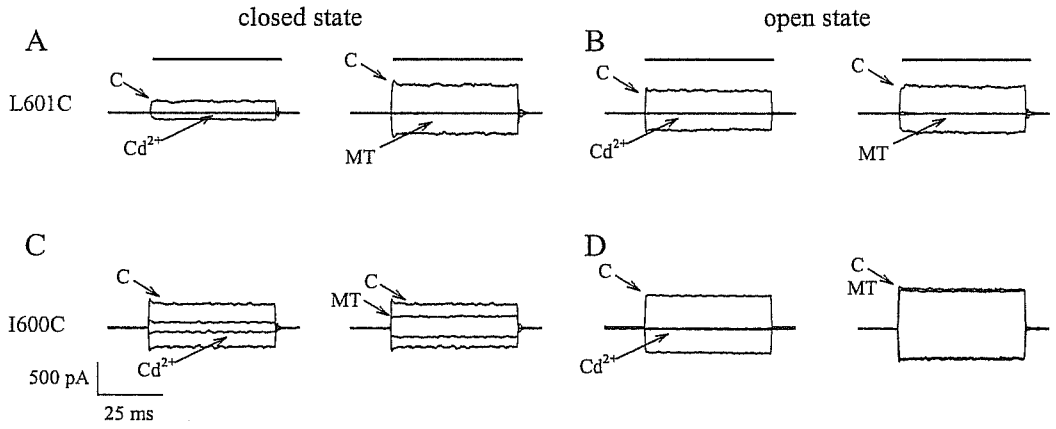

Fig.16: *The effect of Cd^{2+} and MTSET on mutant channels L601C and I600C in the presence and absence of cGMP. **A**: irreversible reduction of the cGMP gated current caused by 100 μM Cd^{2+} (left) and 2.5 mM MTSET (right) added for 5 min in the absence of cGMP in mutant channel L601C. **B**: as in A, but with sulfhydryl reagents added in the presence of 1 mM cGMP. **C**: as in A, but for mutant channel I600C. **D**: as in C, but in the presence of 1 mM cGMP. In A, B, C and D voltage steps are as in Fig. 13.*

The effect of MTSET was rather different: it significantly reduced the current of mutant channel L601C both in the open and in the closed state, while the current of mutant channel G597C was reduced only in the closed state and not in the open state (Matulef et al., 1999). This current reduction was almost complete, i.e., close to 100%. Current reduction induced by MTSET on the other cysteine mutants is reported in Fig.17. MTSET in the open state potentiated mutant channels M602C and Q599C. In the closed state MTSET reduced the current of mutant channels M602C, L601C, I600C, G597C and E594C by 35±5%, 100%, 55±5 %, 100% and 55±2%.

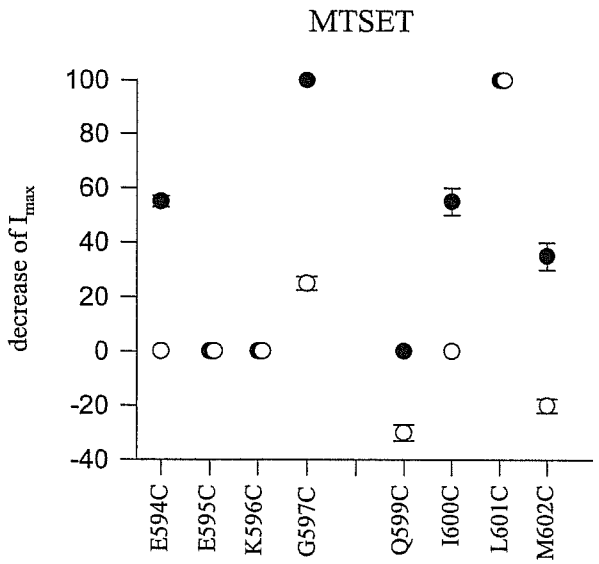

Fig.17: Percentage of 2.5 mM MTSET irreversible currrent reduction in the absence of cGMP (closed circles) and in the presence of 1 mM cGMP (open circles) for cysteine mutants from GLU594 to MET602.

The small effect of MTSET on most of these cysteine mutants, illustrated in Fig.17, does not imply the inaccessibility of these residues to MTSET. As shown in Fig.18, when mutant channels E595C and I600C are first exposed to MTSET in the open state and then exposed to Cd^{2+}, a significantly lower current decrease is observed: the current decrease by Cd^{2+} in mutant channels E595C and I600C in the open state is from 50% and 100% to 10% and 58±4% respectively by MTSET pre-treatment. This pre-treatment of MTSET in the closed and open state reduced the effect induced by Cd^{2+} and by the oxidizing agent CuP in mutant channels I600C, Q599C, K596 and E595, but not in mutant channel E594C. Therefore residues Leu601, Ile600C, Gln599, Arg596 and Glu595 are accessible to MTSET both in the open and closed states.

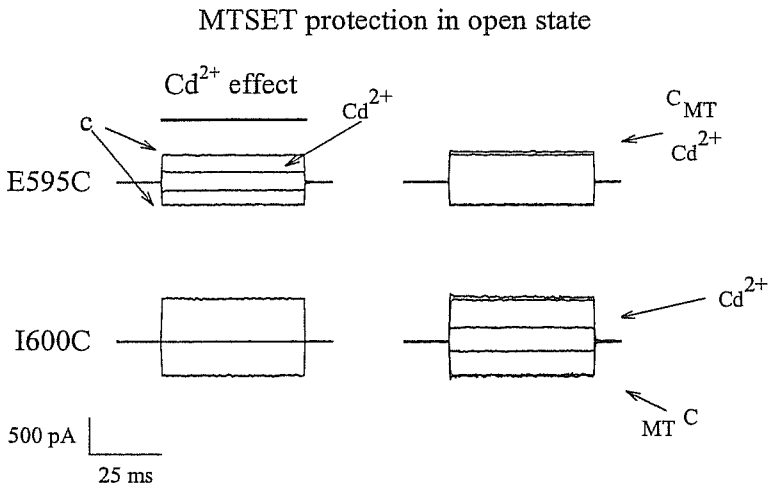

Fig.18: Protection by MTSET of Cd^{2+} current reduction in mutant E595C and I600C. On the left: current traces before and after the addition of 100 µM Cd^{2+} for 5 min in the open state. On the right: effect of 100 µM Cd^{2+} in the open state before and after the application of 2.5. mM MTSET.

As shown in Fig. 19A CuP applied in the closed state caused an irreversible decrease of the cGMP gated current in mutant channel I600C within 2 min in the presence of 1 µM of CuP and within 10 s in the presence of 1 mM CuP. A similar effect was observed also in the closed state for the low and high CuP concentration (see Fig.19B). The time course of this current reduction is shown in Fig.19C: both in the open and closed state CuP completely suppressed the cGMP-gated current in mutant channel I600C within 2 min.

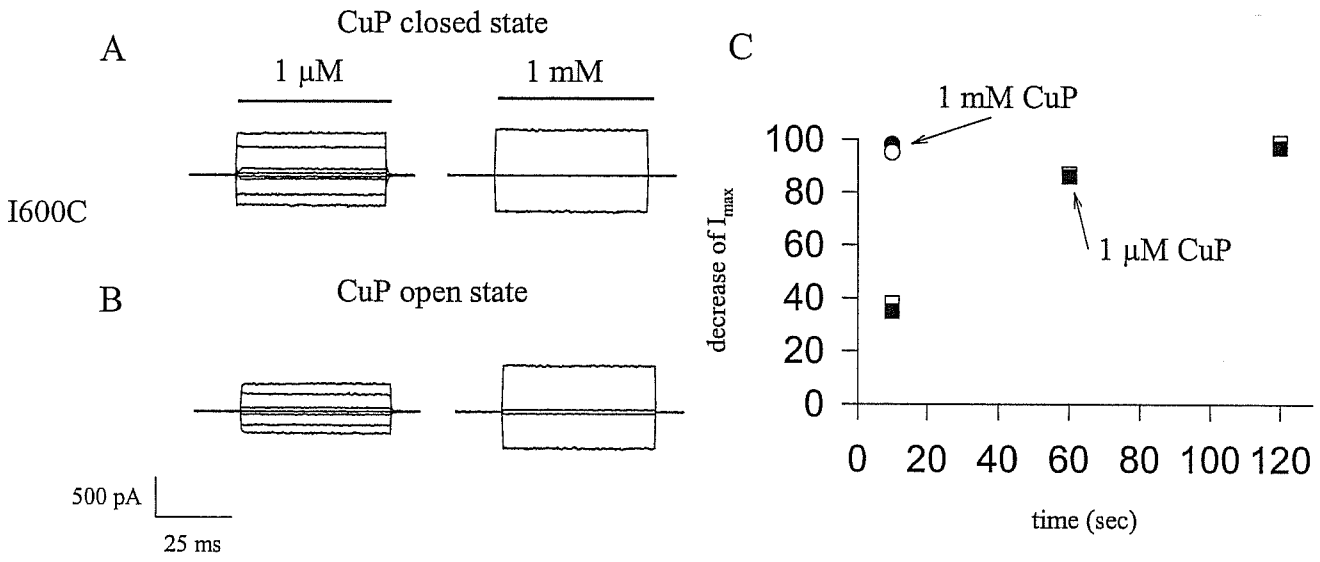

Fig.19: *The effect of CuP on cysteine channels from GLU594 to MET602.* ***A****: irreversible reduction of the cGMP-gated current, in the closed state, caused by an addition of 1 µM CuP and 1 mM CuP for mutant channel I600C.* ***B****: as in A, but in the open state. In A and B voltage steps are as in Fig. 13. The four traces shown in the left panel of A and B were obtained before application of 1 µM CuP and after 10, 60 and 120 s. On the right panel of A and B only the trace obtained before application of 1 mM CuP and after 10 s are shown.* ***C****: time course of current reduction in the open and closed state, in the presence of 1 mM and 1 µM CuP.*

A comparison between the current decrease induced by exposure for 5 min to 100 µM Cd^{2+} and for 2 min to 1 µM CuP is shown in Figs. 20 A and B. In the open state the application of 100 µM Cd^{2+} caused a current decrease in mutant channels M602C, L601C, I600C, Q599C, G597C, K596C, E595C and E594C by 30±3%, 100%, 100%, <5%, 23±4%, 20±5%, 55±4% and 100% respectively. In the open state blockage, by the two sulfhydryl reagents was almost identical except in mutant channel G597C. In this case, the current reduction by CuP is 67±7%, considerably higher than that one induced by Cd^{2+}; this difference could be explained if in G597C the cysteines were close to each other and so deeply buried that they would result inaccessible to Cd^{2+}.

In the closed state the current decrease for the same mutant channels was 65±2%, 100%, 75±5%, 100%, 100%, 100%, 100% and 100% respectively. A very similar effect by CuP was observed for most of these mutant channels, but with some differences: in the closed state Cd^{2+} induced a current reduction in mutant channels E595C, I600C and

M602C by 100%, 75±5% and 65±2% respectively, but the effect of CuP for these same mutant channels was 80±5%, 97±3% and 0% respectively.

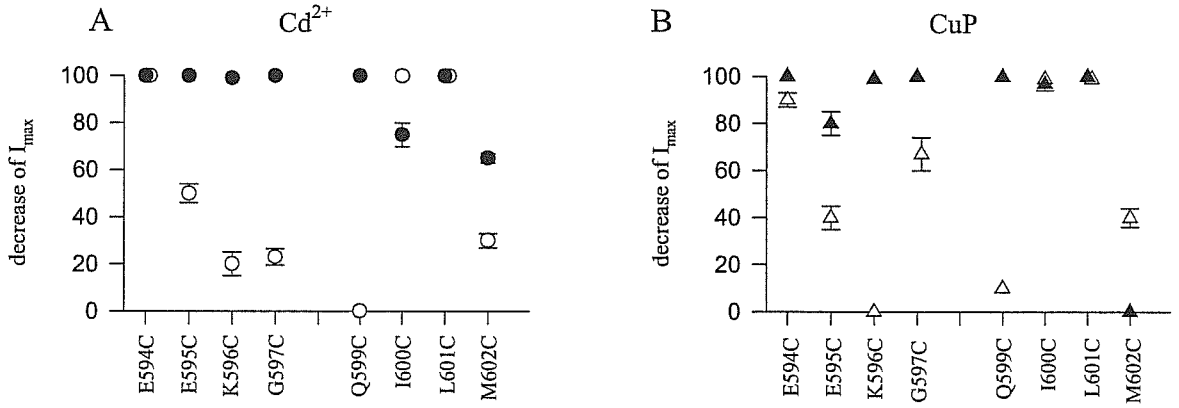

***Fig.20**: A percentage of 100 μM Cd^{2+} irreversible current reduction in the absence (closed circles) and in the presence (open circles) of 1 mM cGMP for cysteine mutants from Glu594 to Met602. **B**: percentage of 1 μM CuP irreversible current reduction in the absence (closed triangles) and in the presence (open triangles) of 1 mM cGMP for cysteine mutants from Glu594 to Met602.*

In the absence of sulfhydryl reagents mutant channels L601C, I600C, G597C and E594C in the presence of 1 mM cGMP exhibited a rundown of the cGMP activated current varying between 5 and 12% within 15 min. This run down was higher than that one observed in the wt channel.

Residues from Pro587 to Met592

Residues from Pro587 to Met592 were sensitive to sulfhydryl reagents similarly to those from Lys603 to Leu607. As shown in Fig.21A in the closed state Cd^{2+} powerfully reduced the cGMP-gated current in mutant channels D588C, K590C and G591C. Current decrease of mutant channels A589C and M592C was 20±4% and 50±5% respectively. Perfusion with 1 μM CuP in the closed state for 2 min had a similar effect on the same mutant channels, as shown in Fig.21B.

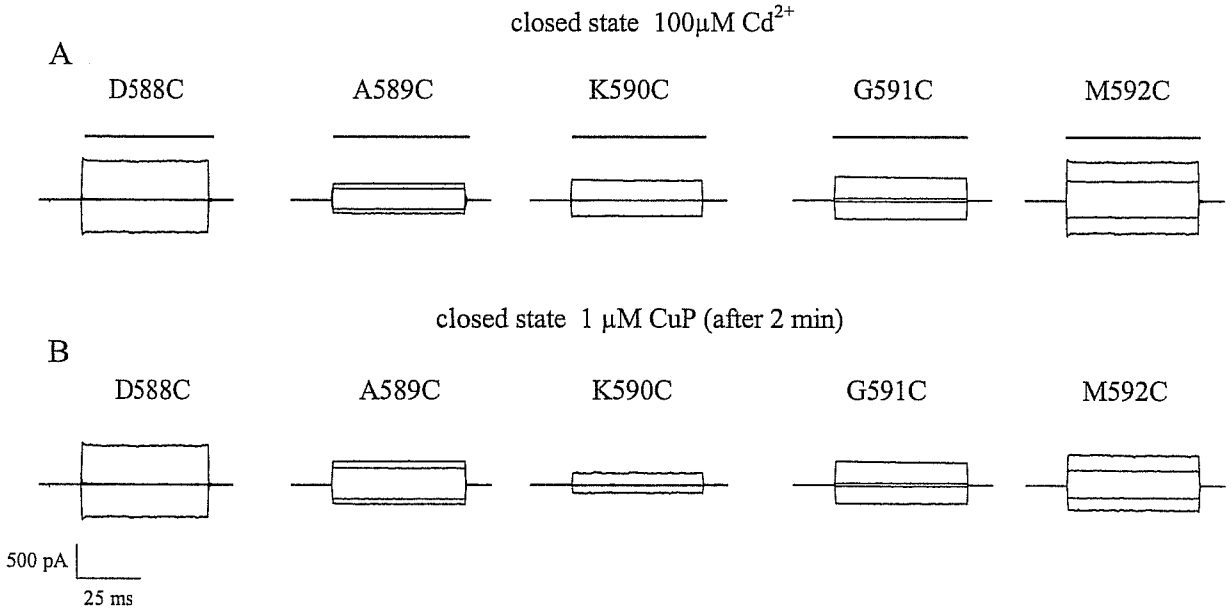

Fig.21: *The effect of Cd^{2+} and CuP applied in the absence of cGMP on cysteine mutants from Asp588 to Met592.* ***A****: current traces before and after the addition of 100 μM Cd^{2+} for 5 min. From right to left recordings from channel mutants M592C, G591C, K590C and A589C and D588C.* ***B****: As in A, but adding 1 μM CuP for 2 min. Voltage steps in A and B as in Fig. 13.*

As shown in Figs. 22 A and B in the open state Cd^{2+} effect was at most 10% and that of CuP was slightly larger, at most 30%. MTSET did not have any significant effect in the open state and decreased by about 25% all these mutant channels, as shown in Fig.23.

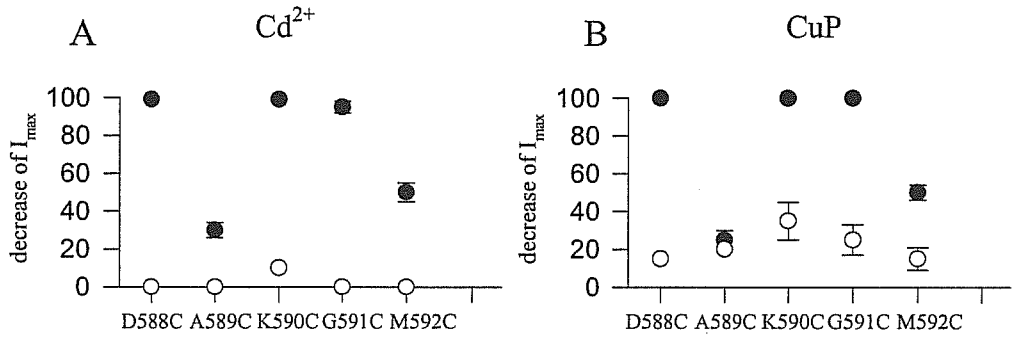

Fig.22: A: percentage of 100 μM Cd^{2+} irreversible current reduction in the absence of cGMP (closed circles) and in the presence of 1 mM cGMP (open circles) for cysteine mutants Asp588 to Met592. ***B****: as in A, but for 1 μM CuP.*

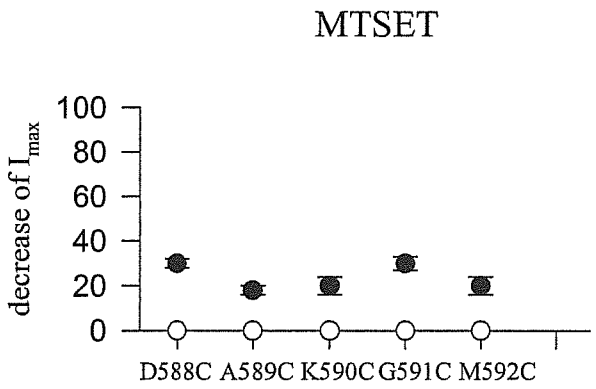

Fig.23: percentage of 2.5 mM MTSET irreversible current reduction in the absence of cGMP (closed circles) and in the presence of 1 mM cGMP (open circles) for cysteine mutants Asp588 to Met592.

Residues from Leu583 to Tyr586

A clear and evident cGMP gated current was recorded from mutant channels E585C and L583C. No cGMP-gated current was recorded from oocytes injected with the mRNA of

mutant channels Y586C and L584C. As shown in Fig.24 100 μM of Cd^{2+} did not produce any irreversible decrease of the cGMP gated current in mutant channels E585C (A and B) and L583C (C and D) neither when Cd^{2+} was applied in the open state (B and D) nor in the closed state (A and C). Similarly, neither the addition of 1 μM or mM CuP to the bathing medium caused any permanent reduction of the cGMP gated current. MTSET caused a current decrease of about 20% when applied in the closed state but none when applied in the open state. Therefore the sensitivity to sulfhydryl reagents of cysteine mutants from Tyr586 to Leu583 is similar to that one observed in the wt channel.

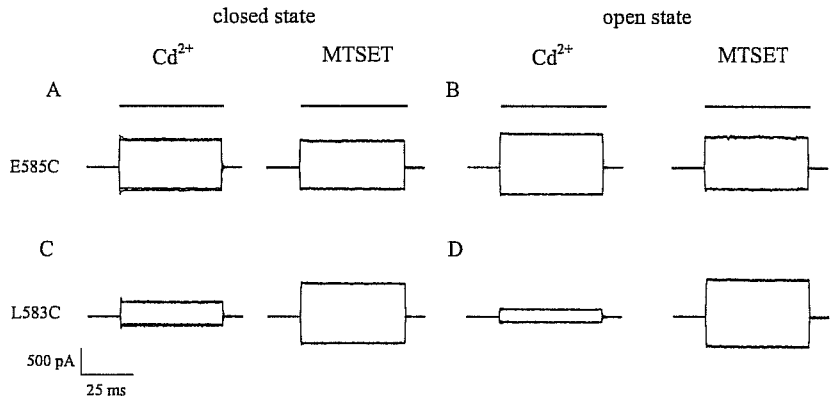

Fig.24: *The effect of Cd^{2+} and MTSET on mutant channels E585C and L583C in the presence and absence of cGMP.* ***A****: irreversible reduction of the cGMP-gated current caused by 100 μM Cd^{2+} (left) and 2.5 mM MTSET (right) added for 5 min in the absence of cGMP in mutant channel E585C.* ***B****: as in A, but with sulfhydryl reagents added in the presence of 1 mM cGMP.* ***C****: as in A, but for mutant channel L583C.* ***D****: as in C, but in the presence of 1 mM cGMP. In A, B, C and D voltage steps as in Fig13.*

2-S6 transmembrane domain and pore region

2.1-S6 TRANSMEMBRANE DOMAIN AND PORE HELIX: AN OVERVIEW

Fig.25 reproduced the overall architecture of the K^+ channel pore. This structure was revealed for the first time in 1998 after the elucidation of the X-ray crystal structure of KcsA, a K^+ channel from *Streptomyces lividans* (Doyle et al., 1998). Subsequently, the same architecture was found in other K^+ channels and is thought to be shared by all the pore regions present in voltage gated channels. All members of this family share a common pore domain that contains two transmembrane (TM) segments named M1 and M2 that correspond to S5 and S6 in the CNG channel. Between this domains there is a loop forming the filter region and an additional small helix, not spanning the lipid membrane, referred as the P-helix. (Doyle et al., 1998; Jiang et al., 2002; Flynn and Zagotta, 2003). S6 and M2 are involved in the gating of K^+ channels, whereas the loop forming the filter region does not change its conformation upon gating. In K^+ channels, the only significant structural difference on passing from the closed to the open conformations is the bending by 30° of the S6/M2 helix towards the lipid phase, around an glycine hinge (Jiang et al., 2002). One of the purposes of my thesis is to test and challenge whether a similar conformational change occurs also in CNG channels.

We know that there are many differences between this region present in K^+ channels and CNG channels but some experiment suggest that the structure and the movement are similar (Flynn and Zagotta et al., 2001; Flynn et al., 2001; Johnson and Zagotta, 2001; Jiang et al., 2002; Flynn and Zagotta, 2003). The hypothesis put forward by Zagotta and his collaborators is that during channel gating the S6 transmembrane domain present in CNGA1 channels moves as in K^+ channels. In particular, it is assume that the KcsA model represents the putative closed state of the channel and the MthK model represents the open state (Flynn and Zagotta, 2003). The analysis performed in the S6 domain of CNGA1 channels from Thr389 to Ser399 (Flynn and Zagotta, 2001 and 2003) suggested that also in CNG channels the S6 domain has an helical configuration, possibly crossing at an hypothetical constriction, located between residue Val391 and Ser399. In this view the inner vestibule of CNG channels has the same structure of K^+ channels, i.e. a bundle of four helices crossing so to form a restriction constituting the gate in the closed state of the channel. The mutant channel V391C is

blocked by MTSET only in the open state, but is blocked by Ag^+ equally well in the closed and open state (Flynn and Zagotta 2001). The former observation suggests the existence also in CNG channels of a gating mechanism similar to that of K^+ channels, while the later shows that Ag^+ ions penetrate the inner vestibule of CNG channels up to residue Val391 both in the open and closed state. Several previous reports have argued or implied that the gate of CNG channels was in the pore itself.

In 1999 Becchetti et al. (Becchetti et al., 1999) have shown that CNG and K^+ channels share the same gross topology and that residues L(358)TTIGETPPP(367) of the CNGA1 channel from bovine rods span the lipid membrane from the intracellular to the extracellular side. These residues form the inner pore of the channel.

Point mutations in the pore itself, primarily of glutamate 363, significantly changed the gating (Bucossi et al., 1997): in mutant channel E363A in the presence of a steady cGMP concentration the cGMP activated current inactivated spontaneously and in mutant channels E363D and T364M single channel properties were markedly different from those observed in the wt CNG channel. Sun et al. (1996) and Liu and Siegelbaum (2000) reported that internal MTSEA blocked both in the open and closed state channel mutants T360C and I361C. However, as shown in Becchetti et al. (1999), methanesulphonate reagents (MTSET and MTSEA) potentiate and do not block the mutant channel T360C. The mutant I361C has a fast run down (Becchetti et al., 1999) and it is impossible to establish unequivocally any effect of methanesulphonate reagents. Fodor et al. (1997) have observed that tetracaine had a 1000-fold higher affinity for the closed CNG channel as compared to the open channel. This rather surprising result, however, does not show or prove that the inner vestibule is equally accessible to permeating ions both in the open and closed state. Karpen et al. (1993) have described a state-independent block of native CNG channels by divalent cations such Ni^{2+} and Zn^{2+}. Rather correctly, these authors have assumed that the observed effect was due to an interaction with the gating machinery and not with the pore itself.

As a consequence the exact location of the gate in CNG channels is yet an open question. The testing and validation of this hypothesis is another objective of my work.

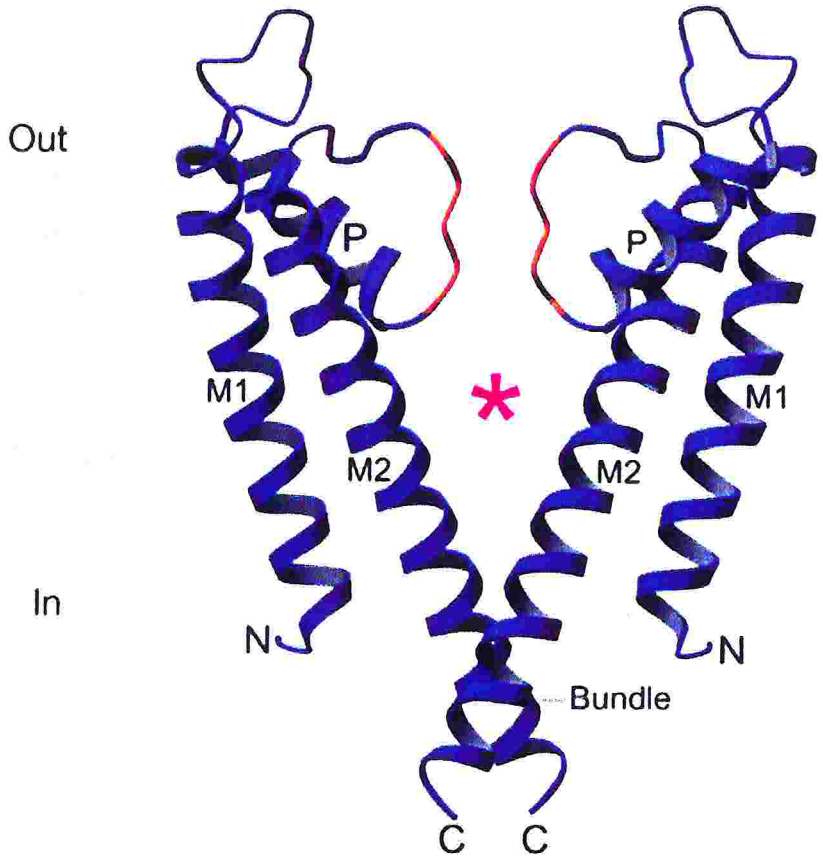

Fig.25: *structural elements of the K+ channel pore. Two subunits of the KcsA channel are shown with the extracellular side on top. The selectivity filter is orange and a red asterisk marks the central cavity. Three helical segments include, from n to C terminus, the outer helix (M1), pore helix (P) and inner helix (M2). The gate is formed by the inner helix (Bundle) (Jiang et al., 2002).*

Before describing my results concerning the S6 transmembrane domain and the pore region I present a brief overview of the experimental results obtained by other groups, discuss their hypothesis on structure of the pore of CNG channels.

A) PREVIOUS INVESIGATION ON THE P-HELIX AND INNER PORE

Three previous SCAM studies identified certain cysteine-substituted residues in the pore-forming P region (S5-S6 linker) of the CNG channels that react with charged, hydrophilic MTS reagents (Sun et al., 1996, Becchetti et al., 1999 and Liu and Siegelbaum, 2000).

The results present in these papers show that several amino acid residues in the P loop of the CNG channel are differently accessible to MTSEA and MTSET. The accessibility

map of the residues tested with MTSET in the work of Torre and collaborator (Becchetti et al., 1999) is consistent with a topological structure of the pore region different from the one previously proposed (Sun et al., 1996), and more similar to that of voltage-dependent potassium channel (Doyle et al., 1998), which have a significant sequence homology with CNG channels. Indeed, the results obtained with MTSEA are in agreement with those reported by Sun et al. (1996) but, the interpretation of the results is basically different. In particular, they identified three residues (V4C, T2C and P22C) that were accessible from both sides of the membrane when the channel was closed, in contrast with results obtained for voltage-gated K^+ channels. To account for this result, they propose that each of the four P regions form a "thin blade of an iris". Becchetti et al. demonstrated that these results are an artefact produced by slight permeation of MTSEA through the plasma membrane. Indeed, this compounds, although unable to permeate the open channel as a charged amine, rapidly crosses the lipid bilayer, probably because the uncharged amine is partially soluble into the plasma membrane (Becchetti et al., 1999). Thus, the accessibility to MTSEA of several P loop residues from the two sides of the membrane could be due to MTSEA permeation through the plasma membrane instead of being a consequence of the CNG channel topology. For this reason they test the accessibility of an MTS derivatives such as MTSET, impermeant the plasma membrane. The results of these experiments indicate a different accessibility for MTSET and MTSEA and suggest that the accessibility of several residues to MTSEA from both sides of the plasma membrane (Sun et al., 1996) is caused by MTSEA permeation through the lipid bilayer. MTSET effects suggest that the distinction between residues outwardly or inwardly accessible is clear-cut, in the P loop of CNG channels, with an overall topology reminiscent of that of K^+ channels.

Becchetti et al. demonstrated that neither MTSEA nor MTSET had any effect on mutants K2C and S6C. cGMP-activated currents from mutant V4C were not affected by MTSET application to the inner side of the plasma membrane, either in the closed or in the open state. On the contrary, MTSET strongly inhibited cGMP-gated currents in mutant V4C, when applied to the outer side of membrane patches, both in the presence and in the absence of cGMP. These results suggest that Val4 is located extracellularly, possibly in the outer pore vestibule. cGMP-activated currents from L7C mutant were scarcely different from those observed in wt channels. They were not affected by

external MTSET. However, MTSET application to the inner side of membrane patches produced a partial but reproducible block: 60% (±9.9%, n=4) in the closed state, and 25% (±3.6%, n=5) in the open state. These results show that Leu7 residue is accessible from the internal side of the plasma membrane. These data indicate that cysteines introduced in positions 9 and 12 are accessible from the inner side of the plasma membrane. Mutants T15C and T16C had similar properties only data from T16C mutant will be presented. The cGMP-gated currents were strongly and rapidly potentiated by intracellular application of MTSET (and MTSEA), in the presence and in the absence of cGMP. MTSET application to the outer face of the plasma membrane produced negligible effects on both T15C and T16C mutants. These results suggest that residues in position 15 and 16 are not accessible from the extracellular side, and that T16C is accessible to MTSET from the inner side of the plasma membrane and may be partially involved in channel gating. cGMP-activated currents recorded from the mutant channel I17C rapidly decayed in inside-out patches. Current did not recover even when patches were maintained several minutes in the absence of cGMP (Lynch, 1998). Cysteines in position 17 of neighbouring subunits should be in closer contiguity than cysteines in the other functional mutants. These results argue that residue in position 17 is accessible from the inner side of the patch membrane. Furthermore, we propose that Ile17 is located near the narrowest section of the channel pore, at its intracellular side. The faster decay in the presence of cGMP suggests also that Ile17 residues of different subunits are closer to each other in the open state. Thr20, Pro21 and Pro22 are extracellular residues. The weak effect on P21C indicates that the side chain of this residue does not line the channel pore lumen. For summarising the effects produced by the application of MTSET on the different cysteine mutants: residues Leu7, Trp9, Leu12, Thr15, Thr16, Ile17 were accessible intracellularly; residues V4, T20, P21, P22 were accessible extracellularly. For Leu7 the effects of MTSET was more pronounced in the closed state than in the open state.

The results of the SCAM study made on the A1 subunit of the bovine rod CNG channel revealed that the accessibility of several residues in the P loop to MTSEA and MTSET is significantly different. The results obtained are only in part in accordance with those reported by Sun et al. (1996). Therefore, the accessibility map of the residues tested

with MTS compounds is consistent with a topological structure of the pore region different from the one previously proposed (Sun et al., 1996).

After the publication of these papers in 1996 and 1999, Liu and Siegelbaum corrected theirs interpretation of the experiments. Moreover, they extend these studies by rescuing nine of the twelve non expressing mutants through construction of tandem dimers that contain one wild type and one cysteine-substituted mutant subunit (Liu and Siegelbaum, 2000). They conclude that there are several fundamental similarities between the structure of the P region of CNG channels with that of KcsA. The accessibility of three residues at the C terminal end of the P region (E19C, T20C and P22C) is consistent with previous SCAM studies on CNG channels (Sun et al., 1996; Becchetti et al., 1999) and voltage-gated shaker (Lu and Miller, 1995). The results are also consistent with the external location of these residues in the KcsA structure (Doyle et al., 1998). The pattern of accessibility of V4C, L7C, T11C and L14C at the amino terminus of the CNG channel P region suggests that this region forms an α helix, consistent with the aligned pore helix of KcsA and regions of helical MTS accessibility patterns in *Shaker* channels (Gross and MacKinnon, 1996). However, there are also some significant differences between these results on CNG channels and previous results in potassium channels. These results show both similarities and differences with those of Becchetti et al. (1999), which studied reactivity of CNG channels with external MTSET using a set of cysteine-substituted mutant monomers. Similarly, the authors observed hat T20C and P22C are modified in both the open and closed state. Although no state dependence of V4C reactivity was observed, the authors used 500 μM cGMP to activate the channels compared to 10 mM cGMP in our experiments. A second discrepancy is that Becchetti et al. (1999) did not observe any effects on extracellular MTSET on L7C mutants. Finally, although Becchetti et al. (1999) found no inhibition of W9C currents with external MTSET, they did not look for any potentiating effects on responses to low concentrations of cGMP.

B) PREVIOUS INVESTIGATION ON THE S6 HELIX

My interest is focused also in the S6 transmembrane domain and also in this case, before describing my results, I analyse briefly the experiments and the conclusions proposed by other authors. In particular, I will discuss and analyse five different papers,

concerning the movement of this region during the gating of channel, I analyse (Flynn and Zagotta, 2001; Johnson and Zagotta, 2001; Flynn et al., 2001; Jiang et al., 2002 and Flynn and Zagotta, 2003).

All these papers suggest that the effects of cysteine modification on permeation give indication of a structural homology between CNG and KcsA channels in this region. In particular all the residues that compose the S6 putative helix are modified in cysteines and the effect of MTSET is tested.

An aim of my thesis is to check the hypothesis proposed in 2001 by Johnson and Zagotta (Johnson and Zagotta, 2001) regarding the rotational movement during cyclic nucleotide-gated channel opening. The author used a histidine scan of the C-linker of the CNGA1 channel and studied the modulation (potentiation or inhibition) caused by 1 μM Ni^{2+}. They conclude that the channel opening involves rotation of the initial C-linker around the central axis without translating radially and probably initiates movement of the S6 and pore opening.

Another objective of my study is to verify if in the open state of CNG channel there is the same bend of S6 transmembrane domain present in the K^+ channel. This similarity is described in 2001 end in 2003 by Flynn and Zagotta (Flynn and Zagotta, 2001; Flynn and Zagotta, 2003).

The experiments of Zagotta and collaborators (2001) suggest that the residues in position 391 and 399 lie on different faces of the S6 helix and the formation of a disulfide bond at both of these positions is consistent with a bundle crossing between S399C and V391C. An important result is also the formation of a spontaneous disulfide bond at S399C in the absence of cGMP; this result suggests that these residues be close together in the closed state. The state dependent formation of a spontaneous disulfide bond in this position reports a conformational change in the helix bundle that is associated with channel gating and suggests that the smokehole may widen as the channel opens. These results are consistent with the hypothesis that CNG channels are structurally similar to KcsA in the helix bundle region and suggest a plausible mechanism for the opening conformational change in CNG channels. The authors propose that the helix bundle opens by a translation and possible rotation of the intracellular ends of the S6 helices, with the extracellular ends constrained by interactions with the pore loop (Flynn and Zagotta, 2001; Flynn et al., 2001).

In the 2003 the same group propose again a model for this region of the channel from the residues in position 384 to 399 using MTSEA to understand the effect cysteines modification. In particular, the behaviour of three important residues (391, 395 and 399) was studied. Currents through S399C channels spontaneously declined immediately after patch excision. They demonstrate that the decline in S399C current is due to the formation of a disulfide bond between the S399C residues from different subunits (Flynn and Zagotta, 2001). An intersubunit disulfide bond also formed in V391C channels, but required the presence of the mild oxidizing agent CuP (Flynn and Zagotta, 2001). Currents through G395C channels decline after a brief exposure to MTSEA. This is an unexpected result and suggests a possible formation of disulfide bond between S atoms of G395C mutants. All these results are consistent with the view that side chains of residues V391, G395 and S399 are pointing toward the centre of the pore. Since, CNGA1 share sequence similarity with KcsA and MthK channels (Jiang et al., 2002), these channels are used as templates for the closed and open state, respectively, and the conclusion of Zagotta end collaborators is that the distances between the residue S399C in the closed and in the open state are respectively of 5-8 Å and 20-30 Å, like the distance in te same position of the mentioned channels.

2.2-TEMPLATE AND SEQUENCE ALIGNMENT

The S6 region of the bovine rod CNG channels (CNG1) shares sequence similarity with KcsA (K^+ channel from *Streptomyces lividans*), *Shaker* (*Drosophila melanogaster* K^+ channel) (Flynn and Zagotta, 2001; Jiang et al., 2002) and MthK channel from *Methanobacterium thermoautotrophicum* (Jiang et al., 2002, Flynn and Zagotta, 2003) (Fig.26).

The principal observation in the sequence alignment is the conservation of amino acids at different position in the inner helix (Fig.26), in particular, in the first position, the gating hinge, it is conserved a glycine; in the second position, at five amino acids later to the gating hinge, in position C-terminal, we observe a conserved glycine or alanine. Notably, the CNG channel is different from KcsA in the selectivity filter, as the first one lack the GYG sequence important for the ion selectivity.

As seen in Fig.26, conservation of the P region motif between CNG and potassium channel sequences is particularly high (about 40%). In the KcsA structure, the motif

corresponds to the pore helix and the pore loop, hence forming the channel selectivity filter. All potassium channels share, in this region, a highly conserved GYG triplet. Deletion-mutants of the Shaker cannel, lacking the YG residue pair, lose much of their preference for K^+ ions (Heginbotham et al., 1992), suggesting that these residues are determinant of K^+ channels selectivity. Not surprisingly, the GYG triplet is not conserved in CNG channels, constituting the major difference whit respect to the KcsA channel P region. In addition to the striking sequence conservation, SCAM experiments argue in favour of a structural similarity between the P region of CNG channels and KcsA. First, accessibility data suggests α helical configuration for the pore region spanning residues Y347 to T359 of the CNG channel and corresponding to the pore helix of the KcsA (Liu and Siegelbaum, 2000). Second, accessibility of CNG channel residues from T359 to P366 correlate well with those of the pore loop residues in the KcsA structure (Becchetti et al., 1999).

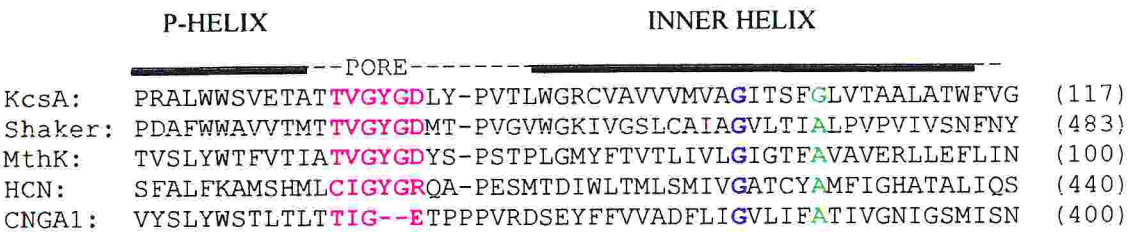

Fig.26: *Amino-acid sequence alignment of the pore helix, selectivity filter and inner helix for same channels of the P-loop-containing family. The selectivity filters is coloured in red, the gating hinge glycine blue and in green the conserved amino acids.*
KcsA is a K^+ channel from Streptomyces lividans, Shaker is a Drosophila melanogaster K^+ channel, MthK channel from Methanobacterium thermoautotrophicum, CNG cyclic nucleotide gated channel (A1 subunit) from bovine rod and HCN, hyperpolarization activated cyclic nucleotide gated channels.

When the whole region, spanning from TM1 to TM2 of the KcsA and from N294 to S396 of the CNG1 channel, is considered, sequence similarity becomes rather low (about 20%). However, experimental data strongly support homology of the entire region. In particular:

1. the experimental residue accessibility in the C terminal part of CNGA1 S6 is fully consistent with the accessibility of the corresponding KcsA residue in TM2 (Johnson and Zagotta, 2001);
2. residue G383, which is located in the middle of the CNGA1 S6, is conserved throughout the whole K^+ and CNG channel families. In K^+ channels, it represent the hinge point (gating hinge) at which the TM2 helix bends (about 30%) to bring the channel into the open state conformation (Jiang et al., 2002). A similar movement, upon channel gating, has been proposed for the S6 of CNG channels (Flynn and Zagotta, 2001, Johnson and Zagotta, 2001). As a consequence, conservation of G383 might correspond to a conserved structural role of this residue;
3. residue A388 is either G or A in all CNGA1 channels and K^+ channels. The presence of a small side-chain at this site is believed t be important in order to avoid blockade of the channel open state configuration (Jiang et al., 2002). Again, the conservation of a residue that is so relevant in K^+ channels argue in favour of the conservation of its structural role in CNG channels subunits.

2.3-EXPERIMENTAL RESULTS

In this part of my thesis, I analyse the effect of Cd^{2+}, MTSET, MTSEA and MTSES when some residues present in the pore region were mutated into a cysteine (i.e. mutant channels V348C, L351C, T359C, T360C and I361) and in many residues that compose the putative S6 transmembrane domain from residues Phe375 to His420, both in the closed and in the open state.

In my experiment I use the wt CNGA1 channel and the residues are mutated in cysteine, one by one. The construct that I used has all the seven endogenous cysteines and it is not the cysteine free CNGA1 channel used by Zagotta and his collaborators. The presence of these cysteines makes the channel under investigation close to the real CNG channel but complicates the interpretation of the experimental results. For example, modification of current amplitude due by the application of MTSET could be caused by an interaction with the native cysteine in position 481 (Brown et al., 1998) and not caused by a direct interaction of MTSET with the exogenously induced cysteines. For this reason it was necessary, every time that I observed a current modification after the application of MTSET or MTSEA to test the effect of MTSES as this last compound does not have any effect in the wt (Brown et al., 1998). In particular, I have studied all these effects on the mutant channels T359C and T360C.

I have tested the effect of MSTES also on some mutant channels in the S6 segment, such as, F380C and G383C mutant channels.

Residues in the N-terminal side of the S6 domain from Phe375 to Ile390

I have replaced one by one all residues from Phe375 to Ile390 with a cysteine and constructed mutant channels from F375C to I390C. These residues compose the N-terminal portion of the S6 transmembrane domain. The application of MTS compounds both in the open and in the closed state does not produce any significant modification on the cGMP-activated current on mutant channels from F375C to I390C. The only significant observation is the large potentiation (90±5%) of current for F380C mutant channel caused by MTSET in the open state, in the closed state any effect was observed. Other residues, in which it is possible measure a small potentiation (<20%) in these condition, are V377C, G383C and I390C; the residue G383C is potentiated, in the same manner, also in the closed state (see table 2). For the mutant channels F380C and

G383C I have also studied the effect of MTSES (2.5 mM) in the open and in the closed state and the effects is different for the two mutants (Fig.27). In particular, MTSES does not have any effect for the mutant G383C in both the channel configurations. Instead, the effect in the F380C is state dependent, in fact, it is potentiated in the open state and no effect is observed in the closed state. Different is the behaviour of MTSEA when I tested on the current of D379C and F380C (Fig.28): in the open state this MTS compound block the D379C channel and potentiated the F380C, instead, in the closed state all the channel currents are potentiated.

The application of 100 μM Cd^{2+} and 1 μM CuP, for all the residues in this region, does not present any important decrease of current (table 2, Fig.27 and Fig.28); indeed, all the decrease of current is smaller than 30%.

	Cd^{2+} open state	*Cd^{2+} closed state*	*CuP Open state*	*CuP Closed state*	*MTSET open state*	*MTSET close state*
F375C	0	0	0	0	0	0
V376C	0	0	0	0	0	0
V377C	<20	0	0	0	<20	0
A378C	<20	<10	0	0	0	0
D379C	0	22±4	23±2	46±3	0	0
F380C	80±10	38±7	30±2.5	30±2.5	90±5	0
I382C	<20	<20	25±2	20±2	0	0
G383C	<20	35±2	45±5	23±2	<20	<20
L385C	30±2	30±2	0	0	0	0
I386C	0	0	0	0	0	0
T389C	10±5	29±2	15±5	40±3	0	0
I390C	0	36±5	15±5	0	<20	0

Table 2: *Summary of results from the residue in position F375 to I390. In this table are represented the percentage (%) of block of current in black and the percentage of potentiation of current in blue. Each value was obtained from at least five patches excised from at least two different injected oocytes.*

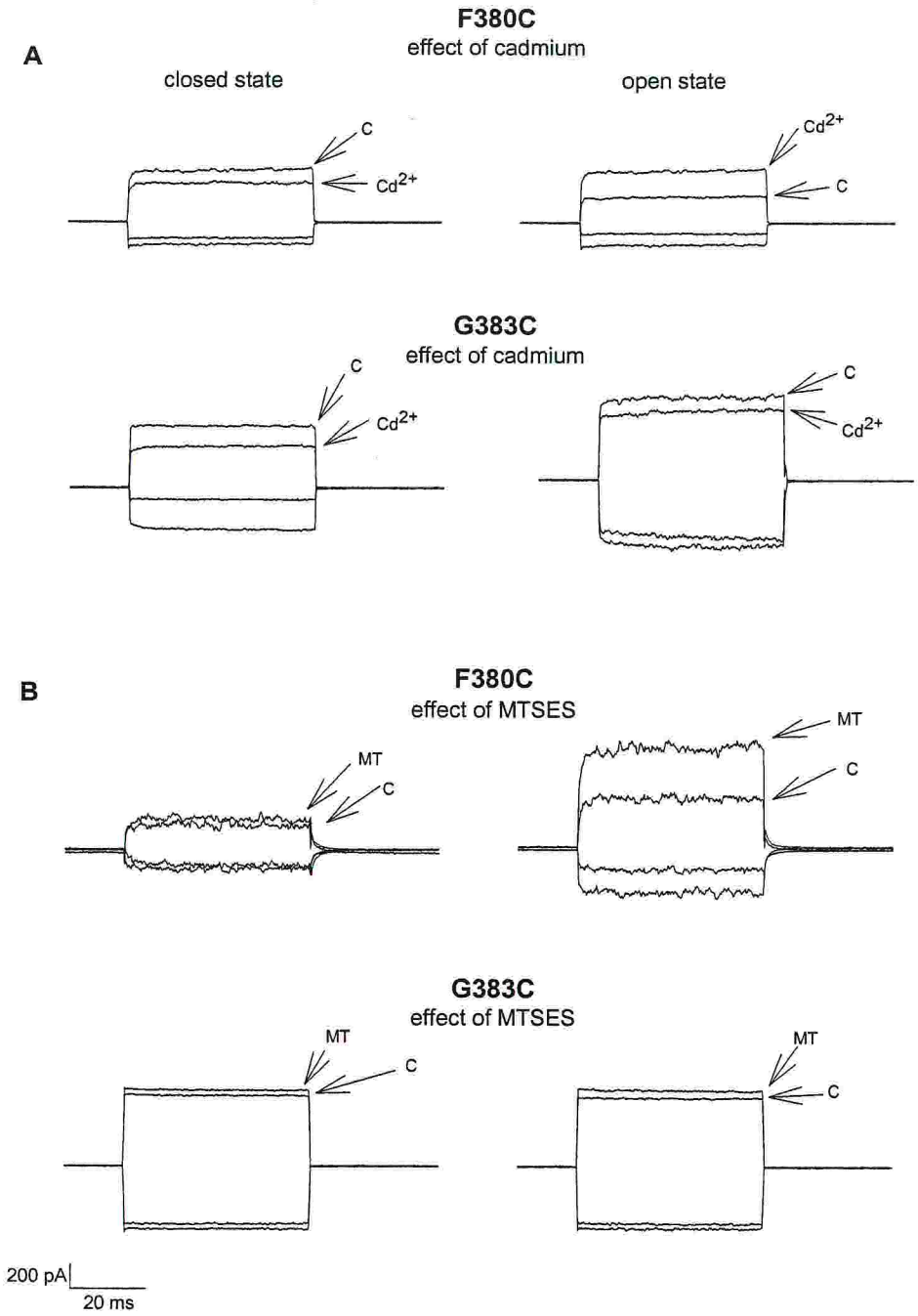

Fig.27: *The effect of Cd^{2+} and MTSES on mutant channels F380C and G383C in the presence and absence of cGMP.* ***A****: reduction of the cGMP-gated current caused by 100 µM Cd^{2+} added for 5 min in the closed state (left) in the open state (right).* ***B****: potentiation of the cGMP-gated current caused by 2.5 mM MTSES added for 5 min in the closed state (left) in the open state (right). In A and B voltage steps from 0 to +/- 60 mV. Each trace is the average of 10 individual trials. The cGMP-gated current was obtained as the difference of the current in the presence and in the absence of 1 mM cGMP. C indicates the control current, Cd^{2+} the current after the exposure for 5 min to 100 µM Cd^{2+} MT the current after the exposure for 5 min to 2.5 mM MTSES.*

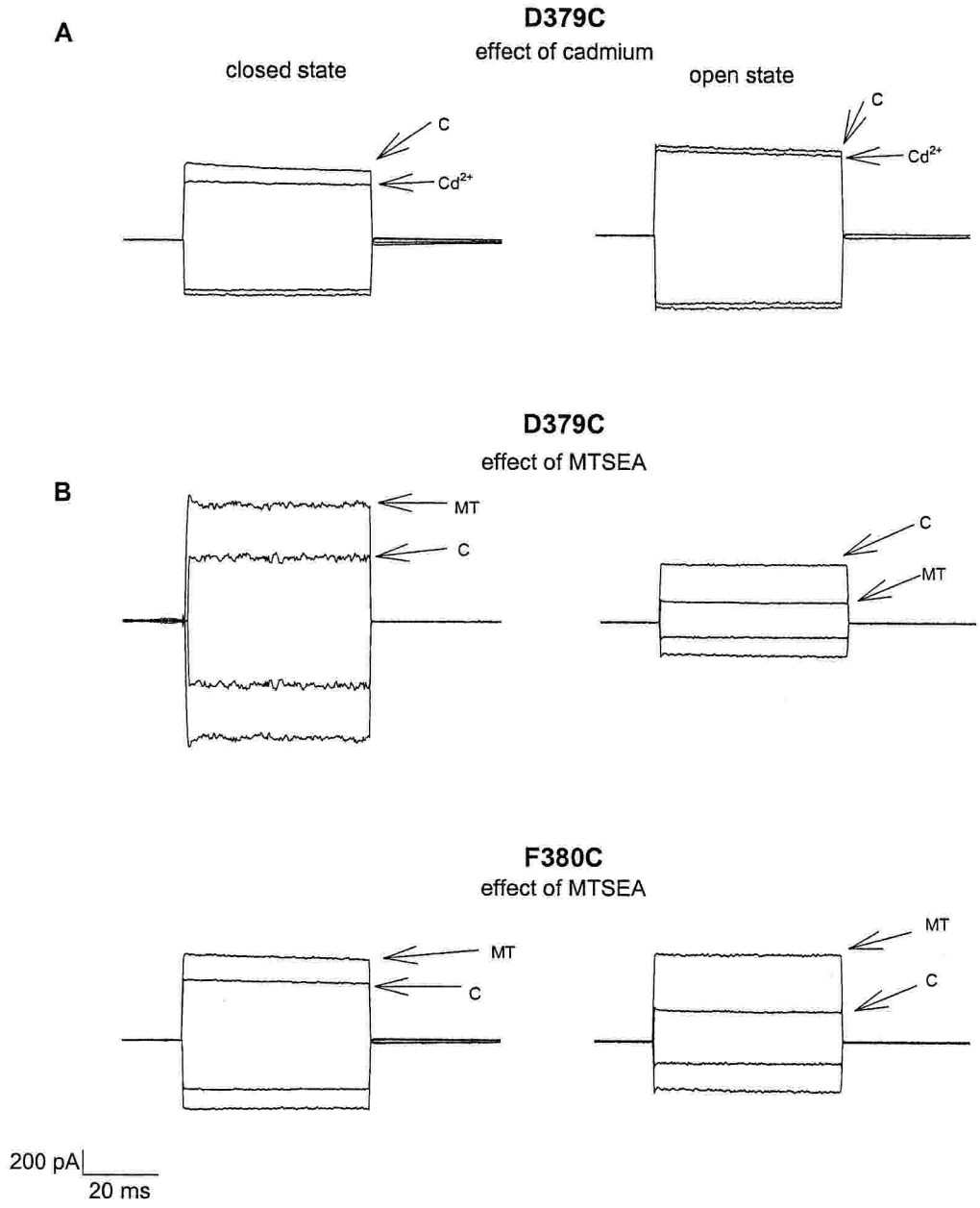

Fig.28: *The effect of Cd^{2+} and MTSEA on mutant channels D379C and F380C in the presence and absence of cGMP.* ***A****: reduction of the cGMP-gated current caused by 100 μM Cd^{2+} added for 5 min in the closed state (left) in the open state (right).* ***B****: potentiation of the cGMP-gated current caused by 2.5 mM MTSEA added for 5 min in the closed state (left) in the open state (right). In A and B voltage steps from 0 to +/- 60 mV. Each trace is the average of 10 individual trials. The cGMP-gated current was obtained as the difference of the current in the presence and in the absence of 1 mM cGMP. C indicates the control current, Cd^{2+} the current after the exposure for 5 min to 100 μM Cd^{2+} MT the current after the exposure for 5 min to 2.5 mM MTSEA.*

In table 2, I do not show results on channel mutants L381C and F387C because I did not obtain functional channels. There are two possible explanations for the lack of functional expression: the first one is the spontaneous formation of disulfide bonds cause by the closeness of introduced cysteines; the second hypothesis is the impossibility to produce a good fold of the channel into the membrane. I do not have data for mutant channels V384C and A388C, as they present a very fast and complete rundown of current probably due to the spontaneous formation of disulfide bond in excised patch. It is likely that the formation of disulfide bridges is prevented inside the intact oocyte, because of the reducing intracellular environment (Creighton, 1993).

Residues in the middle of the S6 domain (position 391, 395, 399 and 406)

The region of the S6 transmembrane domain, from the amino acids Val391 to Ala406, is a very interesting portion of the channel, as the homology with K channels suggests that the S6 transmembrane segments become in close contact and cross. Indeed, the V391C, G395C, S399C and A406C mutant channels present a particular behaviour after the application of Cd^{2+} and MTSET.

The application of 100 μM Cd^{2+} produce, in the V391C mutant channel, a reversible decrease of current respectively of 85±6% (n=5) and 89±4% (n=5) in the open and closed state (Fig.29A). Instead, the application of 2.5 mM MTSET causes a complete decrease of current (100% n=3) in the open state and no effect in the closed state (n=3) (Fig.29B).

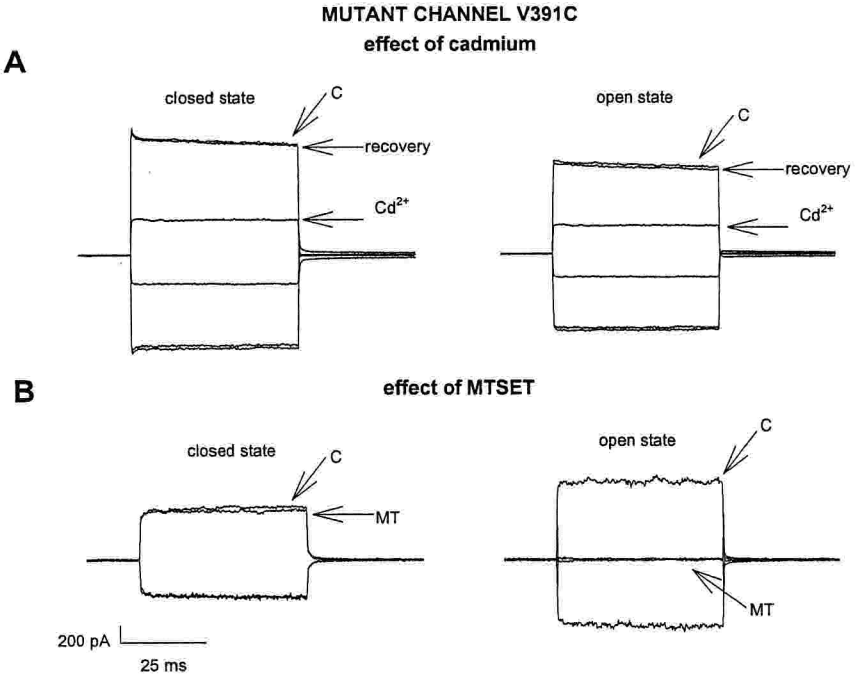

Fig.29: *The effect of Cd^{2+} and MTSET on mutant channel V391C in the presence and absence of cGMP. **A**: reversible reduction of the cGMP-gated current caused by 100 μM Cd^{2+} added for 5 min in the closed state (left) in the open state (right). **B**: irreversible reduction of the cGMP-gated current caused by 2.5 mM MTSET added for 5 min in the closed state (left) in the open state (right). In A and B voltage steps from 0 to +/- 60 mV. Each trace is the average of 10 individual trials. The cGMP-gated current was obtained as the difference of the current in the presence and in the absence of 1 mM cGMP. C indicates the control current, Cd^{2+} the current after the exposure for 5 min to 100 μM Cd^{2+} MT the current after the exposure for 5 min to 2.5 mM MTSET.*

In order to obtain a more quantitative analysis of the blocking effect of Cd^{2+} in the closed and open state I tested also the effect, using the same experimental protocol, of different concentrations of Cd^{2+}, in particular 10, 20 and 50 μM (Fig.30) and the results obtained are very similar for all the different concentrations. When I apply the mild oxidant CuP I obtain the same large effect that I observed whit Cd^{2+} but, in this case the block of current is irreversible [85±5% (n=3) and 87±3% (n=3) in the open and closed state, respectively] (Fig.31).

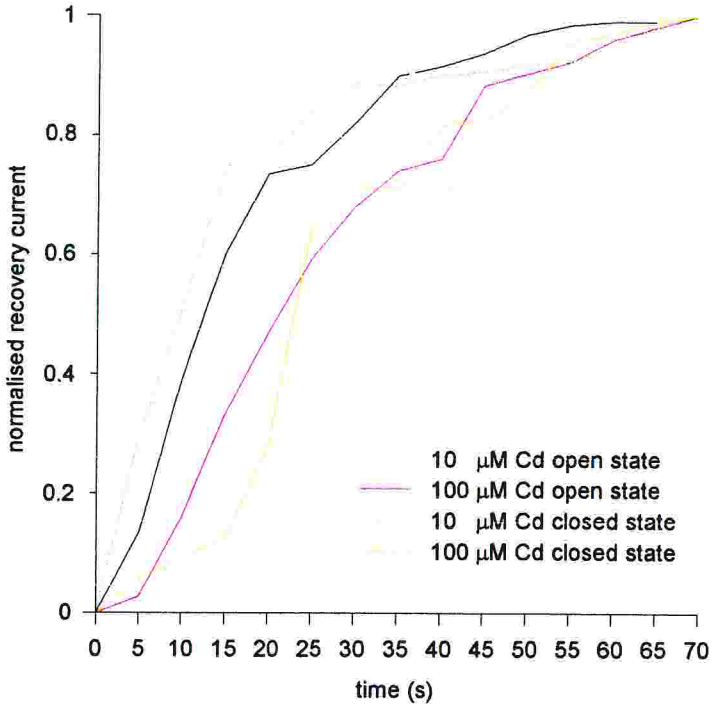

Fig.30: *Time-dependent recovery in current from V391C mutant channel in the open and closed state after application of 10 and 100 µM Cd^{2+} added for 5 min.*

When the neighbouring glycine in position 392 is mutated into a cysteine the mutant channel G392C presents a completely different behaviour. Indeed, no effect was observed in presence of Cd^{2+} (n=5) and MTSET (n=5) in the open state, i.e. in the presence of 1 mM cGMP; only a small decrease of current was observed in the closed state after the addition of 100 µM Cd^{2+} (n=5) (Fig.32).

Another interesting mutant channel is the G395C. Replacing the glycine at position 395 with cysteine produced a channel with such a low open probability that the cGMP-activated currents were so small that only single channel opening could be observed (this effect was observed also by Flynn and Zagotta, 2003). In order to clearly see single channels opening and record single channel currents I used a particular experimental protocol in which I apply first a pulse of -100 mV to inactivate the "stretch activated

channels" and after 1 second a voltage command at -180 mV was delivered (Fig.33). In the open state I observe a decrease of single channel opening after the application of both Cd^{2+} (100% n=4) and MTSET (about 50% n=4). In the closed state I observed a potentiation of current after the application of MTSET (n=4), whereas a complete block is observed after the application of Cd^{2+} (n=4) (Fig.33).

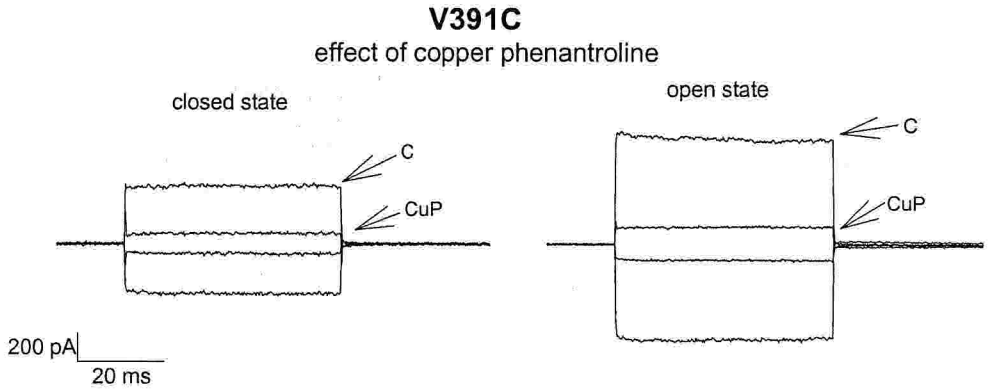

Fig.31: *The effect of CuP on mutant channel V391C in the presence and absence of cGMP. Reduction of the cGMP-gated current caused by 10 μM CuP added for 5 min in the closed state (left) in the open state (right). Voltage steps from 0 to +/- 60 mV. Each trace is the average of 10 individual trials. The cGMP-gated current was obtained as the difference of the current in the presence and in the absence of 1 mM cGMP. C indicates the control current, CuP the current after the exposure for 5 min to 1 μM CuP.*

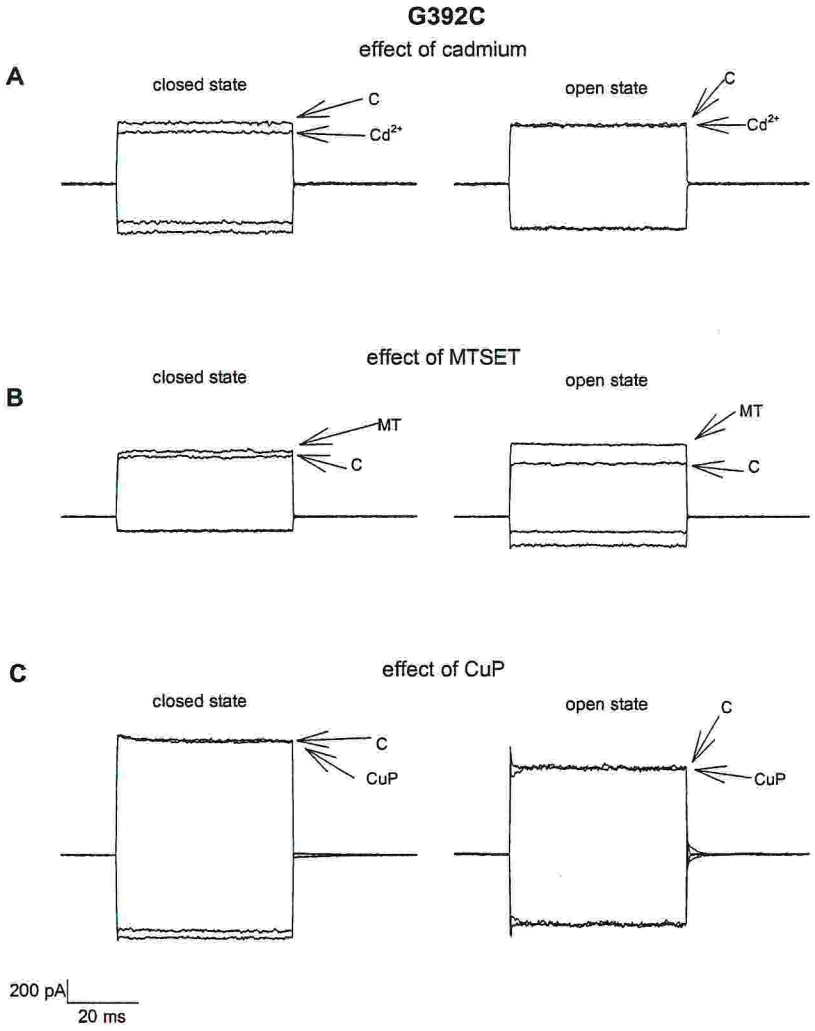

Fig.32: *The effect of Cd^{2+}, MTSET and CuP on mutant channel G392C in the presence and absence of cGMP.* ***A****: reduction of the cGMP-gated current caused by 100 µM Cd^{2+} added for 5 min in the closed state (left) in the open state (right).* ***B****: reduction of the cGMP-gated current caused by 2.5 mM MTSET added for 5 min in the closed state (left) in the open state (right).* ***C****: reduction of the cGMP gated current caused by 10 µM CuP added for 5 min in the closed state (left) in the open state (right). In A B and C voltage steps from 0 to +/- 60 mV. Each trace is the average of 10 individual trials. The cGMP-gated current was obtained as the difference of the current in the presence and in the absence of 1 mM cGMP. C indicates the control current, Cd^{2+} the current after the exposure for 5 min to 100 µM Cd^{2+} MT the current after the exposure for 5 min to 2.5 mM MTSET, CuP the current after the exposure for 5 min to 1 µM CuP.*

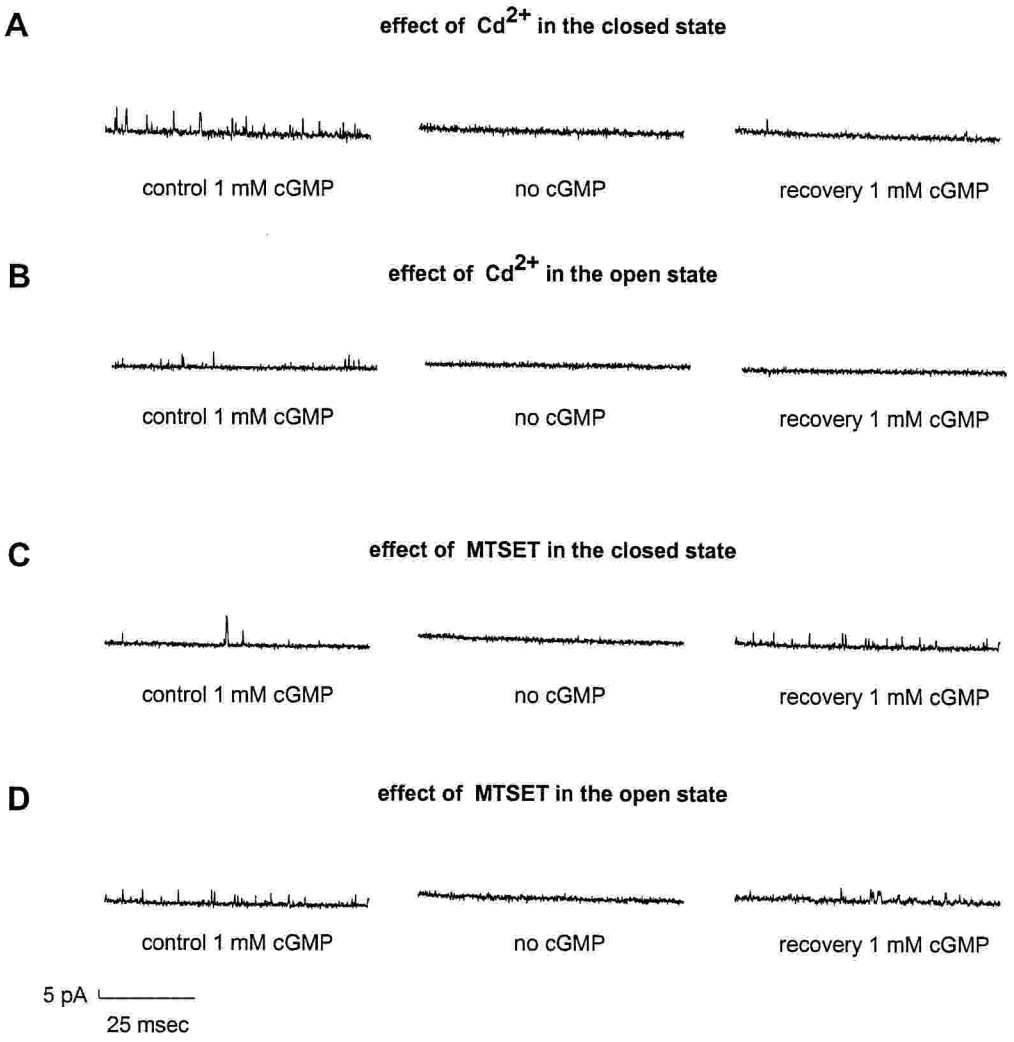

Fig.33: *The effect of Cd^{2+} and MTSET on mutant channel G395C in the presence and absence of cGMP.* ***A****: reversible reduction of the cGMP-gated current caused by 100 μM Cd^{2+} added for 5 min in the absence of cGMP.* ***B****: as in A, but with 100 μM Cd^{2+} added in the presence of 1 mM cGMP.* ***C****: as in A, but in presence of 2.5 mM MTSET.* ***D****: as in C, but in the presence of 1 mM cGMP. In A, B, C and D voltage steps from -100 to - 180 mV.*

Of particular interest was mutant channel S399C. This mutant channel exhibits a spontaneous decline of the cGMP-activated current after patch excision (Fig.34). This decline is likely to be caused by the spontaneous formation of a disulfide bond. For this reason the application of sulfhydryl reagents was performed, not immediately after patch excision, as in the experiments of Flynn and Zagotta (Flynn and Zagotta, 2003), but only after I observed a stabilisation of the current. For this reason I believe that the any effect of MTS compounds that I observed is real and not an artefact due to the rundown of current. By analysing the effect of sulfhydryl reagents after stabilisation of the cGMP activated current, I concluded that both in the open and in the closed state the application of Cd^{2+} produces a reversible block of current of 90±4% (n=7) and 50±8% (n=7), respectively (Fig.35A). The administration of MTSET, however, does not cause any decrease of current in the open (n=6) and closed state (n=6) of channel (Fig.35B). This observation is contrary to what reported by Flynn and Zagotta (2001 and 2003)

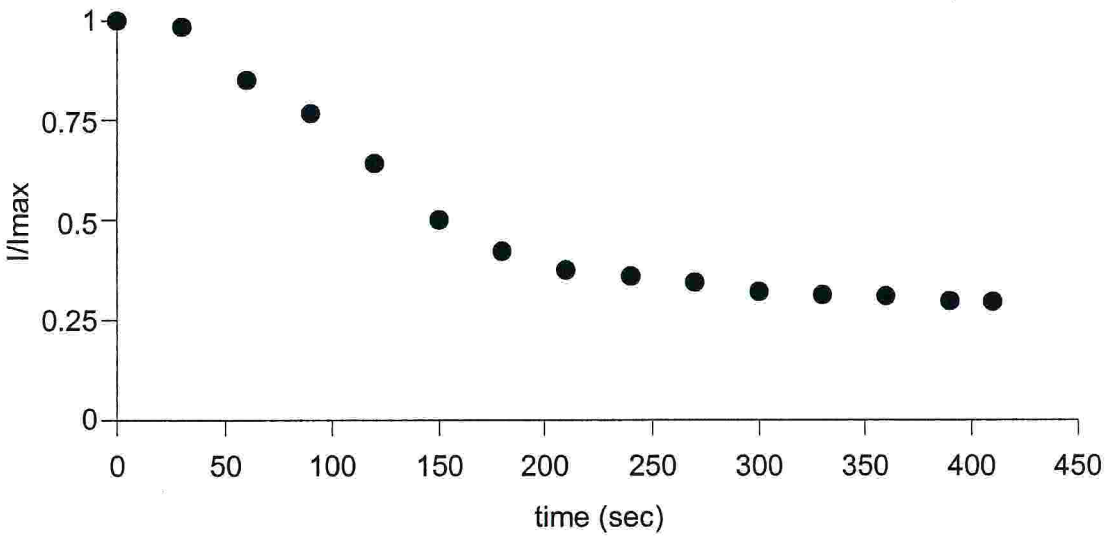

Fig.34: Current rundown of the mutant channel S399C after patch excision in presence of 1 mM cGMP.

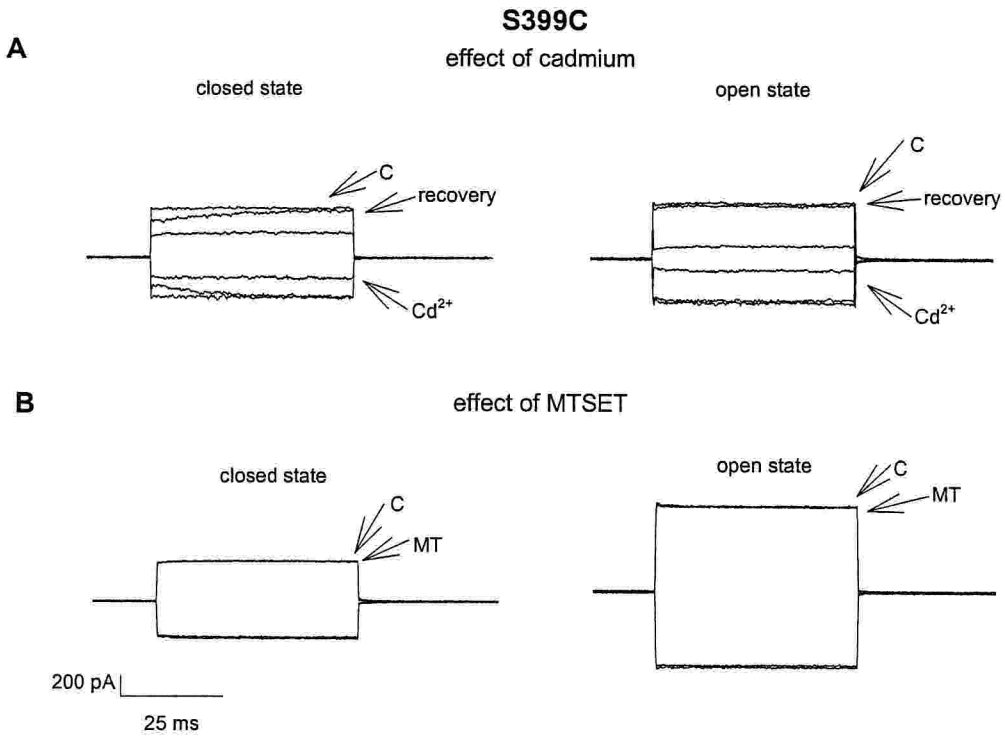

Fig.35: *The effect of Cd^{2+} and MTSET on mutant channel S399C in the presence and absence of cGMP.* ***A****: reversible reduction of the cGMP-gated current caused by 100 μM Cd^{2+} added for 5 min in the closed state (left) in the open state (right).* ***B****: irreversible reduction of the cGMP-gated current caused by 2.5 mM MTSET added for 5 min in the closed state (left) in the open state (right). In A and B voltage steps from 0 to +/- 60 mV. Each trace is the average of 10 individual trials. The cGMP-gated current was obtained as the difference of the current in the presence and in the absence of 1 mM cGMP. C indicates the control current, Cd^{2+} the current after the exposure for 5 min to 100 μM Cd^{2+} MT the current after the exposure for 5 min to 2.5 mM MTSET.*

The last important mutant channel that I analysed in this region of the S6 transmembrane domain is the A406C. Also in this case the application of MTSET does not cause any decrease of current neither in the open (n=4) nor in closed state (n=4) of channel (Fig.36B), whereas, the behaviour of the current after the application of Cd^{2+} is state dependent: indeed, in the open state (n=5) I did not observe any effect and, on the contrary, in the closed state the decrease of current was complete (100% n=5) and not reversible (Fig.36A).

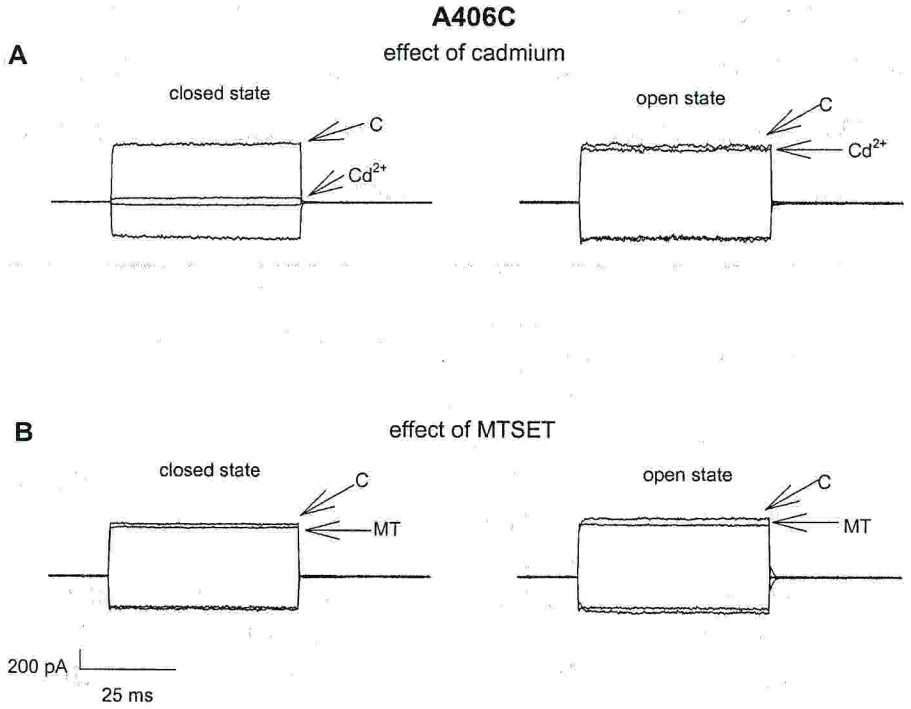

Fig.36: *The effect of Cd^{2+} and MTSET on mutant channel A406C in the presence and absence of cGMP. **A**: irreversible reduction of the cGMP-gated current caused by 100 μM Cd^{2+} added for 5 min in the closed state (left) in the open state (right). **B**: irreversible reduction of the cGMP-gated current caused by 2.5 mM MTSET added for 5 min in the closed state (left) in the open state (right). In A and B voltage steps from 0 to +/- 60 mV. Each trace is the average of 10 individual trials. The cGMP-gated current was obtained as the difference of the current in the presence and in the absence of 1 mM cGMP. C indicates the control current, Cd^{2+} the current after the exposure for 5 min to 100 μM Cd^{2+} MT the current after the exposure for 5 min to 2.5 mM MTSET.*

Residues in the C-terminal side of the S6 domain (position 403, 404, 405, 408, 410, 413, 416, 417 and 420)

The current of the mutant channels of some residues that compose the C-terminal portion of the S6 transmembrane domain is analysed after the application of Cd^{2+} and MTSET in the open and in the closed state. In particular only nine mutant channels are studied: A403C, A404C, R405C, A406C, F408C, D413C, K416C, Q417C and H420C (Table 3 and Fig.37). The MTSET applied in the closed and open state produce a decrease of current of 80±2% and 100%, respectively, only on the D413C mutant channel, in the other three channels no effect was observed. Treatment with Cd^{2+} produces a large decrease of current in the open state of D413C channel (55±5%) and in the closed state of A403C (85±10%), A404C (75±8%), A406C (100%), F408C (100%) and Q417C (95±5%). A small effect was observed in H420C channel in the close state (17±3%) and no effect was observed in the other mutants.

	Cd^{2+} open state	*Cd^{2+} closed state*	*MTSET open state*	*MTSET close state*
A403C	0 (n=3)	85±10 (n=3)		
A404C	0 (n=3)	75±8 (n=3)		
R405C	<20 (n=2)	0 (n=2)		
A406C	0 (n=5)	100 (n=5)	0 (n=4)	0 (n=4)
F408C	100 (n=3)	100 (n=3)		
A410C	0 (n=3)	76±3 (n=3)		
D413C	55±5 (n=4)	<20 (n=4)	100 (n=4)	80±2 (n=4)
K416C	<10 (n=4)	0 (n=4)	0 (n=4)	0 (n=4)
Q417C	0 (n=4)	95±5 (n=4)	0 (n=4)	<20 (n=4)
H420C	0 (n=3)	17±3 (n=3)	0 (n=3)	0 (n=3)

Table 3: *Summary of results from the residue in position from A406 to H420. In this table are represented the percentage (%) of block of current in black and the percentage of potentiation of current in blue.*

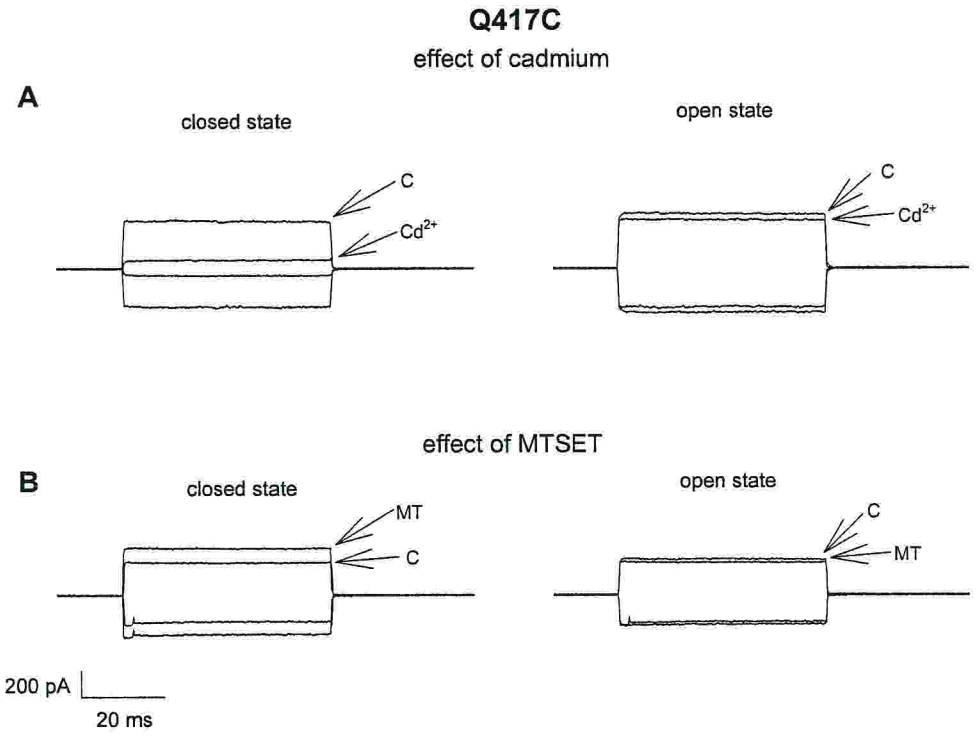

*Fig.37: The effect of Cd^{2+} and MTSET on mutant channel Q417C in the presence and absence of cGMP. **A**: irreversible reduction of the cGMP-gated current caused by 100 µM Cd^{2+} added for 5 min in the closed state (left) in the open state (right). **B**: reduction of the cGMP-gated current caused by 2.5 mM MTSET added for 5 min in the closed state (left) in the open state (right). In A and B voltage steps from 0 to +/- 60 mV. Each trace is the average of 10 individual trials. The cGMP-gated current was obtained as the difference of the current in the presence and in the absence of 1 mM cGMP. C indicates the control current, Cd^{2+} the current after the exposure for 5 min to 100 µM Cd^{2+} MT the current after the exposure for 5 min to 2.5 mM MTSET.*

Residues in the pore helix (position 348, 351)

When I apply 100 μM Cd^{2+} in the inner side of the plasma membrane I do not observe any decrease of current in mutant channel V348C (also referred as V4C) in the open (n=7) and in the closed state (n=7) of the channel (Fig.38A). Also when I apply 2.5 mM MTSET in the intracellular side of the membrane, in the closed (n=7) and in the open state (n=7), I do not observe any change in the amplitude of the current (Fig.38B).

Therefore I conclude that this residue is not accessible to Cd^{2+} and MTSET from the inner side of the plasma membrane. Instead, if I apply the same concentration of MTSET in the outer site of the membrane (in this case the MTS compound is added to the solution contained in the patch pipette) I observe a different behaviour: in particular in the closed state a complete block (100% in 5 minutes of application; n=7) of current is observed (Fig.39A). Also in the open state I observed a block of the cGMP-activated current but occurring in a longer time; after 10 minutes of perfusion in the presence of 2.5 mM MTSET in the extracellular medium I observed a partial block of about but 45±6% (n=7) (Fig.39A). This suggests that the residue in position 348 is accessible from the outer site of the membrane both in the open and closed state: however in the closed state residue in position 348 is more accessible to extracellular MTSET. The same results are obtained measuring the single current (Fig.40).

These results are summarised in Fig.41A. In the figure I plotted the current decrease in inside-out patch in presence and in the absence of cGMP and in presence of saturating concentration of cGMP and in the continuos presence of 2.5 mM MTSET in the external side of the plasma membrane. Initially 1 mM cGMP was continuously present in the intracellular medium and a relative small decline of the cGMP-activated current was observed. When cGMP was removed from the intracellular medium and was briefly added again for 10 seconds when the cGMP activated was measured, the cGMP activated current disappeared irreversibly within a few minutes.

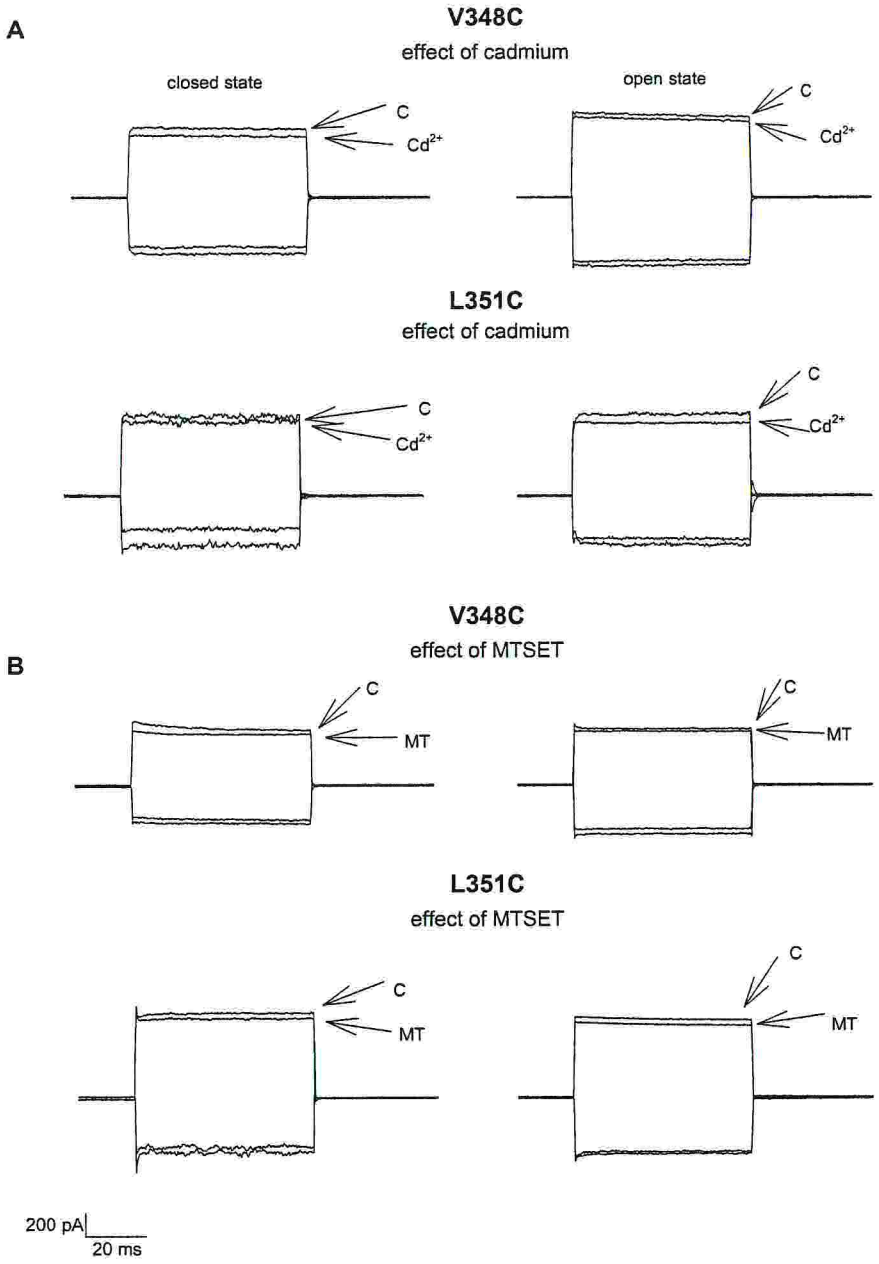

Fig.38: *The effect of Cd^{2+} and MTSET on mutant channels V348C and L351C in the presence and absence of cGMP.* ***A****: reduction of the cGMP-gated current caused by 100 µM Cd^{2+} added for 5 min in the closed state (left) in the open state (right).* ***B****: reduction of the cGMP-gated current caused by 2.5 mM MTSET added for 5 min in the closed state (left) in the open state (right). In A and B voltage steps from 0 to +/- 60 mV. Each trace is the average of 10 individual trials. The cGMP-gated current was obtained as the difference of the current in the presence and in the absence of 1 mM cGMP. C indicates the control current, Cd^{2+} the current after the exposure for 5 min to 100 µM Cd^{2+} MT the current after the exposure for 5 min to 2.5 mM MTSET.*

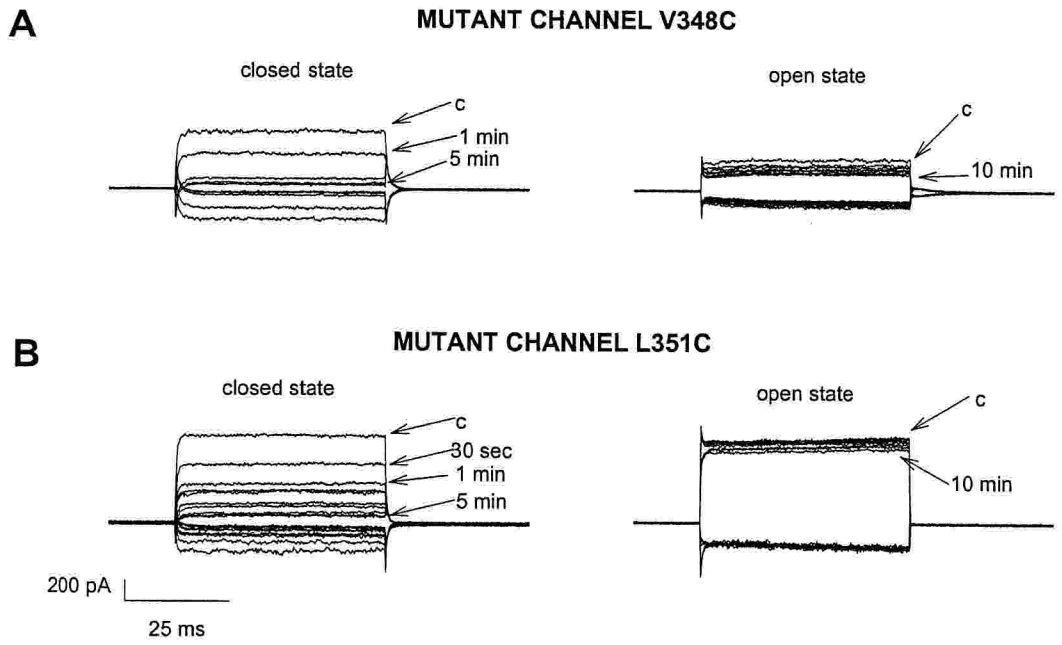

Fig.39: *The effect of MTSET applied in the outer site of plasma membrane on mutant channels V348C and L351C in the presence and absence of cGMP.* ***A****: reduction of the cGMP-gated current caused by 2.5 mM MTSET in the closed state (left) in the open state (right).* ***B****: reduction of the cGMP gated current caused by 2.5 mM MTSET in the closed state (left) in the open state (right). In A and B voltage steps from 0 to +/- 60 mV. Each trace is the average of 10 individual trials. The cGMP-gated current was obtained as the difference of the current in the presence and in the absence of 1 mM cGMP.*

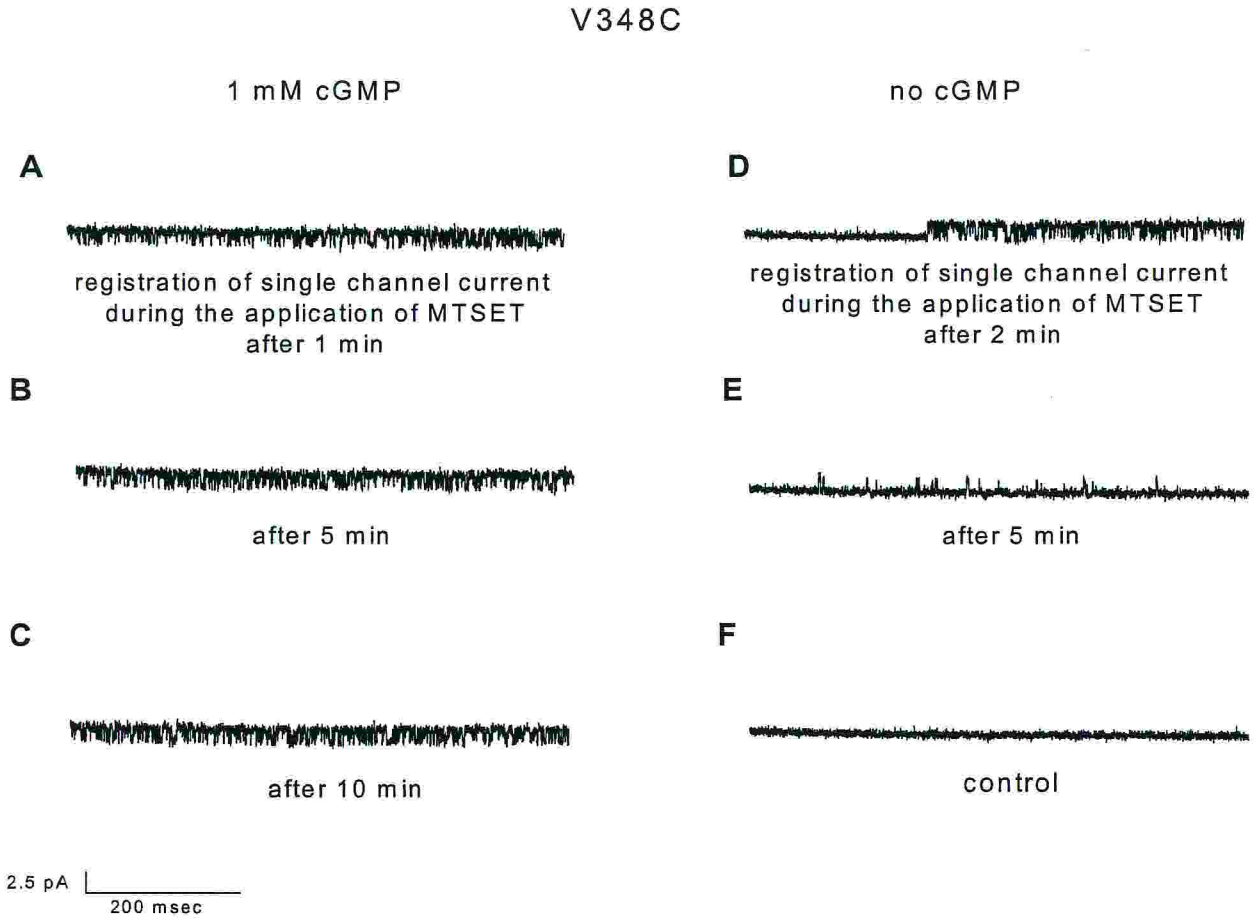

Fig.40: *The effect of MTSET applied in the outer site of plasma membrane on mutant channel V348C in the presence and absence of cGMP.* ***A***, ***B*** *and* ***C****: reduction of the cGMP-gated current caused by 2.5 mM MTSET in the open state.* ***D***, ***E*** *and* ***F****: reduction of the cGMP-gated current caused by 2.5 mM MTSET in the closed state. In A, B, C, D E and F voltage steps from 0 to -100 mV.*

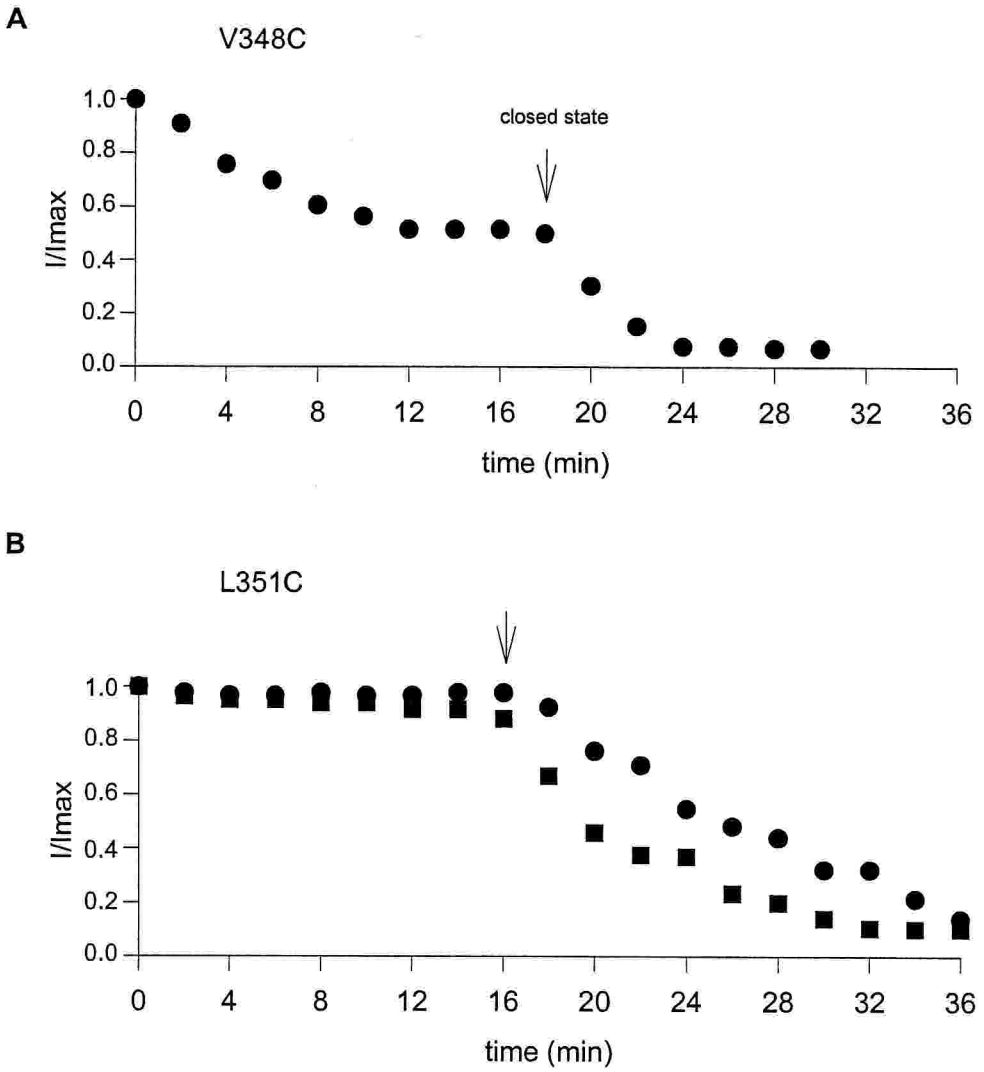

*Fig.41: Time course of V348C and L351C mutant channels. All the plots represent the time course in the open and in the closed state in presence of 2.5 mM MTSET outside the patch membrane. **A** and **B** are the effect in V348C and L351C mutant channels, respectively. The arrows represent the moment in which the channel was closed. In B are plotted the results of two different experiments. The effect of MTSET in open and closed state was tested in the same patch.*

A different behaviour was observed with mutant channel L351C (named also L7C) (Fig.39B). In particular when I add 2.5 mM MTSET in the extracellular site of the plasma membrane, in the open state I do not observe any block of current after 10 minutes (n=7), whereas in the closed state the block of current is slow but complete: in 20 minutes the percentage of block is 100% (n=7). Also in this case the results are better summarised in Fig.41B. In this figure I have plotted the current decrease in inside-out patch in presence and in the absence of saturation concentration of cGMP, but in the continuos presence of 2.5 mM MTSET in the external side of the plasma membrane.

As shown in Fig. 41B extracellular MTSET (2.5 mM) did not appreciably block the mutant channel L351C in the open state, but when cGMP was removed from the medium bathing the cytoplasmic side of the patch, MTSET blocked the mutant channel L351C. Extracellular MTSET blocked the mutant channel V348C, as shown in Fig.41A, both in the open and closed state, but the blocking rate was significantly higher in the closed state. When the excised patch contained only one cGMP activated channel it is possible to monitor in time MTSET blockage. In the presence of 1 mM cGMP in the medium bathing the cytoplasmic side of the membrane and 2.5 mM MTSET in the patch pipette, the mutant channel L351C was most of the time in open state and the open probability was 0.91. With time the open probability decreased but channel openings had the same amplitude and finally after 5 minutes, no channel opening were observed. Similar results were observed with patches containing a single mutant channel Val348C. These results indicate that extracellular MTSET blocks mutant channels V348C and L351C by reducing the open probability and not the single channel conductance, suggesting that Val348 and Leu351 are part of the channel gate. Liu and Siegelbaum (2000) have shown that also Leu358 and Thr355 are accessible to extracellular MTSET in the open state, but Thr355 is not accessible in the closed state. Becchetti et al. (1999) have shown that Trp353 is accessible to intracellular MTSET equally well in the closed and open state.

Residues in the inner pore (position 359, 360 and 361)

I observed a different behaviour in mutant channel T359C (named also T15C) (Fig.42). The application of 100 μM Cd^{2+} in the open (n=6) and in the closed state (n=6) from the inner side of the plasma membrane does not produce any blockage of current. When MTSET is added to the intracellular medium, potentiation of current is observed both in open (n=6) and closed state (n=6) of channel. Instead, the application of the same concentration of this MTS compounds from the outside of the membrane does not produce any significant modification of current (Fig.43A)

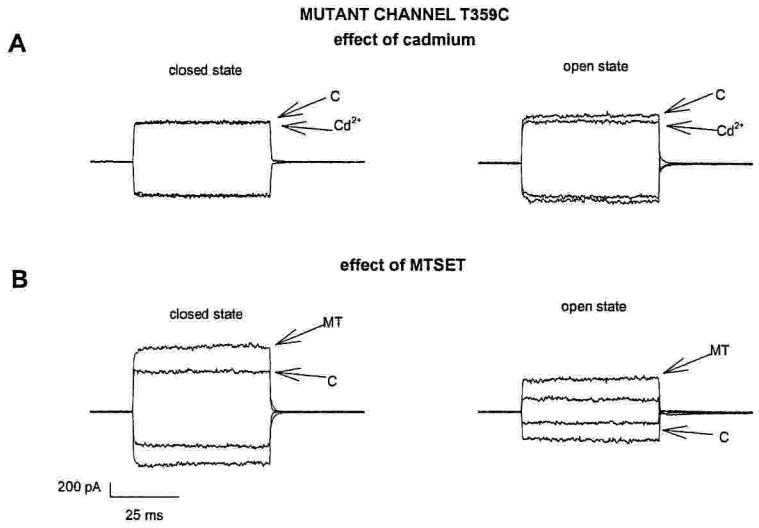

Fig.42: *The effect of Cd^{2+} and MTSET on mutant channel T359C (named also T15C) in the presence and absence of cGMP.* ***A****: reduction of the cGMP-gated current caused by 100 μM Cd^{2+} added for 5 min in the closed state (left) in the open state (right).* ***B****: reduction of the cGMP-gated current caused by 2.5 mM MTSET added for 5 min in the closed state (left) in the open state (right). In A and B voltage steps from 0 to +/- 60 mV. Each trace is the average of 10 individual trials. The cGMP-gated current was obtained as the difference of the current in the presence and in the absence of 1 mM cGMP. C indicates the control current, Cd^{2+} the current after the exposure for 5 min to 100 μM Cd^{2+} MT the current after the exposure for 5 min to 2.5 mM MTSET.*

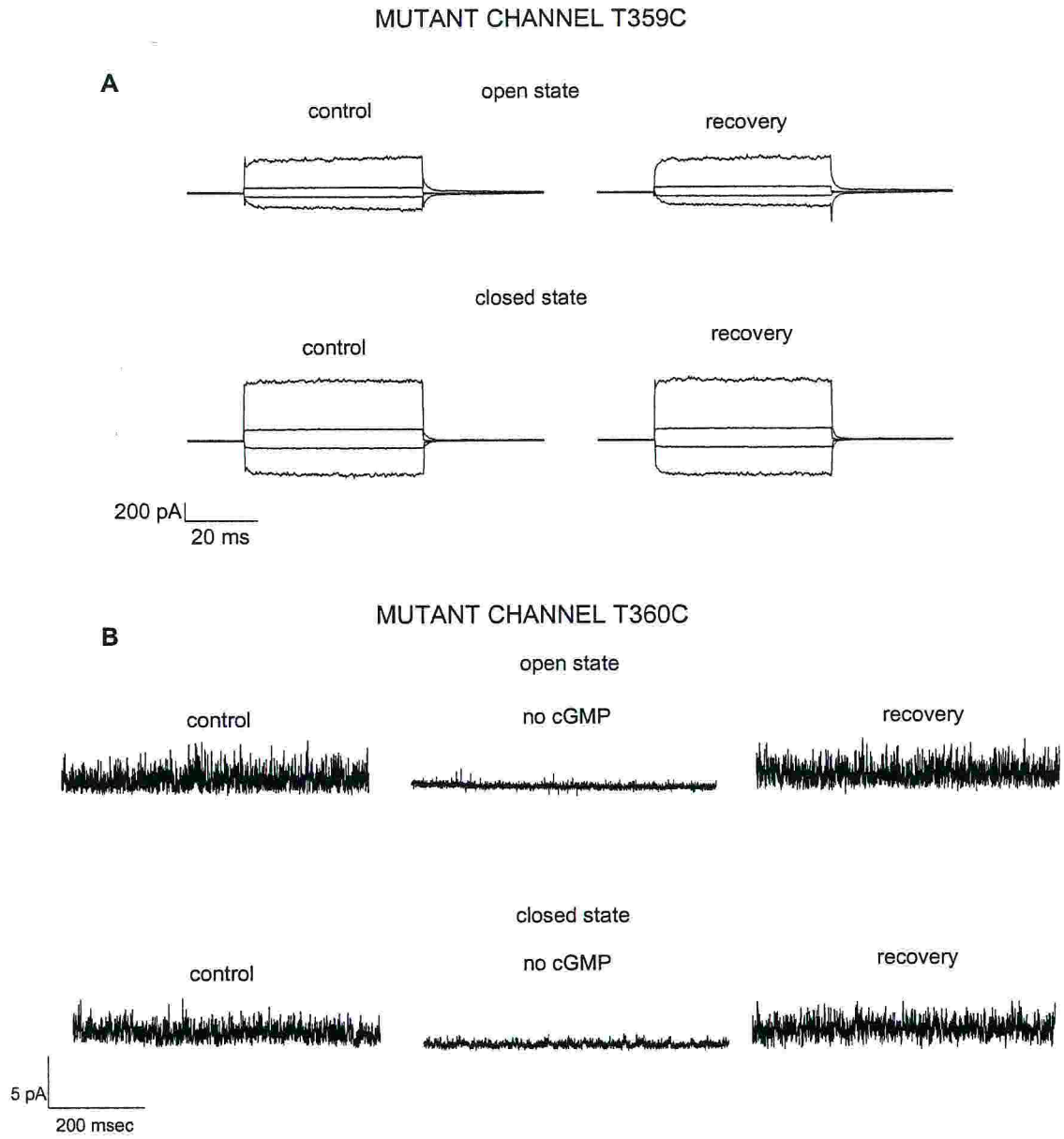

Fig.43: *The effect of MTSET applied in the outside of the plasma membrane on mutant channels T359C and T360C in the presence and absence of cGMP.* ***A****: effect on the macroscopic cGMP-gated current caused by 2.5 mM MTSET added for 15 min in the closed state (bottom) in the open state (top). Each trace is the average of 10 individual trials.* ***B****: effect on single-channel openings of cGMP-gated channels caused 2.5 mM MTSET added for 15 min in the closed state (bottom) in the open state (top). In A voltage steps from 0 to +/- 60 mV. Each trace is the average of 10 individual trials. The cGMP-gated current was obtained as the difference of the current in the presence and in the absence of 1 mM cGMP. In B voltage steps from –100 to –180 mV.*

The mutant channel T360C (named also T16C) (Fig.44) has a different behaviour in the closed and open state after the application from the inner side of the 100 μM Cd^{2+}. In particular, in the closed state (n=6) no blockage of the cGMP-activated current is observed, as observed in mutant channel T359C, whereas in the open state the application of Cd^{2+} produce a complete but reversible block of current (n=6). As in mutant channel T359C, application of MTSET from the inner side produce a potentiation of current both in the open (n=6) and in the closed state (n=6). When MTSET was applied from the extracellular side of the membrane no significant modification of the cGMP-activated current was observed (Fig.43B).

The cGMP-activated current of mutant channel I361C (named also I17C), after the patch excision, spontaneously decay (data not show). This behaviour is probably due to the formation of disulphide bridges between the inserted cysteines, suggesting that the distance between these neighbouring and opposing residues is small so that -S-S- bridges are spontaneously formed.

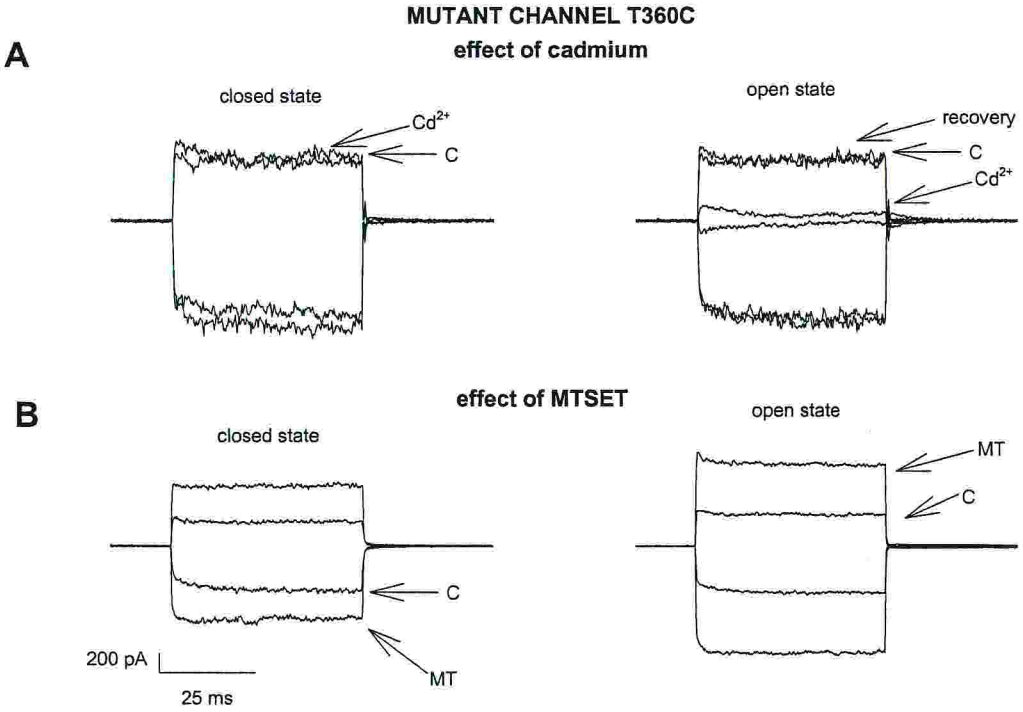

Fig.44: *The effect of Cd^{2+} and MTSET on mutant channel T360C (named also T16C) in the presence and absence of cGMP.* ***A****: reduction of the cGMP-gated current caused by 100 μM Cd^{2+} added for 5 min in the closed state (left) in the open state (right).* ***B****: reduction of the cGMP-gated current caused by 2.5 mM MTSET added for 5 min in the closed state (left) in the open state (right). In A and B voltage steps from 0 to +/- 60 mV. Each trace is the average of 10 individual trials. The cGMP-gated current was obtained as the difference of the current in the presence and in the absence of 1 mM cGMP. C indicates the control current, Cd^{2+} the current after the exposure for 5 min to 100 μM Cd^{2+} MT the current after the exposure for 5 min to 2.5 mM MTSET.*

The observed potentiation in mutant channels T359C and T360C does not necessarily report a direct action of MTSET on the exogenously introduced cysteine, because MTSET is known to potentiated also the wt channel (Brown et al., 1998). Indeed, 2.5 mM MTSET significantly shift the dose response curve to cGMP of the wt channel, by binding to the native cysteine 481 located in the C-linker of the channel. MTSET potentiation of the wt is much faster when MTSET is added in the presence of 1 mM cGMP, i.e. when the channel is open. The same effect was observed in presence of MTSEA, a MTS compound positively charged but smaller then MTSET. Potentiation of the wt channel is not observed when the positively charged MTSET is replaced by the similar compound MTSES, but negatively charged. Fig.45 and Fig.46 illustrate the results of the experiments of T359C and T360C when MTESEA (2.5 mM) and MTSES (2.5 mM and 10 mM) replaced MTSET (2.5 mM). In this case potentiation was observed only in mutant channel T360C and not in mutant channel T359C. MTSES potentiation of mutant channel T360C was observed when MTSES was added in the presence and in the absence of cGMP in the bathing medium. In Fig.47 there is a plot in which there is the comparison between the three different MTS compounds. As a consequence MTSES potentiation is not state dependent: indeed the time course of potentiation was indistinguishable when the channel was either open or closed. The results of these experiments strongly suggest, but not yet prove, that the potentiation effect of MTSES is mediated by a direct binding of the compound to the exogenous cysteine introduced in position 360.

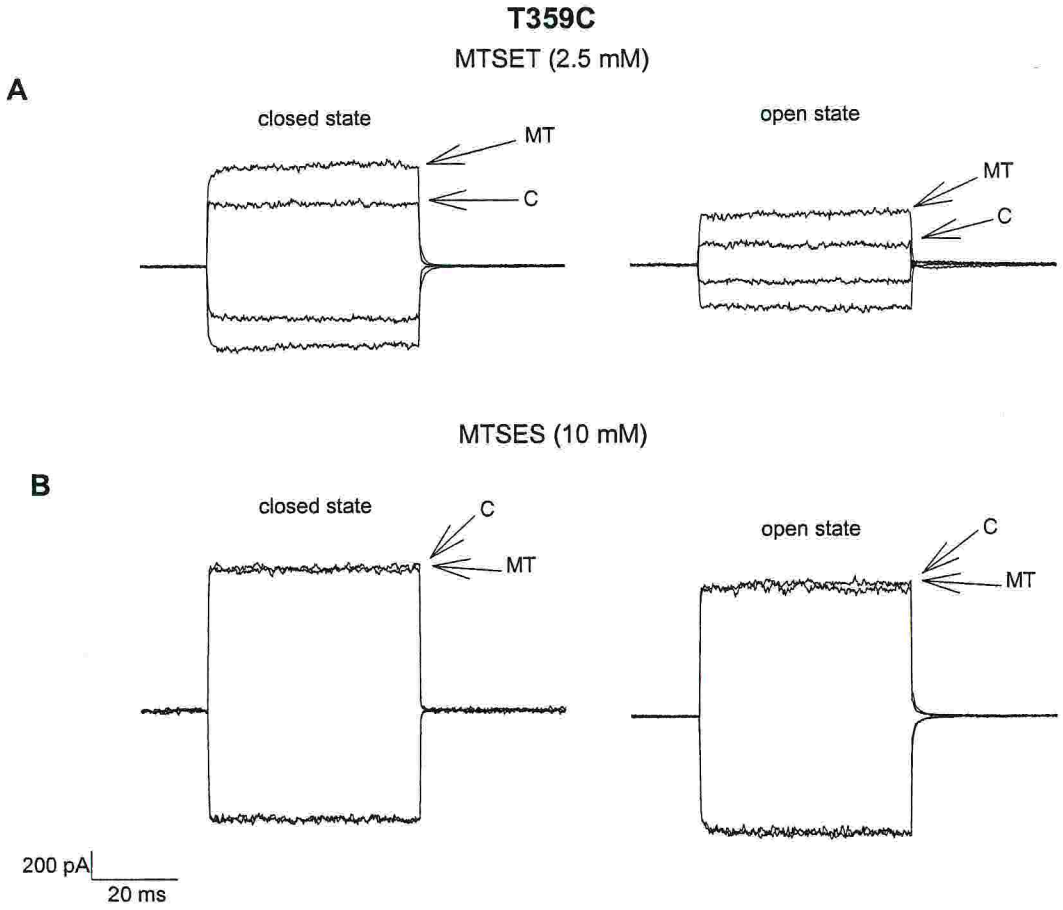

Fig.45: *The effect of MTSET and MTSES on mutant channel T359C in the presence and absence of cGMP.* ***A****: the effect of 2.5 mM MTSET added for 2 minutes in the absence (left) and in the presence of 1 mM cGMP (right) in mutant channels T359C.* ***B****: the effect of 10 mM MTSES added for 2 minutes in the absence (left) and in the presence of 1 mM cGMP (right) in mutant channels T359C In A and B voltage steps from 0 to +/- 60 mV. Each trace is the average of 10 individual trials. The cGMP-gated current was obtained as the difference of the current in the presence and in the absence of 1 mM cGMP.*

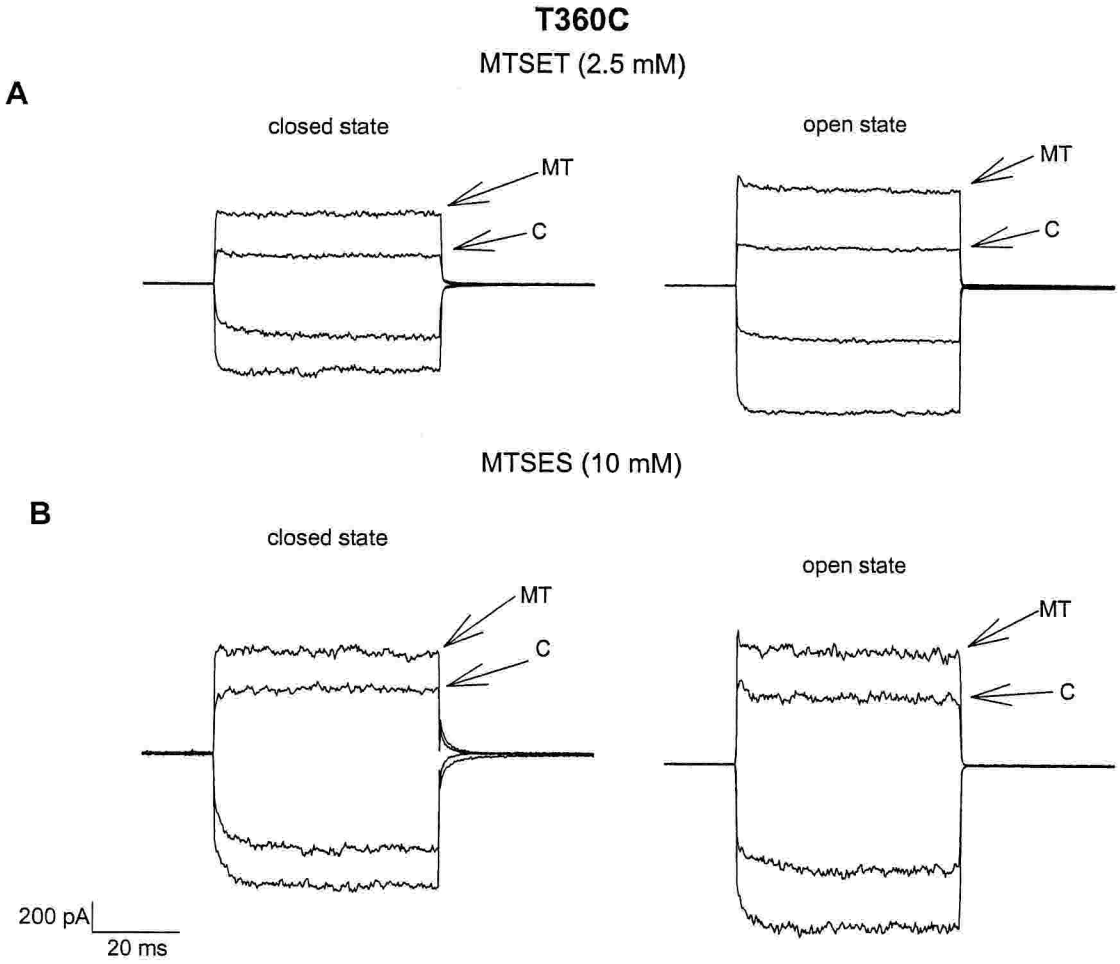

Fig.46: *The effect of MTSET and MTSES on mutant channel T360C in the presence and absence of cGMP.* ***A****: the effect of 2.5 mM MTSET added for 2 minutes in the absence (left) and in the presence of 1 mM cGMP (right) in mutant channels T360C.* ***B****: the effect of 10 mM MTSES added for 2 minutes in the absence (left) and in the presence of 1 mM cGMP (right) in mutant channels T360C In A and B voltage steps from 0 to +/- 60 mV. Each trace is the average of 10 individual trials. The cGMP-gated current was obtained as the difference of the current in the presence and in the absence of 1 mM cGMP.*

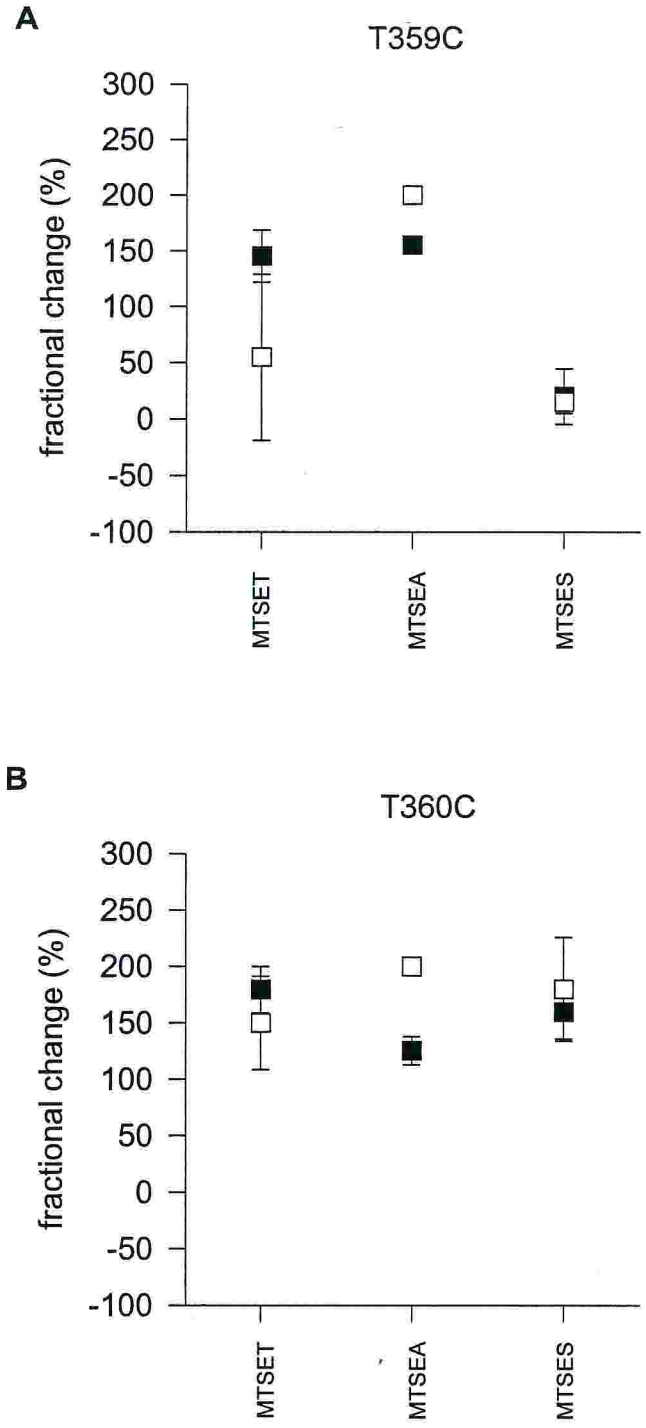

Fig.47: *Fractional potentiation induced by MTSET, MTSEA and MTSES on mutant channels T359C and T360C in the presence and absence of cGMP.* ***A****: the effect of MTS compounds added for 2 minutes, in the absence (closed square) and in the presence of 1 mM cGMP (open square) in mutant channel T359C.* ***B****: the effect of MTS compounds added for 2 minutes, in the absence (closed square) and in the presence of 1 mM cGMP (open square) in mutant channel T360C. In A and B the error bars indicate the standard deviation. Each point was obtained from at least six patches excised from at least two different injected oocytes.*

Cd^{2+} ions are useful probe for the accessibility of native and exogenous cysteines (Becchetti and Gamel, 1999; Becchetti and Roncaglia, 2000; Rothberg et al., 2002). A Cd^{2+} ion by coordinating to two or more cysteines can bind very tightly to cysteines with an affinity varying between 10 and 100 μM (Becchetti and Roncaglia, 2000). Fig.49 illustrates the effect of treating the channel mutant T360C with micromolar amount of Cd^{2+} for 2 minutes in the closed and open state (Fig.48)

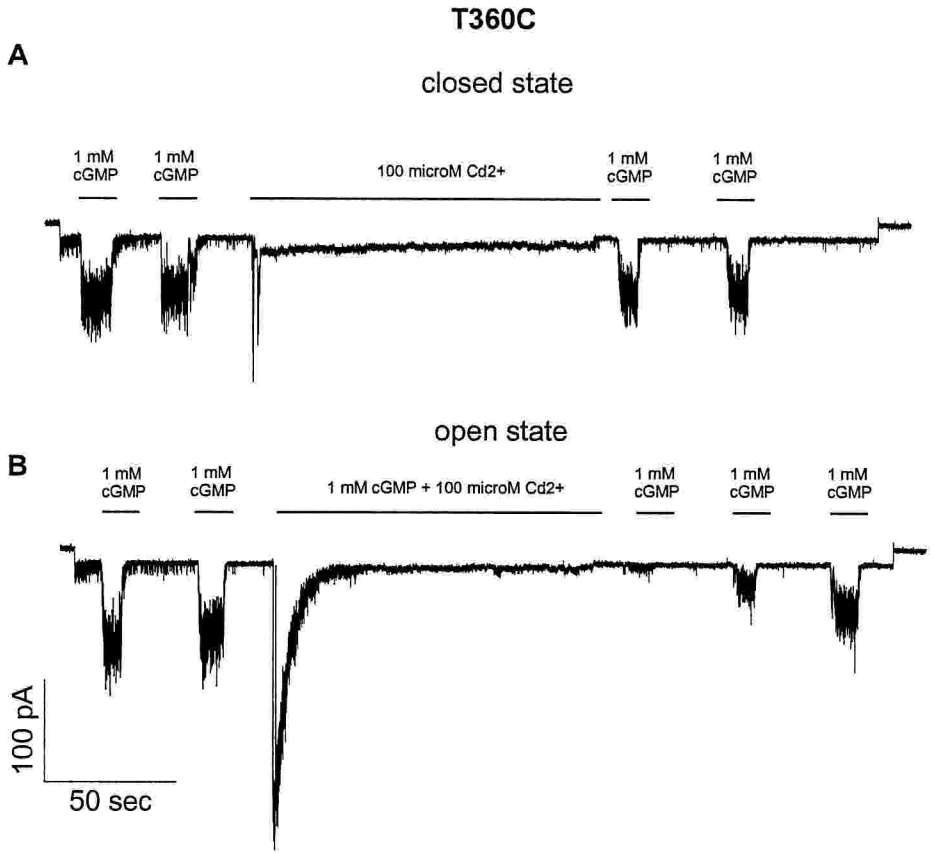

Fig.48: *Effect of 100 μM Cd^{2+} on mutant channels T360C in the open and closed state.* ***A****: the effect of Cd^{2+} added for 2 minutes, in the absence of 1 mM cGMP.* ***B****: the effect of Cd^{2+} added for 2 minutes in the closed presence of 1 mM cGMP.*

When 1 μM Cd^{2+} was added to the intracellular medium, the cGMP-activated current was immediately potentiated and no significant effect on the current was observed when Cd^{2+} was removed from the intracellular medium (Fig.49). When 10 μM was added for 2 minutes, after Cd^{2+} removal the cGMP-activated current was transiently reduced (Fig.49) and was completely blocked when a Cd^{2+} concentration larger than 20 μM was used. Cd^{2+} blockage was reversible, after washing in a Cd^{2+} free solution for more than 3 minutes or so. As shown in Fig.49 the concentration blocking half of the cGMP-activated current was about 10 μM. No significant blockage was observed when the same experiments were repeated with wt channels or mutant channels T359C (Fig.50). When Cd^{2+} was added to the intracellular medium in the absence of cGMP, no blockage was observed for Cd^{2+} concentration below 100 μM, for wt and mutant channels T359C and T360C (Fig.49 and Fig.50).

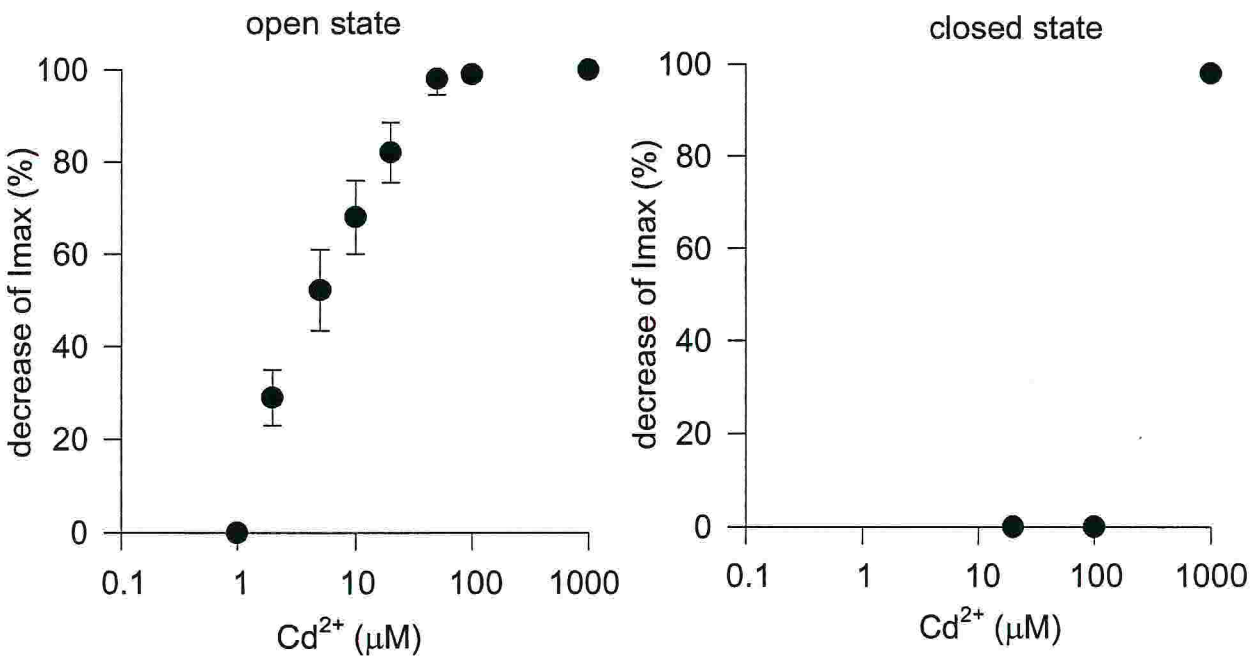

Fig.49: Stoichiometry of Cd^{2+} on mutant channel T360C in the open and closed state. Each point was obtained from at least four patches excised from at least two different injected oocytes.

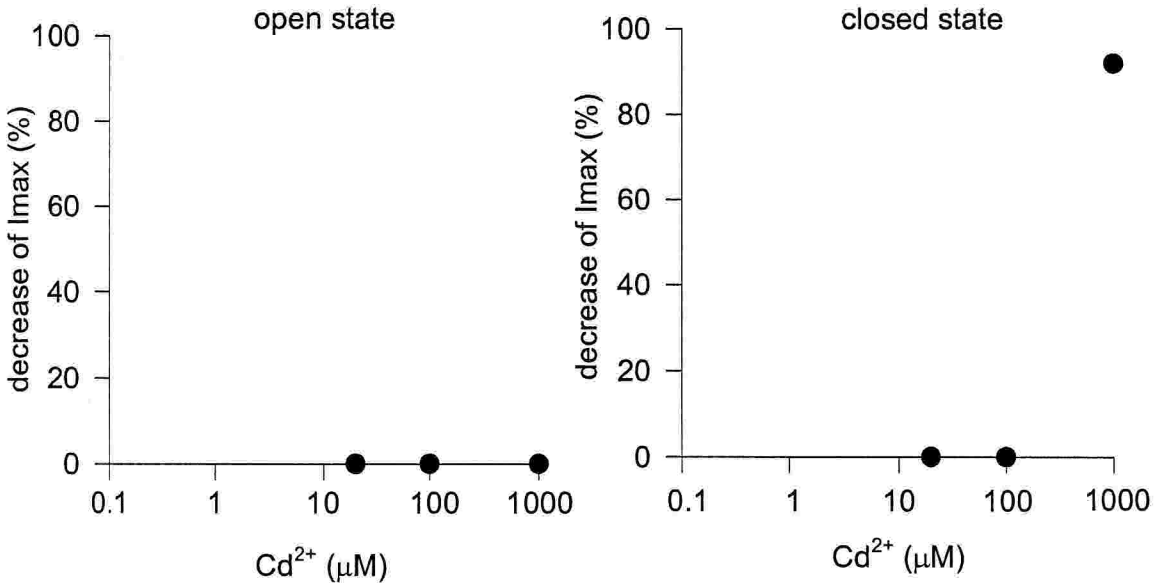

Fig.50: *Stoichiometry of Cd^{2+} on mutant channel T359C in the open and closed state. Each point was obtained from at least four patches excised from at least two different injected oocytes.*

1 mM Cd^{2+} irreversibly blocked the wt and mutant channels T359C and T360C when added in the absence of cGMP, but did not blocked the wt and mutant channel T359C when added in the presence of 1 mM cGMP (Fig.49 and Fig.50). These results indicate multiple actions of Cd^{2+}. At low concentrations around 1 μM potentiate the wt and mutant channels T359C and T360C probably by interacting with an endogenous cysteine, possibly cysteine 481. At the higher concentration around 10 μM Cd^{2+} binds to the cysteines exogenously introduced in mutant channel T360C in the open state. At the concentration of 1 mM Cd^{2+} blocks the wt channel through a low affinity binding, possibly located in the cyclic nucleotide binding domain as blockage is antagonised by the presence of 1 mM cGMP. If the potentiation of mutant channel T360C by MTSES is mediated by a direct binding of MTSES to the cysteines introduced in position 360, MTSES is expected to protect the mutant channel T360C from Cd^{2+} blockage observed in the open state. Before to test the effect of this compound I analyse the effect in the wt channel and in the T369C mutant channel (Fig.51).

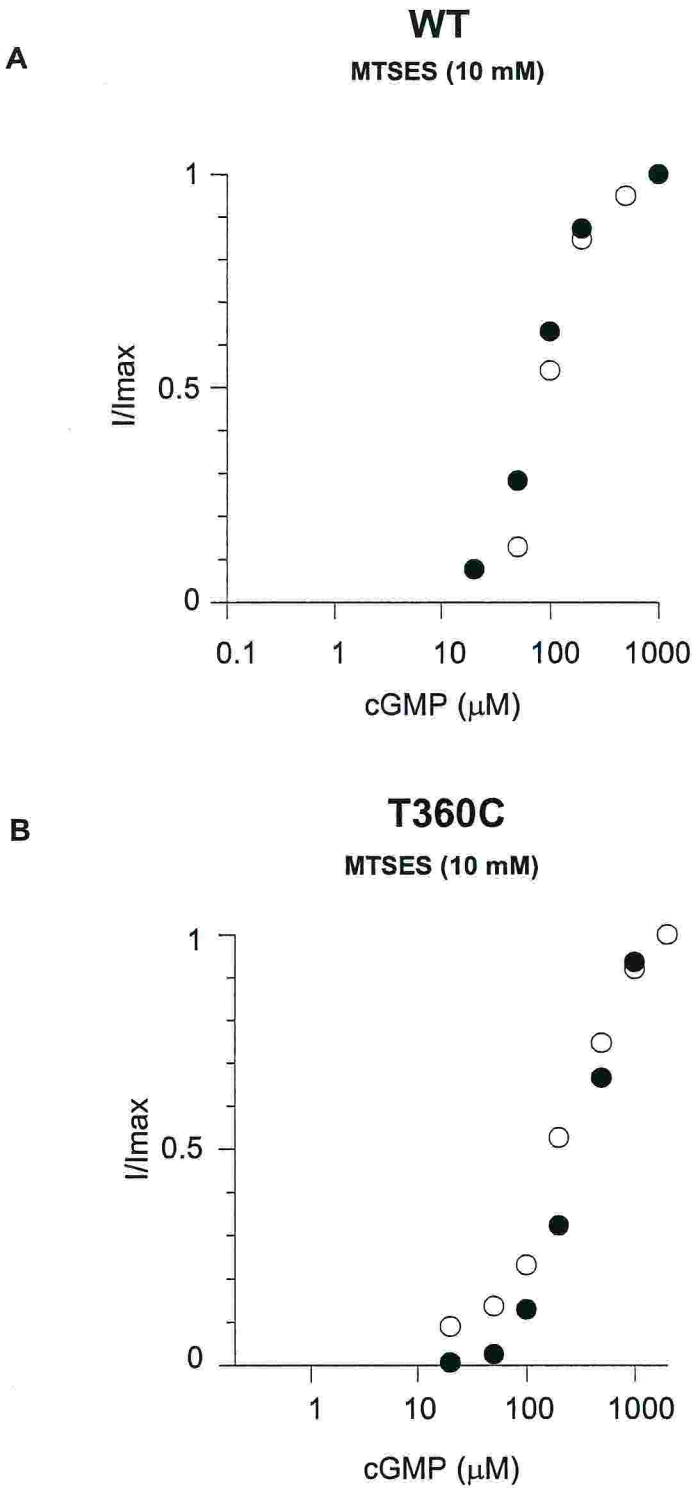

Fig.51: *Stoichiometry of cGMP on WT and in mutant channel T360C in the open state.* ***A:*** *dose-response of cGMP in the wt channel before (open circle) and after (closed circle) the application of 10 mM MTSES for 5 min;* ***B:*** *dose-response of cGMP in the mutant channelT360C before and after the application of 2.5 mM MTSET for 5 min. Each point was obtained from one excised patch.*

Besides pre-treating the patch with MTSES, it is possible to add to the intracellular medium simultaneously MTSES and Cd^{2+}. With this protocol the blocking effect of 10 μM Cd^{2+} (or a higher concentration) is first measured (Fig.52) and after washing out Cd^{2+} and returning to the original amplitude of the cGMP activated current the potentiating effect of 10 mM MTSES was measured. As shown in Fig.52, when Cd^{2+} is added to the intracellular medium in the presence of MTSES, the cGMP activate current was initially potentiated as in the absence of MTSES, indicating that 10 mM MTSES did not chelate Cd^{2+}. When Cd^{2+} was removed from the intracellular medium the cGMP activated current was only slightly reduced, showing that MTSES indeed protected mutant channel T360C from Cd^{2+} blockage observed in the open state.

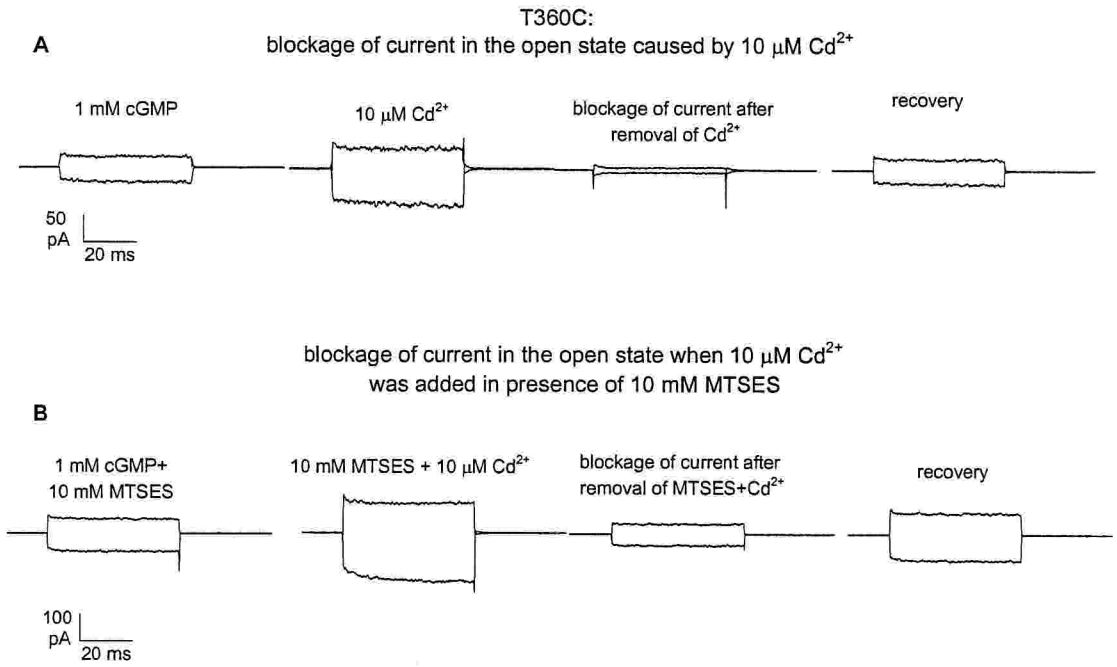

Fig.52: *Effect of 10 μM Cd^{2+} in mutant channel T360C in the open* ***A:*** *effect of cadmium before the application of 10 mM MTSES (solution containing MTSES +Cd^{2+}).* ***B:*** *effect of cadmium after the application of 10 mM MTSES (solution containing MTSES +Cd^{2+}).*

In the presence of 10 mM MTSES the K_D of Cd^{2+} blockage increased from about 10 to 35 μM (Fig.53). These results show that MTSES and Cd^{2+} ions compete for the same binding site. Therefore the potentiation induced by MTSES is caused by a direct binding of the compound to the cysteine exogenously introduced in the mutant channel T360C. The results not only show that MTSES is able to reach in the inner vestibule both in the closed and open state, but indicate that residue in position 360 in the pore moves during channel gating.

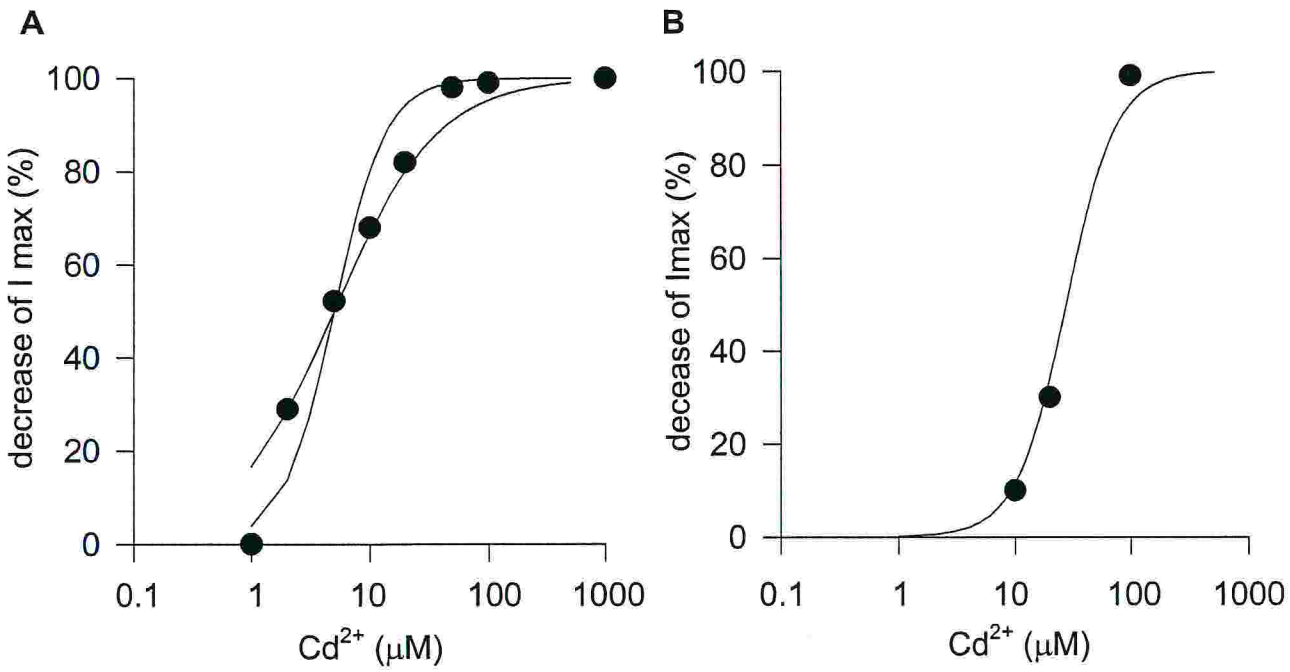

Fig.53: *Stoichiometry of Cd^{2+} in mutant channel T360C in the open state.* ***A:*** *dose-response of Cd^{2+} before the application of 10 mM MTSES for 5 min;* ***B:*** *dose-response after the application of 10 mM MTSES for 5 min. Each point was obtained from one excised patch.*

DISCUSSION AND CONCLUSIONS

In this final part of my thesis, I will discuss the experimental results that I have obtained. I will first discuss the CNBD region and in particular the C-helix and secondly the pore region comprising the pore walls, the S6 transmembrane domain and the P helix. A new model of their structural organisation will be presented and possible conformational changes occurring during the gating will be proposed.

1-Cyclic nucleotide binding domain

The current reduction induced by Cd^{2+} and CuP, is better summarized and rationalized when mapped on an ideal alpha helix and the degree of blockage of the cGMP-gated current in the corresponding cysteine mutant is shown in a color coded scale, as shown in Figs 54A and B. Red indicates reduction higher than 30%, blue indicates the absence of a significant reduction lower than 30%, white indicates residues where the corresponding cysteine mutant did not produce functional channels with a cGMP gated current.

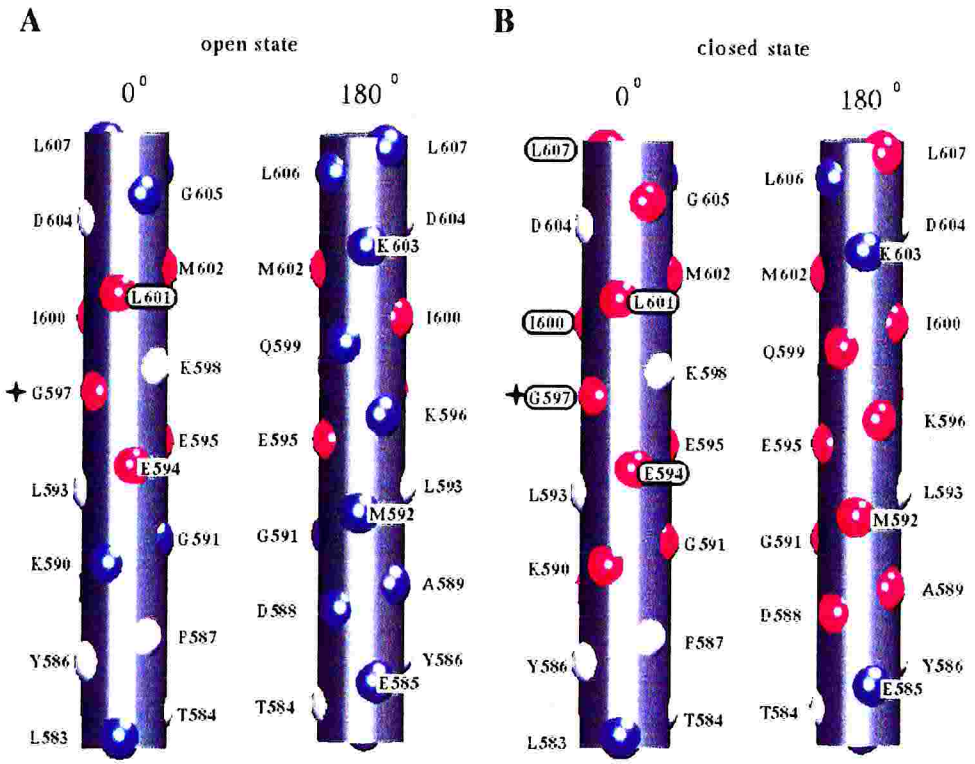

Fig.54: *Map of Cd^{2+} blockage of cysteine mutants from Leu583 to Lys607. In each panel current reduction is shown in a color-coded map (red indicates reduction higher than 30%, blue between 0 and 30%, white indicates residues where the corresponding cysteine mutant did not produce functional channels with a cGMP gated current) with residues located on an ideal alpha helix. Two views of the alpha helix, rotated by 180 degrees around its symmetry axis, are shown. **A**: current reduction in the presence of 1 mM cGMP. **B**: current reduction in the absence of cGMP. The black circles indicate residues where the corresponding cysteine mutant was significantly (more than 40%) blocked by 2.5 mM MTSET. Gly597 is marked with a star since the current of mutant channel G597C is reduced by less than 30% by Cd^{2+} and ~70% by CuP.*

As clearly shown in Fig.54A, the current reduction induced by Cd^{2+} on cysteine mutants in the open state is well localized on one side of the helix covering three turns of the helix from Glu594 to Leu601. The blocking effect of CuP has a similar pattern, with the largest decrease coinciding with that one of Cd^{2+}. The only exception is mutant channel G597C, where CuP excised a fairly stronger current reduction (67±7%) than Cd^{2+} (23±4%). As previously stated, this could be explained by a low accessibility of Gly597 to Cd^{2+}. On the contrary, the current reduction caused by Cd^{2+} and CuP in the closed state is rather diffuse and it is significant for the majority of cysteine mutants from Asp588 to Leu607 (Fig.54B). Sulfhydryl reagents did not have any effect on cysteine mutants downstream to Pro587. In the open state, MTSET caused a current reduction only for the Leu601 cysteine mutant. In the closed state, a current decrease, larger than 40%, caused by MTSET was observed only in cysteine mutants Leu607, Leu601, Ile600, Gly597 and Glu594. Therefore, in the open state the effect of Cd^{2+} and CuP among these mutants coincides almost completely with that of MTSET in the closed state with the exception of Leu607.

The different action of MTSET and by Cd^{2+} and the similar action of Cd^{2+} and CuP in the open state can be rationalized by their different interaction with cysteine mutants. One molecule of MTSET forms a disulfide bond with the thiol group of a single cysteine molecule, whereas one Cd^{2+} atom is usually coordinated by two or more (up to four) cysteines and CuP enhances the formation of disulfide bonds among two cysteines. A Cd^{2+} ion has an approximate diameter of 1.82 Å (Glusker, 1991). Inspection of the 3D structure of metallothioneins deposited in the Protein Data Bank (Berman et al., 2000) indicates that the distance between a Cd^{2+} ion and the sulfur atom of a coordinating cysteine is about 2.5 Å and that distances between the C_α of two cysteines coordinating the same Cd^{2+} ion ranges between 4 and 9 Å (Krovetz et al., 1997; Ermler et al., 1998; Maroney, 1999). The distance between the C_α of two cysteines forming a disulfide bond ranges between 4 and 6.5 Å (Srinivasan et al., 1990). Given the thermal fluctuations of the protein, the maximum distance between the C_α of two cysteines able to form a disulfide bond or to coordinate one Cd^{2+} ion (establishing bonds at the previously reported distances) can be estimated as being around 10 Å

(Johnson and Zagotta, 2001; Careaga and Falke, 1992; Krovetz et al., 1997; Ermler et al., 1998; Maroney, 1999).

The space occupied by a molecule of MTSET is approximately a cylinder with a diameter of 6 Å and a height of 10 Å (Akabas et al., 1992). These distances and the observed effect of the used sulfhydryl reagents will be used to understand the experimental data and to develop a model of the relative location of two C-helices in the open state.

Current reduction in the open state

The clear action of Cd^{2+} and CuP in the open state when residues are mapped on an ideal alpha helix (see Fig.54A) has two major implications. Firstly it gives the evidence that in the open state residues from Asp588 to Leu607 have the secondary structure of an alpha helix. Such a secondary structure was previously assumed to be in analogy with the 3D structure of CAP, but was not supported by any direct experimental evidence. These data, therefore, provide experimental support to the notion that in the open state these residues form an alpha helix, usually referred to as the C-helix. Secondly it strongly suggests that in the open state C-helices from two subunits come in close contact like CAP. In the open state, the action of Cd^{2+} and CuP suggests that the distance between the C_α of residues Leu601, Ile600, Gly597, and Glu594 of C-helices of two subunits is between 4 and 10 Å. Under these conditions in the corresponding cysteine mutants, disulfide bonds can be formed and Cd^{2+} ions find pairs of neighboring cysteines for an energetically favorable coordination. The formation of these bonds between pairs of neighboring cysteines leads, by constraining the C-helices position, to the disruption of the gating mechanism and the subsequent blockage of the cGMP-gated current.

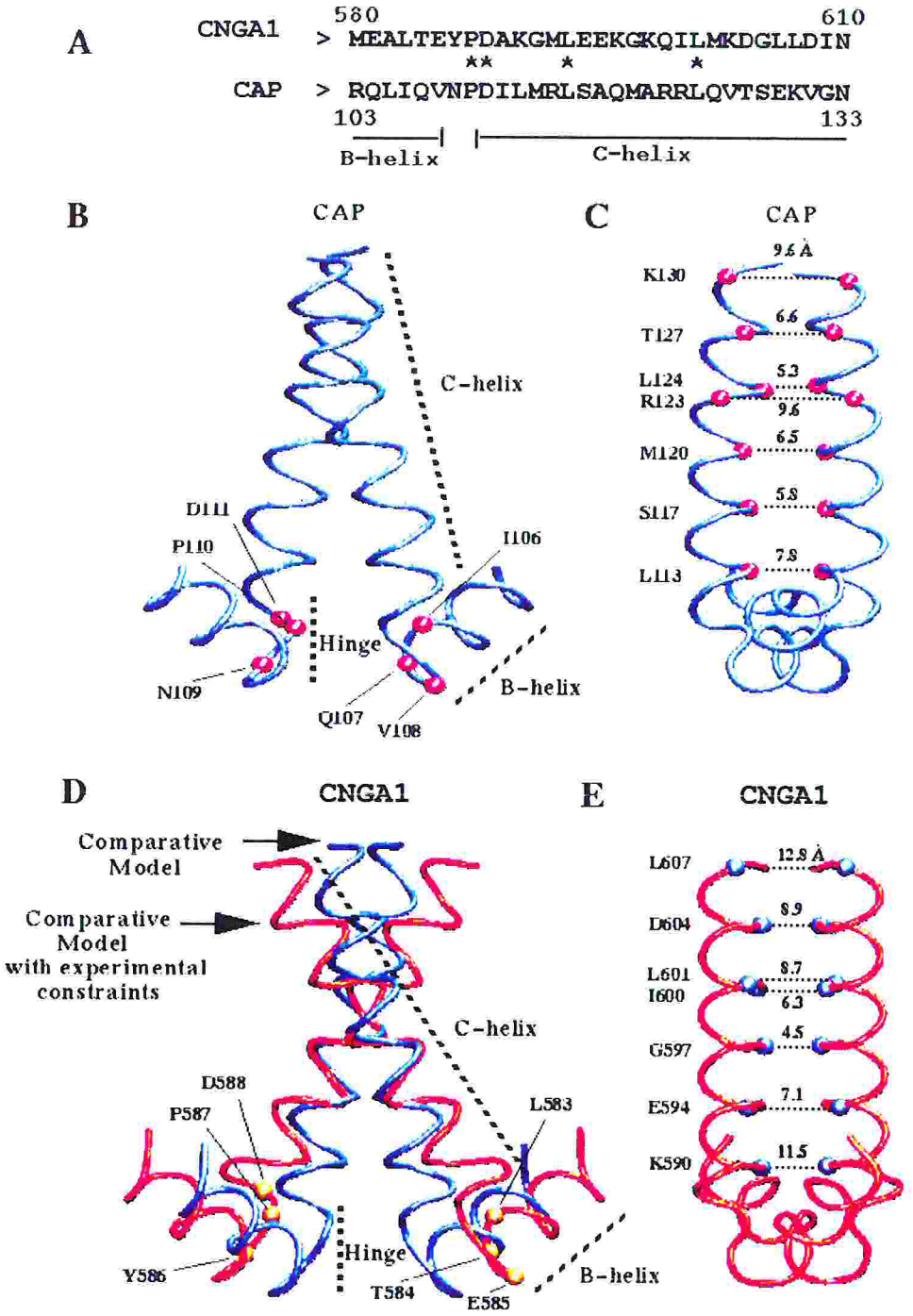

Fig.55: *C-helices in CAP and in CNGA1. **A**: B- and C-helix alignment between CNGA1 and CAP sequences. **B** and **C**: two different views of the 3D location of C-helices in CAP; Cα of the residues at the hinge between B and C-helix (Asn109, Pro110 and Asp111), at the end of the B helix (Ile106, Gln107 and Val108) (B) and at helix-helix interface (Leu113, Ser117, Met120, Arg123, Leu124, Thr127 and Lys130) are shown (C); distances in C are in Angstrom (Å). **D** and **E**: two different views of the putative 3D location of C-helices in the open state of CNGA1. In D, the crossing angle in the comparative model (blue) is compared to that one obtained considering the experimental constraints (red); Cα of the residues at the hinge between B and C-helix (Tyr586, Pro587 and Asp588), at the end of the B helix (Leu583, Thr584 and Glu585) (B) and at helix-helix interface (Lys590, Glu594, Gly597, Ile600, Leu601, Asp604 and Leu607) are shown (E); distances in E are in Angstrom (Å).*

CAP residues forming the C-helix and the hinge with the B helix, from Arg103 to Asn133, are shown in Fig.55A, and are compared to the sequence of residues from Met580 to Asn610 of the CNGA1 channel. Pro110 and Asp111 at the hinge of the B and C-helix of CAP are conserved in the CNGA1 channel and correspond to Pro587 and Asp588. Sequence similarity between CAP and CNGA1 downstream of these two conserved residues is not high. Two views (rotated by 90 degrees around the twofold symmetry axis of the template) of the 3D structure of the two C-helices of CAP and their hinge with B helices are shown in Figs.55B and C. In CAP the two C-helices have their C_α closest contact in correspondence of Leu124, with the C_α at a distance of 5.3 Å. The angle between the two C-helices is about 35°.

If the C-helices of the CNGA1 channel have the same 3D structure of those in CAP using the sequence alignment of Fig.55A the C_α of residues Glu594, Gly597, Leu601 and Asp604 will be at a distance of less than 10 Å in agreement with Cd^{2+} and CuP action in the open state. This comparative model, however, predicts the C_α of Ile600 of two neighboring subunits to be at 12 Å, a distance too high to be in agreement with Cd^{2+} and CuP action on mutant channel I600C. In addition, the comparative model also suggests that the C_α of Leu607 of two neighboring subunits are at 8.5 Å, a distance compatible with a strong Cd^{2+} and CuP on the c-GMP gated current, not experimentally observed.

A way to obtain a better relation between the experimental data and the comparative model of the CNB domain is to increase the crossing angle between the C-helices, as shown in Fig.54D, so that residues Leu601, Ile600, Gly597 and Glu594 of the two C-helices are in close contact. In this case the closest contact between the two C-helices is at Gly597 with the C_α at a distance of 4.3 Å and with the angle between the two C-helices being 60 degrees. With this geometry, the distance between the C_α of Leu607 is 12.8 Å (Fig.55D), too large for the formation of disulfide bond in mutant channel L607C. This distance is compatible with the absence of current reduction by Cd^{2+} and CuP in the mutant channel L607C in the open state.

Residues downstream of Pro587 of two neighboring subunits, such as Glu585 and Leu583, are expected to be rather distant, as mutant channels G585C and L583C are neither affected by Cd^{2+} nor by CuP and they tend to form the B helix of the CNGA1

channel. Residues from Glu585 to Asp588 probably form the hinge between the C and B helices.

The 3D structure of the C-helices shown in Figs.55D and E provides also an explanation for the blocking effect of MTSET. In the open state, MTSET affects only the mutant channel L601C, implying that Leu601 is accessible. Leu601 is indeed at the interface of the two C-helices with a C_α - C_α distance of 8.7 Å and, during its thermal fluctuations, can bind the large compound MTSET. Once bound MTSET is likely to prevent the C-helix from reaching the correct position necessary for triggering channel gating.

Current reduction in the closed state

As summarized in Fig.54B, in the closed state, Cd^{2+} and CuP cause a current decrease in almost all of the cysteine mutants, from Asp588 to Leu607. A significantly lower blockage was observed only in cysteine mutants Leu606, Lys603 and to some extent in MET602, Met592 and Ala589. All these residues, as shown in Fig.54B, are located on the same face of the alpha helix but at the opposite side of those associated with the current reduction of Cd^{2+} and CuP in the open state.

In the closed state, when MTSET binds to the thiol of cysteine mutants the gating mechanism is significantly impaired for mutants L607C, L601C, I600C, G597C and E594C. In the open state Leu601, Ile600, Gly597 and Glu594 are at the interface of the C-helices and, in the closed state, when MTSET binds to the corresponding cysteine mutants, it blocks the motion of the C-helices towards the necessary position for opening the channel. Therefore, the current in residues Leu601, Ile600, Gly597 and Glu594 is decreased by Cd^{2+} and CuP in the open state and by MTSET in the closed state.

In the open state, Leu607 (in the model of Figs.55 D and E) are at a distance of about 13 Å, not enough to accommodate two molecules of MTSET without interfering with the position of the two C-helices. This can provide an explanation for the blockage of MTSET in the closed state of mutant L607C.

In the closed state, MTSET potentiates mutant channels L606C, K603C, K596C and E595C and protects G605C, M602C, I600C and E595C from Cd^{2+} and CuP effect.

Therefore, Leu606, Gly605, Lys603, Met602, Leu601, Ile600, Gly597, Lys596 and Glu595 are accessible to MTSET. Glu594 does not seem to be accessible to MTSET in the closed or in the open state, as the mutant channel E594C is neither potentiated by MTSET nor protected from Cd^{2+} current reduction by MTSET. Mutant channels D604C, K598C and L593C do not produce functional channels with currents gated by cGMP. Asp604 is thought to bind to cGMP and it is expected that the mutation into cysteine is going to be fatal.

The current reduction of Cd^{2+}, CuP and MTSET in the closed state suggest two conclusions: firstly, that in the closed state the great majority of residues from Asp588 to Leu607 are accessible to sulfhydryl reagents, and secondly, that the C-helices undergo a significant rearrangement if it is compared to their open state conformation so that a cysteine introduced in this region could be able to form a disulfide bond with other native cysteines of the channel. Exogenous cysteines introduced in the CNB domain may interact with the endogenous cysteines of the CNB domain such as Cys481 or Cys505 or that one in the N terminal such as Cys35. As a consequence, in the closed state residues from Asp588 to Leu607 either do not form an alpha helix or these C-helices fluctuate significantly, as suggested by the molecular dynamics simulation of these C-helices (Punta et al., 2003). These fluctuations support transient contacts between exogenous cysteines introduced in the C-helix and endogenous cysteines such as Cys35, Cys481 and Cys505.

Also Zagotta and collaborators (Gordon and al., 1997; Matulef and Zagotta, 2002) using the CNGA1 channel and the cys-free channel showed similar conclusions. Indeed, theirs data suggest that the C-helices from all four channel subunits are in close proximity in the closed state and move apart during channel opening

An important observation regarding these results is that, with the experiments, we cannot rule out the possibility that the CNBD of CNGA1 channels come together as a 2-fold symmetric "dimer of dimers" or exhibits 4-fold symmetry. At this time, the only conclusion is the real identification of the point in which the C-helices are in close contact. In the absence of cGMP, C-helices are free to move around their hinge. During these rearrangements C-helices may kink and bend at variable angles and at different residue positions.

2-P helix, S6 transmembrane domain and pore region

In this part of my thesis, I will discuss the architecture and conformational rearrangements of the S6 domain and the pore region occurring during channel gating. These are the questions I will try to answer:

1. Which are the movements of the S6 domain and the P-helix during the gating of the channel?
2. Which conformational rearrangements occur in the pore during the gating?
3. Which are the possible interactions between the S6 domain, the P helix and the pore region during channel gating?

The aminoacid sequence of CNG and K^+ channels shares a significant homology particularly in the pore region (Fig.26). CNG channels do not have the classical signature of K^+ channels, i.e. the GYG motif, however the pore topology of the two channels is likely to be similar (Becchetti et al., 1999) and the S6 transmembrane segments are likely to have a similar helical conformation reminiscent of an inverted "TeePee" (Doyle et al., 1999; Flynn and Zagotta 2001, 2003). During gating K^+ channels do not alter significantly the conformation of the pore region, but when the channel opens the S6 transmembrane segments bend towards the lipid phase by about 30° around a glycine hinge located in the middle of S6. Given the structural similarities between CNG and K^+ channels it is conceivable that the two channels have a similar gating, in which the structure of the inner pore does not change and opening and closing of the channel is caused by conformational changes occurring in the S6 segments.

The analysis of residue accessibility in the pore of CNG channels, based on Cysteine Scanning Mutagenesis (Karlin and Akabas, 1998), has shown that CNG and K^+ channels share the same topology (Becchetti et al., 1999) and that residues L(358)TTIGETPPP(367) of the CNGA1 channel from bovine rods span the lipid membrane from the intracellular to the extracellular side. These residues form the inner pore of the channel. A similar analysis performed in the S6 domain of CNGA1 channels from Thr389 to Ser399 (Flynn and Zagotta, 2001, 2003) suggested that also in CNG channels the S6 domain has an helical configuration, possibly crossing at an hypothetical constriction, located between residue Val391 and Ser399. In this view the

inner vestibule of CNG channels has the same structure of K^+ channels, i.e. a bundle of four helices crossing so to form a restriction constituting the gate in the closed state of the channel. The mutant channel V391C is blocked by MTSET only in the open state, but is blocked by Ag^+ equally well in the closed and open state (Flynn and Zagotta, 2001). The former observation suggests the existence also in CNG channels of a gating mechanism similar to that of K^+ channels, while the later shows that Ag^+ ions penetrate the inner vestibule of CNG channels up to residue Val391 both in the open and closed state. These results could be rationalised by the existence of two gates in CNG channels: a gate located in the S6 domain at the hypothetical constriction between Val391 and Ser399 blocking the access to the inner vestibule to large cations such as MTSET, but not to small cations such as Ag^+ and an other gate located in the pore controlling the permeation of monovalent alkali cations, such as Na^+ and K^+.

Liu and Siegelbaum (2000) have shown that the accessibility to extracellular MTSET of residues in the P-helix changed during gating, indicating the existence of a conformational change. On the basis of the obtained results Liu and Siegelbaum suggested that the P-helix, during gating, rotated around its principal axis.

Several previous reports have suggested that the gate of CNG channels involved also conformational changes in the pore region itself. Karpen et al., (1993) have described a state-independent block of native CNG channels by divalent cations such Ni^{2+} and Zn^{2+}. Rather correctly, these authors have assumed that the observed effect was due to an interaction with the gating machinery and not with the pore itself. Fodor et al., (1997) have observed that tetracaine had a 1000-fold higher affinity for the closed CNG channel as compared to the open channel. This rather surprising result, however, does not show or prove that the inner vestibule is equally accessible to permeating ions both in the open and closed state. Point mutations in the pore itself, primarily of glutamate 363, significantly changed the gating (Bucossi et al., 1997): in mutant channel E363A in the presence of a steady cGMP concentration the cGMP-activated current inactivated spontaneously and in mutant channels E363D and T364M single channel properties were markedly different from those observed in the wt CNG channel. Sun et al., (1996) and Liu and Siegelbaum (2000) reported that internal MTSEA blocked both in the open and closed state mutant channels T360C and I361C. However, as shown in Becchetti et al., (1999) and in the present thesis, methanesulphonate reagents (MTSET and MTSEA)

potentiate and do not block the mutant channel T360C. The mutant channel I361C has a fast run down (Becchetti et al., 1999) and it is impossible to establish unequivocally any effect of methanesulphonate reagents on it. As a consequence the exact location of the gating in CNG channels was not unequivocally proved.

The experiments described in my thesis show that the negatively charged compound MTSES potentiated the mutant channel T360C by about 100% when is applied for 5 minutes or so both in the absence and in the presence of 1 mM cGMP (Fig.46). The positively charged compounds MTSET and MTSEA (Fig.47) induce a similar potentiation of mutant channels T359C and T360C. MTSET and MTSEA potentiate also the wt channel by binding to the native cysteine 481 (Brown et al., 1998). MTSES, on the contrary, does not potentiate the wt channel as shown in Fig.51 (see also Brown et al., 1998). These results indicate that potentiation of CNG channels by the binding of a methanesulphonate reagent to cysteine 481 needs a positively charged reagent, such as MTSET and MTSEA and not MTSES. As a consequence MTSES potentiation of mutant channel T360C occurs by a molecular mechanism different from what occurs when MTSET and MTSEA potentiate the wt and mutant channel T359C. As shown in Fig.54 Cd^{2+} ions block with a K_D of about 10 μM the channel mutant T360C only in the open state. This blockage is antagonised by MTSES: indeed in the presence of 10 mM MTSES the K_D of Cd^{2+} blockage increases to about 35 μM. These experimental results show that the site of MTSES potentiation is indeed the exogenously introduced cysteine. As potentiation is observed when MTSES is added in the absence and in the presence of 1 mM cGMP, it is concluded that residue in position 360 is equally accessible to MTSES in the open and closed state.

As shown in Fig.44 Cd^{2+} blockage of mutant channel T360C is observed only when Cd^{2+} is added in the presence of 1 mM cGMP, i.e. when some channels are in the open state. No blockage was observed when Cd^{2+} was added in the absence of cGMP. These experimental results indicate that residues in position 360 are accessible both in the open and closed state but change their relative conformation so to allow Cd^{2+} blockage in the open state.

Let us now see whether it is possible to propose a molecular model of the pore CNG channels in the closed and open state, based on the homology with the 3D structure of K^+ channels and in agreement with the electrophysiological experiments with mutant

channels. Previous investigations have shown that mutant channels T364C and P366C are blocked by extracellular MTSET equally well in the closed and open state (Becchetti et al., 1999; Liu Siegelbaum, 2000), suggesting that during gating aminoacids in the extracellular vestibule from threonine 360 to proline 366 do not change their configuration significantly. Mutant channels T364C and P366C do not have any significant run down, indicating that the exogenously introduced cysteines are too far apart to form spontaneously disulfide bonds. In patches excised from oocytes, the mutant channel I361C has a fast spontaneous rundown which is faster in the presence of cGMP, suggesting that the side chains of Ile361 point towards the pore axis and that side chains of opposing Ile361 become closer in the closed state. On the basis of these previous results and the effect of MTSES and Cd^{2+} described in the present manuscript a molecular model of the pore region from Leu358 to Pro367 in the open and closed state.

Fig.56A illustrates a model of the backbone of the loop from Leu358 to Pro367 of two opposing subunits in the open (red) and closed (blue) state. The direction of side chains of the different residues for the open and closed state is shown in a symbolic way in Fig.55 B and C respectively. The model was constructed by imposing that in the closed state the distance between opposing C_α of Pro366 to be about 16 Å, of Thr364 to be about 14 Å, of Gly362 to be about 5 Å, of Ile361 to be about 9 Å and finally of Thr360 to be about 14 Å. In this model of the closed pore the tighter restriction is formed by Gly362 approaching almost at the shortest Wan der Waals distance. In the open state Gly362s move apart opening therefore the gate, while Ile361 move slightly closer: the distance between opposing C_α of Gly362 is about 10 Å and of Thr360 is about 9 Å, allowing for the formation of Cd^{2+} binding sites in mutant channels T360C. Distances between the C_α of residues from Glu363 to Pro367 were assumed to be almost identical in the open and closed state. In the closed state residues from Leu358 to Thr360 are assumed to have a helical arrangement and to be part of the P helix starting from Val348. The open and closed state configurations were checked for physical consistency by using Procheck (Laskowski et al., 1996) and Whatif (Vriend, 1990) programs.

Fig.57B shows how the mutant channel T360C can bind one MTSES molecule at each subunit and not been obtruded in the open state. However, Cd^{2+} ions by binding to two

neighbouring cysteines can obtrude the pore in the open state, as shown in Fig.57 C and D, but cannot coordinate to these cysteines in the closed state as they are more than 10 Å apart.

The conformational change of the pore wall underlying the transition between the closed and open state is initiated by the binding of cGMP in the cyclic nucleotide-binding domain. Therefore there is a remarkable sophisticated coupling of conformational changes spanning throughout the entire cytoplasmic domain of the channel. It is rather likely that channel gating is mediated by some movements of the S6 domains which are transmitted to the pore walls. Fig.57A illustrates two possible ingredients for this coupling: an hydrophobic interaction between the side chain of Phe360 in S6 and the side chain of Leu356 or Trp353 (Becchetti et al., 1999) possibly coupling S6 and the P helix; similarly the P helix can be coupled to the pore walls by an hydrophobic interaction between side chains of Ile361 and Leu358.

Contrary to what proposed by Flynn and Zagotta (2001 and 2003) my data do not support a view of the gating in which there is a large bending of the S6 domain towards the lipid phase in the open conformation around an hinge located between Val391 and Ser399. Indeed, the application of Cd^{2+} ions in the closed state and open state has the same blocking effect on mutant channels V391C (Fig.29), G395C (Fig.33) and S399C (Fig.35). My experiments also do not support the view that in CNG channels there is a large movement in which the smokehole enlarges during channel opening as a consequence of a significant displacement of Ser399. Indeed, whereas Flynn and Zagotta reported a different sensitivity to MTSET of mutant channel S399C in the closed and open state, I observe a very similar effect of MTSET in both the states. Another important residue is that in position Ala406. This is the first mutant channel in which I observed a clear differential effect of Cd^{2+} in the open and in the closed state. In the closed state there is a complete block of current (100%) but none in the open state; I did not detect any blockage by MTSET either in the closed or in the open state.

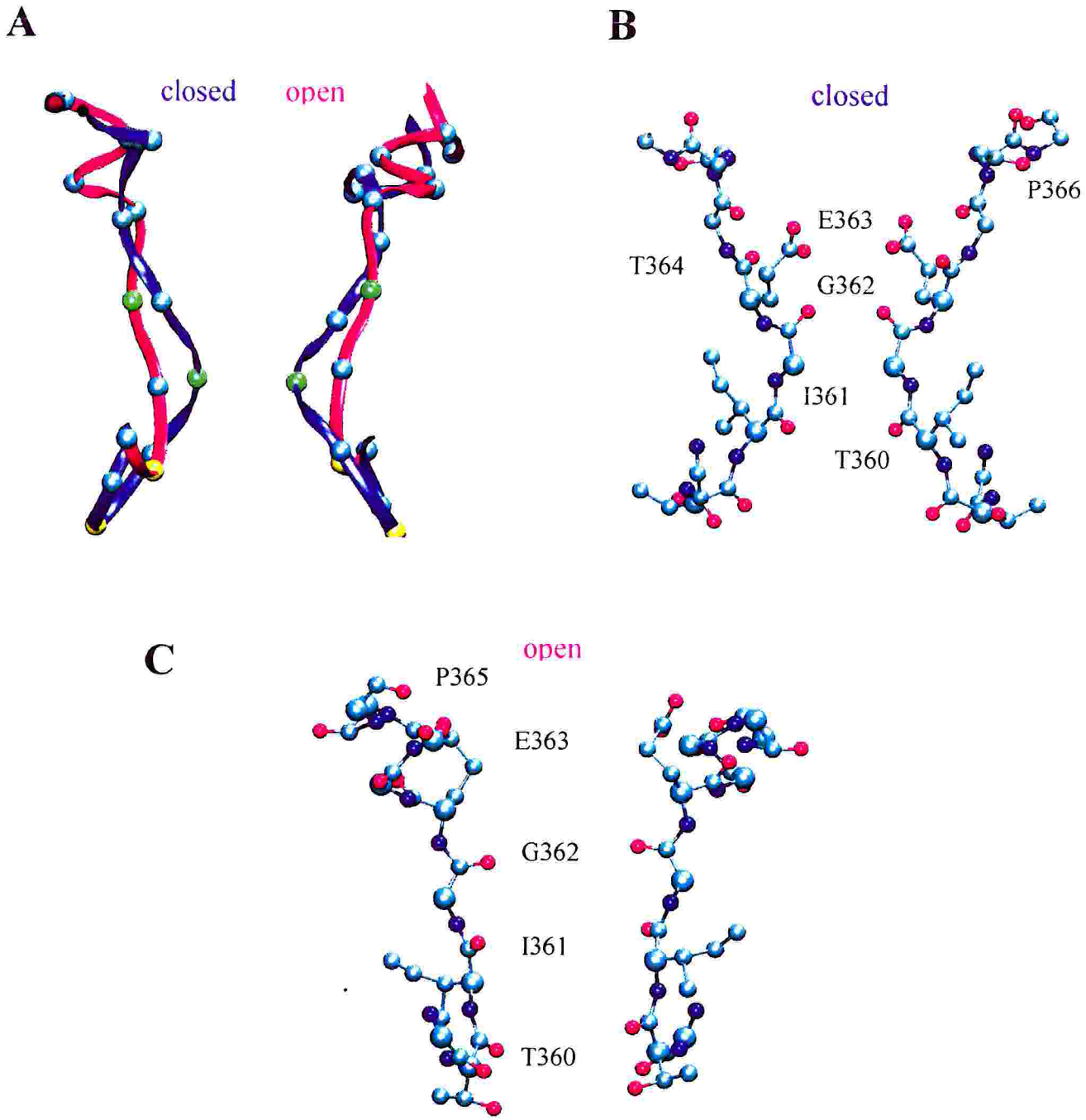

Fig.56: *Molecular models of the pore of cGMP-gated channel in the open and closed state.* ***A****: Molecular models of the pore of cGMP-gated channel in the open (red) and closed state (blue): model of the backbone of the loop from Leu358 to Pro367 of two opposing subunits in the open and closed state. Possible movements of the P helix from the closed to the open state.* ***B*** *and* ***C****: Side chains of the different residues for the closed and open state respectively.*

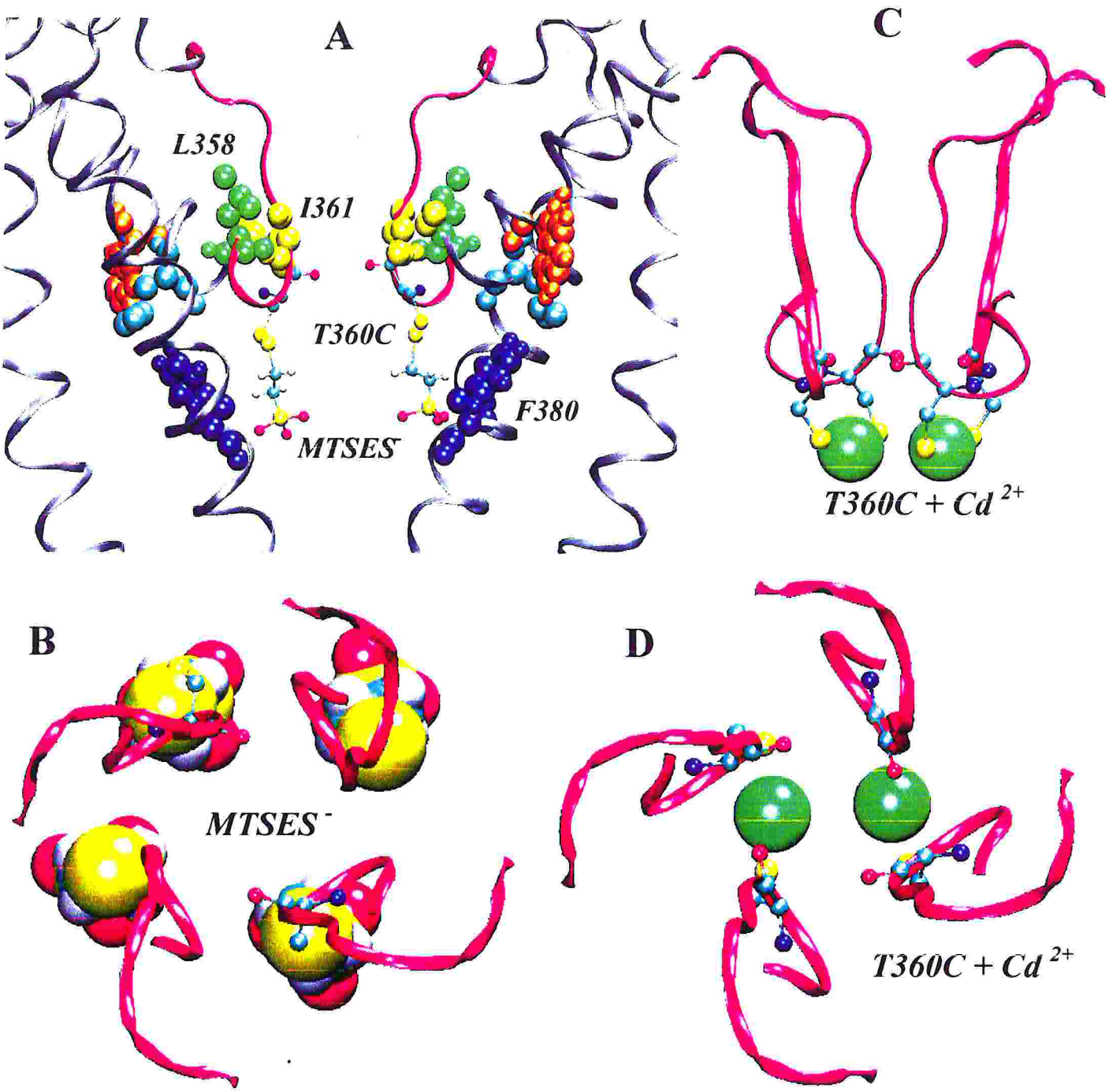

Fig.57: *Binding of MTSES and Cd^{2+} ions to mutant channel T360C.* ***A:*** *side view of two neighboring subunits; a S-S bridge binding between cysteine and MTSES (in yellow). In red is the pore backbone here modeled, in gray is the possible structure of the P helix and the S6 transmembrane segment obtained by homology with the KcsA channel. Possible hydrophobic interaction between the side chain of Ile361 and Leu358 possibly mediating the coupling between the P helix and the pore wall and possible hydrophobic interaction between the side chain of Phe380 and Leu356 or Thr353) possibly mediating the coupling between the S6 segment and the P helix. binding of MTSES and Cd^{2+} ions to mutant channel T360C in the open state, respectively.* ***B:*** *top views of the four subunits binding 4 MTSES.* ***C*** *and* ***D:*** *side views of four subunits binding 2 Cd^{2+} ions (in green), each Cd^{2+} ion is coordinated by two S atoms of neighboring cysteines.*

3-...Conclusions

Let us summaries the main conclusions of my thesis:

A) The CNBD of CNGA1 channels come together as a 2-fold symmetric "dimer of dimers" . My experiments identify the residues, in which the C-helices are in close contact (see Fig.54). Therefore the conformation of the CNBD of CNGA1 channels is different from that determined for the CNBD in HCN2 channels (Zagotta et al., 2003). I propose that in the absence of cGMP, C-helices are free to move around their hinge. During these rearrangements C-helices are likely to kink and to bend at variable angles and at different residue positions.

B) In CNG channels the S6 domain does not have the large movement observed during gating in K channels. This conclusion is primarily based on my observation that the blocking effect of Cd^{2+} on mutant channels V391C (Fig.29), G395C (Fig.33) and S399C (Fig.35) in the absence and in the presence of 1 mM cGMP is almost identical. As Cd^{2+} blockage is a good reporter of distance among the S atoms of exogenously introduced cysteines, I conclude that during gating S6 domains of CNG channels do not move as much as in K^+ channels. I conclude also that Ala388 in CNG channels is not the hinge of the large bending of S6 underlying gating in K^+ channels. My experiments are consistent with a conformational rearrangement producing a movement of the S6 helices leading to changes in distances between the C_α of homologous residues in position 391, 395 and 399 not larger than some Å. I suggest that, in CNG channels, the gating is primarily localised at the pore level.

C) Gating of CNG channels is caused by a small movement of the pore (possibly about 1-2 Å) producing a conformational rearrangement of the pore walls. This conclusion is primarily based on the potentiation of channel mutant T360C by MTSES both in the open and closed state (see Fig.46). This result indicates that the S6 bundles do not form the gate in CNG channels and therefore the gate resides in the pore itself.

D) I speculate that a translation and/or rotation of the S6 domain initiate the movement of the pore walls. This coupling is likely to be mediated by hydrophobic interactions between the P helix and the S6 domain and between the P helix and the pore walls. This hypothesis is supported by the potentiation observed in mutant channels F380C (Fig.27), G383C (Fig.27) and T360C (Fig.46), in the presence of MTSES. In

particular, these interactions could be mediated by the side chains of the residues Phe380/Trp353/Leu356 and Ile361/Leu358, respectively, as proposed in Fig.57A.

With my thesis I hope to have contributed to unravelling the beautiful mechanisms underlying gating in CNG channels.

REFERENCES

Ache, B.W. and A. Zhainarov. 1995. Dual second-messenger pathways in olfctory transduction. *Curr. Opin. Neurobiol.* 5:461-466.

Aggarwal, S. K., and R. MacKinnon. 1996. Contribution of the S4 segment to the gating charge in the Shaker K^+channel. *Neuron* 16:1169-1177.

Akabas, M. H., D. A. Stauffer, M. Xu, and A. Karlin. 1992. Acetylcoline receptor channel structure probed in cysteine-substitution mutants. *Science.* 258:307-310.

Almers, W. and E.W. McCleskey. 1984. Nonselective conductance in calcium channels of frog muscle: calcium selectivity in a single-file pore. *J. Physiol.* 353:585-608.

Altenhofen, W., J. Ludwig, E. Eismann, W. Kraus, W. Bönigk, and U. B. Kaupp. 1991. Control of ligand specificity in cyclic nucleotide-gated channels from rod photoreceptors and olfactory epithelium. *Proc. Natl. Acad. Sci. USA.* 88:9868-9872.

Altschul, S. F., W. Gish, W. Miller, E. W. Myers, and D. J. Lipman. 1990. Basic local alignment search tool. *J. Molo. Biol.* 215:403-410.

Ardell M.D., I. Aragon, L. Oliveira, G.E. Porche, E. burke, and S.J. Pittler. 1996. The β subunit of human rod photoreceptor cGMP-gated cation channel is generated from a complex transcription unit. *FEBS Lett.* 389:213-218.

Armstrong, C.M. and J. Neyton. 1992. Ion permeation through calcium channels. *Ann. NY Acad. Sci.* 635:18-25.

Ashcroft, M. F. 2000. Ion channels and disease. Academic press.

Bairoch, A., and R. Apweiler. 1999. The SWISS-PROT protein sequence data bank and its supplement TrEMBL in 1999. *Nucleic Acids Res.* 27:49-54.

Balasubramanian, S., J.W. Lynch and P.H. Barry. 1996. Calcium-dependent modulation of the agonist affinity of the mammalian olfactory cyclic nucleotide-gated channel by calmodulin and a novel endogenous factor. *J. Membr. Biol.* 152:13-23.

Barker, W. C., J. S. Garavelli, D. H. Haft, L. T. Hunt, C. R. Marzec, B. C. Orcutt, G. Y. Srinivasarao, L. S. Yeh, R. S. Ledley, H. W. Mewes, F. Pfeiffer, and A. Tsugita. 1998. The PRI-International Protein Sequence Database. *Nucleic Acids Res.* 26:27-32.

Barnstable, C.J. and J.-Y. Wei. 1995. Isolation and characterization of the alpha-subunit of rod photoreceptor cGMP-gated cation channel. *J. Molec. Neurosci.* 6:289-302.

Baumann A., S. Frings, M. Godde, R. Seifert and U.B. Kaupp. 1994. Primary structure and functional expression of a *Drosophila* cyclic nucleotide-gated channels present in eyes and antennae. *EMBO J.* 13:5040-5050.

Baylor, D., T.D. Lamb and K.-W. Yau. 1979. The membrane current of single rod outer segments. *J. Physiol. London* 288:589-611.

Baylor, D. 1996. How photons start vision. *Proc. Natl. Acad. Sci.* USA 93:560-565.

Becchetti, A., K. Gamel, and V. Torre. 1999. Cyclic nucleotide-gated channels. Pore topology studied through the accessibility of receptor cysteines. *J. Gen. Physiol.* 114:377-392.

Becchetti, A. and K. Gamel. 1999. The properties of cysteine mutants in the pore region of cyclic-nucleotide-gatedchannels. *Pflugers arch.* 438:587-596.

Becchetti, A., and P. Roncaglia. 2000. Cyclic nucleotide-gated channels: intra- and extracellular accessibility to Cd^{2+} of substituted cysteine residues within the P-loop. *Pflugers Arch.* 440:556-565.

Belluscio, L., G.H. Gold, A. Nemes and R. Axel. 1998. Mice deficient in G_{olf} are anosmic. *Neuron* 20:69-81.

Benitah J. P., G. F. Tomaselli, E. Marban. 1996. Adiacent pore-lining residues within sodium channels identified by paired cysteine mutagenesis. *Proc. Natl. Acad. Sci. USA.* 93:7373-7396.

Benson, D. A., M. S. Boguski, D. J. Lipman, J. Ostell, and B. F. Ouellette. 1998. GenBank. *Nucleic Acids Res.* 26:1-7.

Berghard, A., L.B. Buck and E.R. Liman. 1996. Evidence for distinct signalling mechanisms in two mammalian olfactory sense organs. *Proc. Natl. Acad. Sci. USA* 93:2365-2369

Berman, H. M., J. Westbrook, Z. Feng, G. Gilliland, T. N. Bhat, H. Weissig, I. N. Shindyalov, and P. E. Bourne. 2000. The Protein Data Bank. *Nucleic Acids Res.* 28:235-242.

Biel, M., W. Altenhofen, R. Hullin, J. Ludwig, M. Freichel, V. Flockerzi, N. Dascal, U.B. Kaupp and F. Hofmann. 1993. Primary structure and functionnal expression of a cyclic nucleotide-gated channel from rabbit aorta. *FEBS Lett.* 329:134-138.

Biel, M., X. Zong, M. Distler, E. Bosse, N. Klugbauer, M. Murakami, V. Flockerzi and F. Hoffmann. 1994. Another member of cyclic nucleotide-gated channels family expressed in testis, kidney, and heart. *Proc. Natl. Acad. Sci. U.S.A.* 91:3505-3509.

Biel, M., X. Zong, and F. Hofmann. 1995. Molecular diversity of cyclic nucleotide-gated cation channels. *Naunyn schmiedebergs Arch. Pharmacol.* 353:1-10.

Biel, M., A. Ludwing, X. Zong and F. Hofmann. 1999. Hyperpolarization-activated cation channels: a multi-gene family. *Rev Physiol Biochem Pharmacol.* 136:165-182.

Biel, M., X. Zong and F. A. Ludwing, A. Sautter, and Hofmann. 1999. Structure and function of cyclic nucleotide-gated channels. *Rev Physiol Biochem Pharmacol.* 135:151-171.

Boekhoff, I., E. Tareilus, J. Strotmann and H. Breer. 1990. Rapid activation of alternative second messenger pathways in olfactory cilia by different odorants. *EMBO J.* 9:2453-2458.

Boekhoff, I. and H. Breer. 1992. Termination of second messenger signaling in olfaction. *Proc. Natl. Acad. Sci. U.S.A.* 89:471-474.

Boekhoff, I., S. Schleicher, J. Strotmann and H. Breer, 1992. Odor-induced phosphorylation of olfactory cilia proteins. *Proc. Natl. Acad. Sci. U.S.A.* 89:11983-11987.

Bonigk, W., W. Altenhofen, F. MŸller, A. Dose, M. Illing, R.S. Molday and U.B. Kaupp. 1993. Rod and cone photoreceptor cells express distinct genes for cGMP-gated channels. *Neuron* 10:865-877.

Bonigk, W., J. Bradley, F. MŸller, F. Sesti, I. Boekhoff, G.V. Ronnett, U.B. Kaupp and S. Frings. 1999. The native rat olfactory cyclic nucleotide-gated channel is composed of three distinct subunits. *J. Neurosci.* 19:5332-5347.

Borisy, F.F., G.V. Ronnett, A.M. Cunningham, D. Juifs, J. Beavo and S.H. Snyder. 1992. Calcium/calmodulin-activated phosphodiesterase expressed in olfactory receptor neurons. *J.Neurosci.* 12:915-923.

Bradley, J., J. Li, N. Davidson, H.A. Lester and K. Zinn. 1994. Heteromeric olfactory cyclic nucleotide-gated channels: a subunit that confers increased sensitivity to cAMP. *Proc. Natl. Acad. Sci. USA.* 91:8890-8894.

Bradley, J., Y. Zhang, R. Bakin, H.A. Lester, G.V. Ronett and K. Zinn. 1997. Functional expression of the heteromeric olfactory cyclic nucleotide-gated channel in the hippocampus : a potential effector of synaptic plasticity in brain neurons. *J. Neurosci.* 17:1993-2005.

Bradley, J., S. Frings, K.-W. Yau, and R. Randall. 2001. Nomenclature for Ion Channel Subunits. *Science.* 294:2095-2096.

Breer, H., and I. Boekoff. 1991. Odorants of the same class activate different second messenger pathways. *Chem. Senses* 16:19-29.

Broillet, M.-C. and S. Firestein. 1996. Direct activation of the olfactory cyclic nucleotide-gated channel through modification of sulfhydryl groups by NO compounds. *Neuron* 16:377-385.

Broillet, M.-C. and S. Firestein. 1997. β-subunits of the olfactory cyclic nucleotide-gated channel form a nitric oxide activated Ca^{2+} channel. *Neuron* 18:951-958.

Brown, L.R., R. Gramling, R.J. Bert and J.W. Karpen. 1995. Cyclic-GMP contact points within the 63 kDa subunit and the 240 kDa associated protein of retinal rod cGMP-activated channels. *Biochemistry* 34:8365-8370.

Brown, L.R., S.D. Snow, and T.L. Haley 1998. Movement of gating machinery during the activation of rod cyclic nucleotide-gted channels. *Biophys J.* 75:825-833.

Brown, L.R., T.L. Haley, K.A. West and J.W. Crabb. 1999. Pseudechetoxin: a peptide blocher of cyclic nucleotide-gated ion channels. *Proc. Natl. Acad. Sci. USA* 96:754-759.

Brune, B. and V. Ullrich. 1987. Inhibition of platelet aggregation by carbon monoxide is mediated by activation of guanylyl cyclase. *Mol. Pharmacol.* 32:497-504.

Brunet, L.J., G.H. Gold and J. Ngai. 1996. General anosmia caused by a targeted disruption of the mouse olfactory cyclic nucleotide-gated cation channel. *Neuron* 17:681-693.

Buck L., and R. Axel. 1991. A novel multigene family may encode odorant receptors: a molecular basis for odor recognition. *Cell* 65:175-187.

Bucossi, G., E. Eismann, F. Sesti, M. Nizzari, M. Seri, U.B. Kaupp and V. Torre. 1996. Time dependent current decline in cyclic GMP gated channels caused by point mutations in the pore region. *J. Physiol.* 493: 409-418.

Bucossi, G., M. Nizzari and V. Torre. 1997. Single-channel properties of ionic channels by cyclic nucleotides. *Biophys. J.* 72:1165-1181.

Capovilla, M., A. Caretta, L. Cervetto and V. Torre. 1983. Ionic movements through light-sensitive channels of toad rods. *J. Physiol.* 343:295-310.

Careaga, C. L., and J. J. Falke. 1992. Thermal motions of surface alpha-helices in the D-galactose chemosensory receptor. *J. Mol. Biol.* 226:1219-1235.

Catteral, W.A. 1986 Voltage-dependent gating of sodium channels: correlating structure and function. *Trends Neurosci.* 9:7-10.

Chang G., R.H. Spencer, A.T. Lee, M.T. Barclay, and D.C Rees. 1998. Structure of the MscL homolog from *Mycobacterium tubercolosis*: a gated mechanosensitive ion channel. *Science* 282:2220-2226.

Chen, T.Y., Y.W. Peng, R.S. Dhallan, B. Ahamed, R.R. Reed and K.-W. Yau. 1993. A new subunit of the cyclic nucleotide-gated cation channel in retinal rods. *Nature* 362:764-767.

Chen T.Y. and K.-W. Yau. 1994. Direct modulation by Ca^{2+}-calmodulin of cyclic nucleotide-activated channel of rat olfactory receptor neurons. *Nature* 368:545-548.

Chen T.Y., M. Illing, L.L. Molday, Y.T. Hsu, K.-W. Yau and R.S. Molday. 1994. Subunit 2 (or beta) of retinal rod cGMP-gated cation channel is a component of the 240-kDa channel-associated protein and mediates Ca^{2+}-calmodulin modulation. *Proc. Natl. Acad. Sci. USA* 91:11757-11761.

Chen, F.H., M. Ukhanova, D. thomas, G. Afshar, S. Tanda, B-A. Battelle and R. Payne. 1999. Molecular cloning of a putative cyclic nucleotide-gated ion channel cDNA from Limulus polyphemus. *J. Neurochem.* 72:461-471.

Coburn C.M., and C.I. Bargmann. 1996. A putative cyclic nucleotide-gated channel is required for sensory development and function in *C. elegans. Neuron* 17:695-706.

Colamartino, G., A. Menini, and V. Torre. 1991. Blockage and permeation of divalent cations through the cyclic GMP-activated channel from tiger salamander retinal rods. *J. Physiol. (Camb.)* 440:189-206

Colville C.A., and R.S. Molday. 1996. Primary structure and expression of the human β-subunit and related proteins of the rod photoreceptor cGMP-gated channel. *J. Biol. Chem.* 271:32968-32974.

Cook, N. J., W. Hanke, and U. B. Kaupp. 1987. Identification, purification, and functional reconstitution of the cyclic GMP-dependent channel from rod photoreceptors. *Proc. Natl. Acad. Sci. USA*. 84:585-589.

Creighton, T.E. 1993. Structures and molecular properties. 2nd ed. WHFreeman and Co., New York. NY. 507 pp

Crowther, R. A., R. Henderson, and J. Smith. 1996. MRC image processing programs. *J. Struct. Biol.* 116:9-16.

Dhallan, R. S., K. W. Yau, K. A., Schrader, and R. R. Reed. 1990. Primary structure and functional expression of a cyclic nucleotide-activated channel from olfactory neurons. *Nature.* 347:18-27.

Dhallan, R.S., J.P. Macke, R.L. Eddy, T.B. Shows and R.R. Reed. 1992. Human rod photoreceptor cGMP-gated channel: amino acid sequence, gene structure, and functional expression. *J. Neurosci.* 12:3248-3256.

Doyle, D. A., J. M. Cabral, R. A. Pfuetzner, A. Kuo, J. M. Gulbis, S. L. Cohen, B. T. Chait, and R. MacKinnon. 1998. The structure of the potassium channel: Molecular basis of K^+ conduction and selectivity. *Science.* 280:69-77.

Durell, S.R., and H.R. Guy. 1992. Atomic scale structure and functional models of voltage-gated potassium channels. *Biophys. J.* 62:238-250.

Durell, S.R., and H.R. Guy. 1996. Structural model of the outer vestibule and selectivity filter of the Shaker voltage-gated K^+ channel. *Neuropharmacology*. 35:761-773.

Dzeja, C., V. Hagen, U. B. Kaupp, and S. Frings. 1999. Ca^{2+} permeation in cyclic nucleotide-gated channels. *EMBO J.* 18:131-144.

Eismann, E.F., W. Bšnigk and U.B. Kaupp. 1993. Structural features of cyclic nucleotide-gated channels. *Cell. Physiol. Biochem.* 3:332-351.

Eismann, E., F. Muller, S.H. Heinemann and U.B. Kaupp. 1994. A single negative charge within the pore region of a cGMP-gated channel controls rectification, Ca^{2+} blockage, and ionic selectivity. *Proc. Natl. Acad. Sci. USA.* 91:1109-1113.

Emeis, D., H. Kuhn, J. Reichert and K.P. Hofmann. 1982. Complex formation between metarhodopsin II and GTP-binding protein in bovine photoreceptor membranes leads to a shift of the photoproduct equilibrium. *FEBS Lett.* 143, 29-34.

Ermler, U., W. Grabarse, S. Shima, M. Goubeaud, and R. K. Thauer. 1998. Active sites of transition metals enzymes with a focus on nickel. *Curr. Opin. Struct. Biol.* 8:749-758.

Fesenko, E. E., Kolesnikov, S. S., Lyubarsky, A. L. 1985. Induction by cyclic GMP of cationic conductance in plasma membrane of retinal rod outer segment. *Nature* 313: 310-13.

Fain, G.L., H.R. Matthews and W.C. Cornwall. 1996. Dark adaptation in vertebrate photoreceptors. *Trends Neurosci.* 19:502-507.

Filatov, G.N., A.B. Jainazarov, S.S. Kolesnikov, A.L. Lyubarsky and E.E. Fesenko. 1989. The effect of ATP, GTP and cAMP on the cGMP-dependent conductance of the fragments from frog rod plasma membrane. *FEBS Lett.* 245:185-188.

Finn, J. T., M. E. Grunwald, and K-W. Yau. 1996 Cyclic nucleotide-gated ion channels: an extended family with diverse functions. *Annu. Rev. Physiol.* 58:395-426.

Flynn, G. E., and W. N. Zagotta. 2001. Conformational changes in S6 coupled to the opening of cyclic nucleotide-gated channels. *Neuron.* 30:689-698.

Flynn, G. E., J. P. Johnson, and W. N. Zagotta. 2001. Cyclic nucleotide-gated channels: shedding light on the opening of a channel pore. *Nat. Rev. Neurosci.* 2:643-651.

Flynn, G. E., and W. N. Zagotta. 2003. A cysteine scan of the inner vestibule of cyclic nucleotide-gated channels reveals architecture and rearrangement of th epore. *J. Gen. Physiol.* 121:563-582.

Fodor, A.A., S.E. Gordon, and W. Zagotta. 1997. Mechanism of tetracaine block of cyclic nucleotide-gated channels. *J. Gen. Physiol.* 109: 3-14.

Frank, J., M. Radermacher, T. Wagenknecht, and A. Verschoor. 1988. Studying ribosome structure by electron microscopy and computer-image processing. In Methods in Enzymology, Vol. 164, Ribosomes. H.F.Jr. Noller and K. Moldave, eds. (San Diego: Academic Press, Inc.), pp. 3-35.

Frings, S., J.W. Lynch and B. Lindemann. 1992. Properties of cyclic nucleotide-gated channels mediating olfactory transduction: activation, selectivity and blockage. *J. Gen. Physiol.* 100:45-67.

Frings, S., R. Seifert, M. Godde and U.B. Kaupp. 1995. Profoundly different calcium permeation and blockage determine the specific function of distinct cyclic nucleotide-gated channels. *Neuron* 15:169-179.

Furchgott, R.F. and D. Jothianandan. 1991. Endothellium-dependent and -independent vasodilatation involving cyclic GMP: relaxation induced by nitric oxide, carbon monoxide and light. Blood Vessels 28:52-61.

Furman, R.E. and J.C. Tanaka. 1990. Monovalent selectivity of the cyclic guanosine monophosphatactivated ion channel. *J. Gen. Physiol.* 96:57-82.

Gamel, K. and V. Torre. 2000. The interaction of Na^+ and K^+ in the pore of cyclic nucleotide-gated channels. *Biophysical J.* 79:2475-2493.

Gerstner, A., X. Zong, F. Hofmann and M. Biel. 2000. Molecular cloning and functional characterization of a new modulatory cyclic nucleotide-gated channel subunit from mouse retina. *J. Neurosci.* 20(4):1324-1332.

Glusker, J. P. 1991. Structural aspects of metal liganding to functional groups in proteins. *Adv. Prot. Chem.* 42:1-76.

Gold, G.H. 1999. Controversial issues in vertebrate olfactory transduction. *Annu. Rev. Physiol.* 61:857-871.

Gorczyca, W.A., M.P. Gray-Keller, P.B. Detwiler and K. Palczewski. 1994. Purification and physiological identification of a guanylate cyclase activating protein from retinal rods. Proc. Natl. Acad. Sci. USA. 91:4014-4018.

Gordon, S.E., D.L. Brautigan and A.L. Zimmerman. 1992. Protein phosphatases modulate the apparent agonist affinity of the light-regulated ion channel in retinal rods. 1992. *Neuron* 9:739-748.

Gordon, S.E., and W. N. Zagotta. 1995a. A histidine residue associated with the gate of the cyclic nucleotide-activated channels in rod photoreceptors. Neuron. 14: 177-183.

Gordon, S.E., and W. N. Zagotta. 1995b. Localization of regions affecting an allosteric transition in cyclic nucleotide-activated channels. *Neuron.* 14:857-864

Gordon, S.E., and W. N. Zagotta. 1995c. Subunit interactions in coordination of Ni^{2+} in cyclic nucleotide-gated channels. *Proc. Natl. Acad. Sci. USA.* 92:10222-10226.

Gordon, S.E., J. Downing-Park, B. Tam and A.L. Zimmerman. 1995. Diacylglycerol analogs inhibit the rod cGMP-gated channel by a phosphorylation-independent mechanism. *Biophys. J.* 69:409-417.

Gordon, S.E., J.C. Oakley, M.D. Varnum, and W. N. Zagotta. 1996. Altered ligand specificity by protonation in the ligand binding domain of cyclic-nucleotide gated channels. *Biochemistry* 35:3994-4001.

Gordon, S.E., M.D. Varnum, and W. N. Zagotta. 1997. Direct interaction between amino- and carboxyl-terminal domains of cyclic-nucleotide-gated channels. *Neuron* 19:431-441.

Goulding, E.H., J. Ngai, R.H. Kramer, S. Colicos, R. Axel, S.A. Siegelbaum and A. Chess. 1992. Molecular cloning and single-channel properties of the cyclic-nucleotide-gated channel from catfish olfactory neurons. *Neuron*. 8:45-58.

Goulding, E.H., G.R. Tibbs, D. Liu and S.A. Siegelbaum. 1993. Role of H5 domain in determining pore diameter and ionic permeation through cyclic nucleotide-gated channels. *Nature* 364: 61-64.

Goulding, E.H., G.R. Tibbs and S.A. Siegelbaum. 1994. Molecular mechanism of cyclic nucleotide-gated channel activation. *Nature* 372: 369-374.

Gray-Keller, M., A. Polans, K. Palczewski and P. Detwiler. 1993. The effect of recoverin-like calcium-binding proteins on the photoresponse of retinal rods. *Neuron* 10:523-531.

Gray-Keller M.P.,and P.B. Detwiler. 1994. The calcium feedback signal in the phototransduction cascade of vertebrate rods. *Neuron* 13:849-861.

Gross, A., and R. MacKinnon. 1996. Agitoxin footprinting the Shaker potassium channel pore. *Neuron* 16:399-406.

Grunwald M.E., W-P Yu, H-H Yu, and K-W Yau. 1998. Identification of a domain on the β-subunit of the rod cGMP-gated cation channel that mediates inhibition b calcium-calmodulin. *J. Biol. Chem.* 273:9148-9157.

Grunwald M.E., H. Zhong, J. Lai and K-W Yau. 1999. Molecular determinants of the modulation of cyclic nucleotide-activated channels by calmodulin. *PNAS* 96:13444-49.

Guy, H.R. and F. Conti. 1990. Pursuing the structure and function of voltage-gated channels. *TINS* 13:201-206.

Guy, H.R. and S.R. Durell. 1995. Structural models of Na^+, Ca^{2+}, and K^+ channels. In: Ion channels and genetic diseases. The Rockefeller University Press: 1-16.

Hagins, W.A., R.D. Penn and S. Yoshikami. 1970. Dark current and photocurrent in retinal rods. *Biophys. J.* 10:380-412.

Hamill, O. P., A. Marty, E. Neher, B. Sakmann, and F. J. Sigworth. 1981. Improved patch-clamp techniques for high-resolution current recording from cells and cell-free membrane patches. *Pflugers Arch.* 391:85-100.

Hastrup, H., A. Karlin, and J. A. Javvitch. 2001. Symmetrical dimer of the human dopamine transporter revealed by cross-linking cys-306 at the extracellular end of the sixth transmembrane segment. *PNAS.* 98:10055-10060.

Haynes, L.W., A.R. Kay and K.W. Yau. 1986. Single cyclic GMP-activated channel activity in excised patches of rod outer segment membrane. *Nature* 321:66-70.

Haynes, L.W. 1992. Block of the cyclic GMP-gated channel of vertebrate rod and cone photoreceptors by l-cis-diltiazem. *J.Gen.Physiol.* 100:783-801.

Haynes, L.W. 1995. Permeation and block by internal and external divalent cations of the catfish cone photoreceptor cGMP-gated channel. *J. Gen. Physiol.* 106:507-523.

He, Y., M. L. Ruiz, and J. W. Karpen. 2000. Constraining the subunit order of rod cyclic nucleotide-gated channels reveals a diagonal arrangement of like subunits. *Proc. Natl. Acad. Sci. USA.* 97:895-900.

Heginbotham L., T. Abramson and R. McKinnon. 1992. A functional connection between the pores of distantly related ion channels as revealed by mutant K^+ channels. *Science* 258: 1152-1155.

Heginbotham L., Z. Lu, T. Abramson and R. McKinnon. 1994. Mutations in the K^+ channel signature sequence. *Biophys. J.* 66:1061-1067.

Henderson, R. 1995. The potential and limitations of neutrons, electrons and X-rays for atomic resolution microscopy of unstained biological molecules. *Q. Rev. Biophys.* 28:171-193.

Henn, D. K., A. Baumann, and U. B. Kaupp. 1995. Probing the transmembrane topology of cyclic nucleotide-gated ion channels with a gene fusion approach. *Proc. Natl. Acad. Sci. USA.* 92:7425-7429.

Hess, P. and R.W. Tsien. 1984. Mechanism of ion permeation through calcium channels. *Nature* 309:453-456.

Hilbert, M., G. Böhm, and R. Jaenicke. 1993. Structural relationships of homologous proteins as a fundamental principle in homology modeling. *Proteins.* 17:138-151.

Higgins, M. K., D. Weitz, T. Warne, G. F. Schertler, and U. B. Kaupp. 2002. Molecular atchitecture of a retinal cGMP-gated channels: the arrangement of a cytoplasmic domains. *EMBO J.* 21:2087-94.

Hille, B. 2001. Ion Channels of Excitable Membranes, Third edition. Sinauer Associates, Sunderlands, MA, USA.

Holmgren, M., K. S. Shin, and G. Yellen. 1998. The activation gate of a voltage-gated K+ channel can be trapped in the open state by an intersubunit metal bridge. *Neuron.* 21:617-621.

Hsu, Y.T. and R. S. Molday. 1993. Modulation of the cGMP-gated channel of rod photoreceptor cells by calmodulin. *Nature.* 361:76-79.

Ildefonse, M., and N. Bennett. 1991. Single-channel study of the cGMP-dependent conductance of retinal rods from incorporation of native vesicles into planar lipid bilayers *J. Memb. Biol.* 123: 133-147.

Ildefonse, M., S. Crouzy, and N. Bennett. 1992. Gating of retinal rod cation channel by different nucleotides: comparative study of unitary currents. *J. Membrane Biol.* 130:91-104.

Jiang, Y., A. Lee, J. Chen, M. Cadene, B. T. Chalt, and R. MacKinnon. 2002. The open pore conformation of potassium chammels. *Nature.* 417:523-526.

Johnson, J. P., and W. N. Zagotta. 2001. Rotation movement during cyclic nucleotide-gated channel opening. *Nature.* 412:917-921.

Karlin, A., and M. H. Akabas. 1998. Substituted–cysteine accessibility method. *Methods Enzymol.* 293:123-145.

Karpen, J.W., A.L. Zimmerman, L. Stryer and D.A. Baylor. 1988. Gating kinetics of the cyclic-cGMP-activated channel of retinal rods: flash photolysis and voltage-jump studies. *Proc Natl Acad Sci USA* 85: 1287-1291.

Karpen, J.W., D.A. Loney and D.A. Baylor. 1992. Cyclic GMP-activated channels of salamander retinal rods : spatial distribution and variation of responsiveness. *J. Physiol.* 448:257-274.

Karpen, J.W., R. L. Brown, L. Stryer, and D.A. Baylor. 1993. Interactions between divalent cations and the gating machinery of cyclic GMP-activated channels in salamander retinal rods. *J.Gen.Physiol.* 101:1-25.

Kaupp, U. B., T. Niidome, T. Tanabe, S. Terada, W. Bönigk, W. Stühmer, N. J. Cook, K. Kangawa, H. Matsuo, T. Hirose, T. Miyata, and S. Numa. 1989. Primary structure and functional expression from complementary DNA of the rod photoreceptor cyclic GMP-gated channel. *Nature.* 342:762-766.

Kaupp, U. B. 1995. Family of cyclic nucleotide gated ion channels. *Curr. Opin. Neurobiol.* 5:434-442.

Kaupp, U. B., R. Seifert. 2002. Cyclic nucleotide gated channels. *Physiol. Rev.* 82:769-824

Kharitonov, V.G., V.S. Sharma, R.B. Pilz, D. Magde and D. Koesling. 1995. Basis of guanylate cyclase activation by carbon monoxide. *Proc. Natl. Acad. Sci. USA* 92:2568-2571.

Kingston, P.A., F. Zufall and C.J. Barnstable. 1996. Rat hippocampal neurons express genes for both rod retinal and olfactory cyclic nucleotide-gated channels: novel targets for cAMP/cGMP function. *Proc. Natl. Acad. Sci. USA* 93:10440-10445.

Kleene, S.J. 1995. Block by external calcium and magnesium of the cyclic nucleotide-activated current in olfactory cilia. *Neurosci.* 66:1001-1008.

Koch W.H. and U. B. Kaupp, 1985. Cyclic GMP directly regulates a cation conductance in membranes of bovine rods by a cooperative mechanism. *J. Biol. Chem.* 260:6788-6800.

Koch, W.H. and L. Stryer. 1988. Highly cooperative feedback control of retinal rod guanylate cyclase by calcium ions. *Nature* 334:64-66.

Koch, K.W. 1992. Biochemical mechanism of light adaptation in vertebrate photoreceptors. *Trends Biochem. Sci.* 17(8):307-311.

Kolesnikov, S.S., A.B. Zhainazarov and A.V. Kosolapov. 1990. Cyclic-nucleotide-activated channel in the frog olfactory receptor plasma membrane. *FEBS Lett.* 266:96-98.

Komatsu, H., Y.H. Jin, N. L'Etoile, I. Mori, C.L. Bargmann and N. Akaike. 1999. Functional reconstruction of a heteromeric cyclic nucleotide-gated channel of Caenorhabditiselegans in cultured cells. *Brain Res.* 821(1):160-8.

Körschen, H. G., M. Illing, R. Seifert, F. Sesti, A. Williams, S. Gotzes, C. Colville, F. Müller, A. Dosé, M. Godde, L. Molday, U. B. Kaupp, and R. S. Molday. 1995. A 240 kDa protein represents the complete β subunit of the cyclic nucleotide-gated channel from rod photoreceptor. *Neuron.* 15:627-636.

Körschen, H.G., M. Beyermann, F. Muller, M. Heck, M. Vantler, K-W Koch, R. Kellnet, U. Wolfrum, C. Bode, K.P Hofmann and U.B Kaupp. 1999. Interactions of glutamic-acid-rich proteins with the cGMP signaling pathway in rod photoreceptors. *Nature* 400:761-766.

Koutalos, Y. and K.W. Yau. 1996. Sensitivity regulation in rod photoreceptors by calcium. *Trends Neurosci.* 19:73-81.

Kramer, R.H. and S.A. Siegelbaum. 1992. Intracellular Ca^{2+} regulates the sensitivity of cyclic nucleotide-gated channels in olfactory receptor neurons. *Neuron* 9:897-906.

Kramer, R.H., E. Goulding and S.A. Siegelbaum. 1994. Potassium channel inactivation peptide blocks cyclic nucleotide-gated channels by binding to the conserved pore domain. *Neuron* 12:655-662.

Krovetz, H. S., H. M. A. VanDongen, and A. M. J. VanDongen. 1997. Atomic distances estimates from disulfides and high-affinity metal-binding sistes in a K channel pore. *Biophysical J.* 72:117-126.

Kumar, V.D. and I.T. Weber. 1992. Molecular model of the cyclic GMP-binding domain of the cyclic GMP-gated ion channel. *Biochemistry* 31:4643-4649.

Kurahashi T., and A. Menini. 1997. Mechanism of odorant adaptation in the olfactory receptor cell. *Nature* 385:725-729.

Laio, A., and V. Torre. 1999. Physical Origin of selectivity in ionic channels of biological membranes. *Biophys. J.* 76:129-148.

Lagnado, L., D.A. Baylor. 1994. Calcium controls light-triggered formation of catalitically active rhodopsin. *Nature* 367:273-277.

Lander, H.M. 1997. An essential role for free radicals and derived species in signal transduction. *FASEB J.* 11:118-124.

Laskowski, R.A., J.A. Rullmann, M.W. MacArthur, R. Kaptein, and J.M. Thornton. 1996. AQUA and PROCHECK-NMR: programs for cheching the quality of protein structure solved by NMR. *J.Biomol. NMR* 8(4):477-86.

Leu S.F., C.H. Baker, E.J. Lee, and J.G. Harman. 1999. Position 127 amino acids substitutions affect the formation of CRP:cAMP:lacP complex but not CRP:cAMP:RNA polymerase complexes at lacP. *Biochemistry* 38:6222-6230.

Li, M., N. Stauffer, Y.N. Jan, and L.Y. Jan. 1994. Images of purified Shaker potassium channels. *Curr. Biol.* 4(2):110-5.

Li, J., and H. A. Lester. 1999. Functional roles of aromatic residues in the ligand-binding domain of cyclic nucleotide-gated channels. *Mol. Pharmacol.* 55:873-882.

Liman, E.R. and L.B. Buck. 1994. A second subunit of the olfactory cyclic nucleotide-gated channel confers high sensitivity to cAMP. *Neuron* 13:611-621.

Lynch J.W., and B. Lindermann. 1994. Cyclic nucleotide-gated channels of rat olfactory recepror cells: divalent cations control the sensitivity of cAMP. *J.Gen. Physiol.* 103:87-106.

Lynch J.W. 1998. Nitric oxide inhibition of the rat olfactory cyclic nucleotide-gated ion channel. *J. Membr. Biol.* 165:227-234.

Liu, M., T. Y. Chen, B. Ahamed, J. Li, and K. W. Yau. 1994. Calcium-calmodulin modulation of the olfactory cyclic nucleotide-gated cation channel. *Science.* 266:1348-1354.

Liu, D. T., G. R. Tibbs, and S. A. Siegelbaum. 1996. Subunit stoichiometry of cyclic nucleotide-gated channels and effects of subunit order on channel function. *Neuron.* 16:983-990.

Liu, D. T., G. R. Tibbs, and P. Paoletti. 1998 Constraining ligand-binding site stoichiometry suggests that a cyclic nucleotide-gated channel is composed of two functional dimers. *Neuron.* 21:235-248.

Liu, J. and S. A. Siegelbaum. 2000. Change of pore helix conformational state upon opening of cyclic nucleotide gated channels. *Neuron.* 28:899-909.

Lolley, R.N. and E. Racz. 1982. Calcium modulation of cyclic GMP synthesis in rat visual cells. *Vision Res.* 22:1481-1486.

Loussouarn, G., E. N. Makhina, T. Rose. And C. G. Nichols. 2000. Structure and dynamic of the pore of inwardly rectifying Katp channels. *J. Biol. Chem.* 275:1137-1144.

Lowe, G., T. Nakamura, G.H. Gold. 1989. Adenylate cyclase mediates olfactory transduction for a wide variety of odorants. Proc. Natl. Acad. Sci. USA. 86:5641-5645.

Lu, Q., and C. Miller. 1995. Silver as a probe of pore-forming residues in a potassium channel. *Science* 268:304-307.

Lu, Z. and L. Ding. 1999. Blockade of a retinal cGMP-gated channel by polyamines. *J. Gen. Physiol.* 113:35-43.

Ludwig, J., T. Margalit, E. Eismann, D. Lancet and U.B. Kaupp. 1990. Primary structure of cAMP-gated channel from bovine olfactory epithellium. *FEBS Lett.* 270:24-29.

Luehring, H., W. Hanke, R. Simmoteit and U.B. Kaupp. 1990. Cation selectivity of the cyclic GMP-gated channel of mammalian rod photoreceptors. In Sensory transduction (Borselino, L., L. Cervetto and V. Torre). Plenum Press, N-Y 169-174.

MacKinnon, R. 1991. Determination of th esubunit stoichiometry of a voltage-activated potassium channel. *Nature* 350(6315):232-5.

Maroney, M. J., 1999. Structure/function relationships in nickel metallobiochemistry. *Curr. Opin.Chem. Biol.* 3:188-199.

Matulef, K., G. E. Flynn, and W. N. Zagotta. 1999. Molecular rearrangements in the ligand-binding domain of cyclic nucleotide-gated channels. *Neuron.* 24:443-452.

Matulef, K., and W. N. Zagotta. 2002. Probing the quaternary structure of cyclic nucleotide-gated channels. *Biophysical J.* 82:276a (Abstracts).

Matulef, K., G. E. Flynn, and W. N. Zagotta. 2002. Multimerization of the ligand binding domains of cyclic nucleotide gated channels. *Neuron.* 36:93-103.

Matthews, G. and S.-I. Watanabe. 1987. Properties of ion channels closed by light and opened by 3',5'-cyclic monophosphate in toad retinal rods. *J. Physiol.* 389:691-715.

Matthews, G. and S.-I. Watanabe. 1988. Activation of single ions channels from toad retinal rod inner segments by cyclic GMP: concentration dependence. *J.Physiol. London* 403:389-405.

McGeoch, J.E.M., M.W. McGeoch and G. Guidotti. 1995. Eye CNG channel is modulated by nicotine. *Biochem. Biophys. Res. Commun.* 214:879-887.

McKay, D.B. and T.A. Steitz. 1981. Structure of catabolite gene activator protein at 2.9 Angstršm resolution suggests binding to left-handed B-DNA. *Nature* 290:744-749.

McLatchie, L.M. and H.R. Matthews. 1992. Voltage-dependent block by l-cis-diltiazem of the cyclic GMP-activated conductance of salamender rods. *Proc. R. Soc. Lond.* (B) 247:113-119.

Menini, A., G. Rispoli and V. Torre. 1988. The ion selectivity of the light-sensitive current in isolated rods of the tiger salamander. *J. Physiol.* 402:279-300.

Menini, A. 1990. Currents carried by monovalent cations through cyclic GMP-activated channels in excised patches from salamander rods. *J. Physiol.* 424: 167-185.

Menini, A. 1995. Cyclic nucleotide-gated channels in visual and olfactory transduction. *Biophys. Chem.* 55:185-196.

Miledi, R, I. Parker, and H. P. Zhu. 1984. Extracellular ions and excitation-contraction coupling in frog twitch muscle fibers. *J. Physiol.* 351:687-710.

Mindell, J. A., M. Maduke, C. Miller, N. and Grigorieff. 2001. Projection structure of a CIC-type chloride channel at 6.5 Å resolution. *Nature.* 409:219-223.

MisakaT., Y. Kusakabe, Y. Emori, T. Gonoi, S. Arai, and K. Abe. 1997. Taste buds have a cyclic nucleotide-activated channel, CNGgust. *J. Biol. Chem.* 272:22623-22629.

Molday, R. S., L. L. Molday, A. Dose, I. Clark-lewis, M. Illing, N. J. Cook, E. F. Eismann, and U. B. Kaupp. 1991. The cGMP-gated channels of the rod photoreceptor cell characterization and orientation of the aino terinus. *J. Biol. Chem.* 266:21917-21922.

Molday, R.S. 1996. Calmodulin regulation of cyclic-nucleotide-gated channels. *Curr Opin Neurobiol* 6:445-452.

Molokanova, E., B. Trivedi, A. Savchenko, and R.H. Kramer. 1997. Modulation of photoreceptor cyclic nucleotide-gated channels by tyrosine phosphorylation. *J. Neurosci.* 17:9068-9076.

Molokanova, E., F. Maddox, C.W. Luetje and R.H. Kramer. 1999a. Activity dependent modulation of rod photoreceptor cyclic nucleotide-gated channels mediated by phosphorylation of a specific tyrosine residue. *J. Neurosci.* 19:4786-4795.

Molokanova, E., A. Savchenko and R.H. Kramer. 1999b. Noncatalytic inhibition of cyclic nucleotide-gated channels by tyrosine kinase induced by genistein. *J. Gen. Physiol.* 113:45-56.

Molokanova, E., A. Savchenko and R.H. Kramer. 2000. Interaction of cyclic nucleotide-gated channel subunits and protein tyrosine kinase probed with genistein. *J. Gen. Physiol.* 115:685-696.

Molokanova, E., and R.H. Kramer. 2001. Mechanism of inhibition of cyclic nucleotide-gated channel by protein tyrosine kinase probed with genistein. *J. Gen. Physiol.* 117:219-233.

Moore J.L., I.I Gorshkova, J.W. Brown, K.H. McKenney, and F.P. Schwartz. 1996. Effect of cAMP binding site mutations on the interaction of cAMP receptors protein with cyclic nucleoside monophosphate ligands and DNA. *J. Biol. Chem.* 271:21273-21278.

Muller, F., W. Bonigk, F. Sesti and S. Frings. 1998. Phosphorylation of mammalian olfactory cyclic nucleotide-gated channels increases ligand sensitivity. *J. Neurosci.* 18:164-173.

Nakamura, T., and G. H. Gold. 1987. A cyclic nucleotide-gated conductance in olfactory receptor cilia. *Nature.* 325:442-444.

Nakatani, K. and K.-W. Yau. 1988. Calcium and magnesium fluxes across the plasma membrane of the toad rod outer segment. *J. Physiol.* 395:695-729.

Nakatani, K., Y. Koutalos and K.-W. Yau. 1995. Ca^{2+} modulation of the cGMP-gated channel of bullfrog retinal rod photoreceptors. *J. Physiol.* 484:69-76.

Neher, E., and B. Sakmann. 1976. Single-channel recorded from membrane in denervated frog muscle fibres. *Nature* 260(5554):799-802.

Nicol, G.D. 1993. The calcium channel antagonist, pimozide, blocks the cyclic GMP-activated current in rod photoreceptors. *J. Pharmac. exp. Ther.* 265:626-632.

Nizzari, M., F. Sesti, M. T. Giraudo, C. Virginio, A. Cattaneo, and V. Torre. 1993. Single-channel properties of cloned cGMP-activated channels from retinal rods. *Proc. R. Soc. Lond.* B Biol. Sci. 254:69-74.

North, A. 1995. Hanbook of receptors and channels. CRC Press. 1-151.

Nunn, B.J. 1987. Ionic permeability ratios of the cyclic GMP-activated conductance in the outer segment membrane of salamander rods. *J. Physiol.* 394, 17P.

Oda, Y., L.C. Timpe, R.C. McKenzie, D.N. Sauder, C. Largman and T. Mauro. 1997. Alternatively spliced forms of the cGMP-gated channel in human keratinocytes. *FEBS Lett.* 414:140-145.

O'Dell, T.J., R.D. Hawkins, E.R. Kandel and O. Arancio. 1991. Tests od the roles of two diffusible substances in long-term potentiation: evidence for nitric oxide as a possible early retrograde messenger. *Proc. Natl. Acad. Sci. USA* 88:11285-11289.

Paoletti, P., E. C. Young, and S. A. Siegelbaum. 1999. C-linker of cyclic nucleotide-gated channels controls coupling of ligand binding to channel gating. *J. Gen. Physiol.* 113:17-33.

Palczewisky, K., A.S. Polans, W Baehr and J.B. Ames. 2000. Ca2+-binding proteins in the retina: structure, function, and the etiology of human visual diseases. *BioEssays* 22:337-350.

Papizan D.M., T.L. Schwarz, B.L. Tempel, Y.N. Jan, and L.Y. Jan. 1987. Cloning of genomic and complementary DNA from Shaker, a putative potassium channel gene from *Drosophila. Science* 237:749-753.

Passner, J. M., S.C. Schultz, and T. A. Steitz. 2000. Modeling the cAMP-induced allosteric transition using the crystal structure of CAP-cAMP at 2.1 A resolution. *J. Mol. Biol.* 304:847-59.

Pearson, W. R.. 1998. Empirical statistical estimated for sequence similarity searches. *J. Mol. Biol.* 276:71-84.

Picco, C., and A. Menini. 1993. The permeability of the cGMP-activated channel to organic cations in retinal rods of the tiger salamander. *J. Physiol.* 460:741-758.

Picones, A. and J.I. Korenbrot. 1995a. Permeability and interaction of Ca^{++} with cGMP-gated ion channels differ in retinal rod and cone photoreceptors. *Biophys. J.* 69:120-127.

Picones, A. and J.I. Korenbrot. 1995b. Spontaneous, ligand-independent activity of the cGMP-gated ion channels in cone photoreceptors of fish. *J. Physiol.* 485:699-714.

Pittler, S.J., A.K. Lee, M.R. Altherr, T.A. Howard, M.F. Seldin, R.L. Hurwitz, J.J. Wasmuth and W. Baehr. 1992. Primary structure and chromosomal localization of human and mouse rod photoreceptor cGMP-gated cation channel. *J. Biol. Chem.* 267:6257-6262.

Punta, M., A. Cavalli, V. Torre, and P. Carloni. 2003. Molecular modelling studies on CNG channel from bovine retinal rod: a structural model of the cyclic nucleotide-binding domain. *Proteins* 52:332-338.

Quandt, F.N., G.D. Nicol and P.P.M. Schnetkamp. 1991. Voltage-dependent gating and block of the cyclic-GMP-dependent current in bovine rod outer segments. *Neurosci.* 42:629-638.

Richards, M. J., and S. E. Gordon. 2000. Cooperativity and cooperation in cyclic nucleotide-gated ion channels. *Biochemistry.* 39:14003-14011.

Rieke, F. and E.A. Schwartz. 1994. A cGMP-gated current can control exocytosis at cone synapses. *Neuron* 13:863-873.

Robinson, R.B., and S.A. Siegelbaum. 2003. Hyperpolarization-activated cation current: from molecules to physiological function. *Annu. Rev. Physiol.* 65:453-80.

Roncaglia, P., A. Becchetti. 2001. Cyclic-nucleotide-gated channels: pore topology in desensitizing E19A mutants. *Pflugers Arch.* 441:772-780.

Root, M.J., and R. MacKinnon. 1993. Identification of an external divalent cation-binding site in the pore of a cGMP-activated channel. *Neuron.* 11:459-466.

Root, M.J., and R. MacKinnon. 1994. Two identical non interacting sites in an ion channel revealed by proton transfer. *Science* 265:1852-1856.

Rosembaum, T., L.D.Islas, A.E.Carlos, and S.E. Gordon. 2003. Dequalinium: a novel, high-affinity blocher of CNGA1 channels. *J. Gen.Physiol.* 121(1):37-47.

Rost B., and C. Sander. 1993. Improved prediction of protein secondary structure by use of sequence profiles and neural networks. *Proc. Natl. Acad. Sci. USA* 90:7558-7562.

Rothberg, B. S., K. S. Shin, P. S. Phale, and G. Yellen. 2002. Voltage-controlled gating at the intracellular entrance to a hyperpolarization-activated cation chaannels. *J. Gen. Physiol.* 119:83-91.

Ruiz, M.L. and J.W. Karpen. 1997. Single cyclic nucleotide-gated channels locked in different ligand-bound states. *Nature* 389:389-392.

Ruiz, M.L. and J.W. Karpen. 1999. Opening mechanism of a cyclic nucleotide-gated channel based on analysis of single channels locked in each liganded state. *J. Gen. Physiol.* 113:873-895.

Sali, A., and T. L. Blundell. 1993. Comparative protein modelling by satisfaction of spatial restraints. *J. Mol. Biol.* 234:779-815.

Sambrook J., E.F. Fritsch and T. Maniatis. 1989. Molecular Cloning: A Laboratory Manual. 2nd ed. Cold Spring Harbor Laboratory Press, Cold Spring Harbor, New York.

Sato, C., Y. Ueno, K. Asai, K. Takahashi, M. Sato, A. Engel, and Y. Fujiyoshi. 2001. The voltage-sensitive sodium channel is a bell-shaped molecule with several cavities. *Nature.* 409:1047-1051.

Sautter A., M. Biel, f. Hofmann. 1997. Molecular cloning of cyclic nucleotide gated cation channel subunits from rat pineal gland. *Brain res Mol Res.* 48:171-175.

Sautter, A., X. Zong, F. Hoffmann and M. Biel. 1998. An isoform of the rod photoreceptor cyclic nucleotide-gated channel β-subunit expressed in olfactory neurons. *Proc. Natl. Acad. Sci. USA*. 95:4696-4701.

Sautter, A., X. Zong, F. Hoffmann and M. Biel. 1998. An isoform of the rod photoreceptor cyclic nucleotide-gated channel β-subunit expressed in olfactory neurons. *Proc. Natl. Acad. Sci. USA*. 95:4696-4701.

Savchenko, A., S. Barnes and R.H. Kramer. 1997. Cyclic-nucleotide-gated channels mediate synaptic feedback by nitric oxide. *Nature* 390:694-698.

Sundermann E.R., and W.N. Zagotta. 1999. Sequence of events underlying the allosteric transition of rod cyclic nucleotide-gated channels. *J. Gen. Physiol.* 113:621-640.

Schuman, E.M. and D.V. Madison. 1994. Nitric oxide and synaptic function. *Annu. Rev. Neurosci.* 17:153-183.

Scott, S. P. and J. C. Tanaka. 1998. Three residues predicted by molecular modeling to interact with the purine moiety alter ligand binding and channel gating in cyclic nucleotide-gated channels. *Biochemistry.* 37:17239-17252.

Scott, S. P., I. T. Weber, R. W. Harrison, J. Carey, and J. C. Tanaka. 2001. A functioning chimera of the cyclic nucleotide-binding domain from the bovine retinal rod ion channel and the DNA-binding domain from catabolite gene-activating protein. *Biochemistry.* 40:7464-7473.

Shammat, I. M. and S. E. Gordon. 1999. Stoichiometry and arrangement of subunits in rod cyclic nucleotide-gated channels. *Neuron.* 23:809-819.

Seifert, R., E. Eismann, J. Ludwig, A. Baumann and U.B. Kaupp. 1999. Molecular determinants of a Ca^{2+}-binding site in the pore of cyclic nucleotide gated channels: S5/S6 segments control affinity of intrapore glutamates. *EMBO J.* 18:119-130.

Sesti, F., M. Straforini, T.D. Lamb and V. Torre. 1994. Gating, selectivity and blockage of single channels activated by cyclic GMP in retinal rods of the tiger salamander. *J. Physiol. (Lond.)* 474:203-222.

Sesti, F., E. Eismann, U. B. Kaupp, M. Nizzari, and V. Torre. 1995 The multi-ion nature of the cGMP-gated channel from vertebrate rods. *J. Physiol.* 487:17-36.

Sesti, F., M. Nizzari, and V. Torre. 1996 Effect of changing temperature on the ionic permeation through the cyclic CGM-activated channel from vertebrate photoreceptors. *Biophys. J.* 70:2616-2639.

Shammat, I. M., and S. E.Gordon. 1999. Stoichiometry and arrangement of subunits in rod cyclic nucleotide-gated channels. *Neuron.* 23:809-819.

Shabb, J.B., L. Ng and J.D. Corbin. 1990. One amino acid change produces a high affinity cGMP-binding site in cAMP-dependent protein kinase. *J. Biol. Chem.* 265:16031-16034.

Shabb, J.B., and J.D. Corbin. 1992. Cyclic nucleotide binding domains in proteins having diverse functions. *J. Biol. Chem.* 267:5723-5726.

Shapiro M.S., and W.N. Zagotta. 2000. Structural basis for ligand selectivity of heteromeric olfactory cyclic nucleotide gated channels. *Biophys. J.* 78:2307-2320.

Sklar P.B., R.R.H. Anholt, and S.H. Snyder. 1986. The odorant-sensitive adenylate cyclase of olfactory receptor cells. Differential stimulation by distinct classes of odorants. *J.Biol. Chem.* 261:15538-15543.

Sokolova, O., L. Kolmakova-Partensky, and N. Grigorieff. 2001. Three-dimensional structure of a voltage-gated potassium channel at 2.5 nm resolution. *Structure.* 9:215-220.

Srinivasan, N., R. Sowdhamini, C. Ramakrishnan, and P. Balaram. 1989 Conformations of disulfide bridges in proteins. *Int. J. Peptide Res.* 36:147-155.

Stern, J.H., U.B. Kaupp and P.R. MacLeish. 1986. Control of the light regulated current in rod photoreceptors by cyclic GMP, calcium and l-cis-diltiazem. *Proc. Natl. Acad. Sci. USA.* 83:1163-1167.

Stevens, C.F. and Y. Wang. 1993. Reversal of long-term potentiation by inhibitors of heme oxygenase. *Nature* 364:147-149.

Stryer, L. 1987.Visual transduction: design and recurring motifs. *Chem. Scr.* 27B:161-71.

Su, Y., Dostmann, W. R. G. Herberg, F. W. Durick, K. Xuong, N. H. Ten Eyck, L. Taylor, S. S. and K. I. Varughese. 1995. Regulatory subunit of protein kinase A: Structure of deletion mutant with cAMP binding domains. *Science.* 269:807-813.

Sudlow L.C., R-C Huang, d.J. Green and R. Gilette. 1993. cAMP-activated sodium current of molluscan neurons is resistant to kinase inhibitors and is gated by cAMP in the isolated patch. *J. Neurosci.* 13:5188-5193.

Sun, Z. P., m. H. Akabas, E. H. Goulding, A. Karlin, and S. A. Siegelbaum. 1996. Exposure of residues in the cyclic nucleotide-gated channel pore: P region structure and function in gating. *Neuron.* 16:141-149.

Sunderman, E. R. and W. N. Zagotta. 1999. Mechanism of allosteric modulation of rod cyclic nucleotide-gated channels. *J. Gen. Physiol.* 113:601-619.

Tanaka, J.C. 1993. The effects of protons on 3', 5' -cGMP-activated currents in photoreceptor patches. *Biophys. J.* 65:2517-2523.

Tang C.-Y. and D.M. Papazian. 1997. Transfer of voltage independence from a rat olfactory channel to the Drosophila ether-a-go-go K^+ channel. *J Gen Physiol* 109: 301-311.

Tibbs, G. R., D. T. Liu, B. G. Leypold, and S. A. Siegelbaum. 1998. A state-independent interaction between ligand and a conserved arginine residue in cyclic nucleotide-gated channels reveals a functional polarity of the cyclic nucleotide binding site. *J. Biol. Chem.* 273:4497-4505.

Torre, V., M. Straforini, F. Sesti and T.D. Lamb. 1992. Different channel-gating properties of two classes of cyclic GMP-activated channel in vertebrate photoreceptors. *Proc. R. Soc. B* 250:209-215.

Torre, V. and A. Menini. 1994. Selectivity and single channel properties of the cGMP-activated channel in amphibian retinal rods. Handbook of membrane channels.

Unger, V. M., P. A. Hargrave, J. M. Baldwin, and G. F. X. Schertler. 1997. Arrangement of rhodopsin transmembrane α-helices. *Nature.* 389:203-206.

Varnum, M. D., K. D. Black, and W. N. Zagotta. 1995. Molecular mechanism for ligand discrimination of cyclic nucleotide-gated channels. *Neuron.* 15:619-625.

Varnum, M.D., and W.N. Zagotta. 1996. Subunits interactions in the activation of cyclic nucleotide-gated ion channels. *Biophys. J.* 70:2667-2679.

Vriend, G. 1990. WHAT IF: a molecular modelling and drug design program. *J. Mol. Graph.* 8(1):52-6,29.

Watanabe, S.-I. and G. Matthews. 1988. Regional distribution of cGMP-activated ion channels in the plasma membrane of the rod photoreceptor. *J. Neurosci.* 8:2334-2337.

Watanabe, S.-I. and J. Shen. 1997. Two opposite effects of ATP on the apparent sensitivity of the cGMP-gated channel of the carp retinal cone. *Vis. Neurosci.* 14:609-615.

Weber, I. T., and T. A. Steitz. 1987. Structure of a complex of catabolite gene activator protein and cyclic AMP refined at 2,5 A resolution. *J. Mol. Biol.* 198:311-26.

Weber, I., J. Shabb and J. Corbin. 1989. Predicted structures of cGMP-binding domains of the cGMP-dependent protein kinase: a key alanine/threonine difference in evolutionary divergence of cAMP and cGMP binding sites. *Biochemistry* 28:6122-6127.

Weyand, I., M. Godde, S. Frings, J. Weiner, F. Muller, W. Altenhofen, H. Hatt and U.B. Kaupp. 1994. Cloning and functional expression of a cyclic nucleotide-gated channel from mammalian sperm. *Nature* 368:859-863.

Weitz, D., M. Zoche, F. Müller, M. Beyermann, H. G. Körschen, U. B. Kaupp, and K. W. Koch. 1998. Calmodulin controls the rod photoreceptor CNG channel through an unconventional binding site in the N-terminus of the β-subunit. *EMBO J.* 17:2273-2284.

Weitz, D., N. Ficek, E. Knemmer, P.J. Bauer and U.B. Kaupp. 2002. Subunit stoichiometry of the CNG channel of rod photoreceptors. *Neuron* 36(5):881-9.

Wiesner, B., J. Weiner, R. Middendorff, V. Hagen and U.B. Kaupp. 1998. Cyclic nucleotide-gated channels on the flagellum control Ca2+ entry into sperm. *J.Cell Biol.* 2:473-484.

Yang, J., P.T. Ellinor, W.A. Sather, J.-F. Zhang and R.W. Tsien. 1993. Molecular determinants of Ca^{2+} selectivity and ion permeation in L-type Ca^{2+} channels. *Nature* 366:158-161.

Yang, N., and R. Horn. 1995. Evidence for voltage-dependent S4 movement in sodium channels. *Neuron* 15:213-218.

Yang, N., A.L.Jr. George and R. Horn. 1996. Molecular basis of charge movement in voltage-gated sodium channels. *Neuron* 16:113-122.

Yau, K.-W. and K. Nakatani. 1984. Cation selectivity of light-sensitive conductance in retinal rods. *Nature* 309:352-354.

Yau, K.-W. and K. Nakatani. 1985. Light-induced reduction of cytoplasmic free calcium in retinal rod outer segment. *Nature* 313:579-582.

Yau, K. W., and D. A. Baylor. 1989. Cyclic GMP-activated conductance of retinal photoreceptor cells. *Annu. Rev. Neurosci.* 12:289-327.

Yoshizawa, T. and G. Wald. 1963. *Nature* 197:1279-1286.

Young, E. C., D. M. Sciubba, and S. A. Siegelbaum. 2001. Efficient coupling of ligand binding to channel opening by the binding of a modulatory (beta) subunit of the olfactory cyclic nucleotide-gated channel. *J. Gen. Physiol.* 118:523-46.

Yusaf, S.P., D. Wray and A. Sivaprasadarao. 1996. Measurement of the movement of the S4 segment during the activation of a voltage-gated potassium channel. *Eur. J. Physiol.* 433:91-97.

Zagotta, W.N. 1996. Molecular mechanisms of cyclic nucleotide-gated channels. *J. Bioenerg. Biomembr.* 28:269-278.

Zagotta, W.N., and S. A. Siegelbaum. 1996. Structure and function of cyclic nucleotide-gated channels. *Annu. Rev. Neurosci.* 19:235-263.

Zagotta, W.N., N.B. Olivier, K.D. Black, E.C. Young, R. Olson and E. Gouaux. Structura basis for modulation and agonist specificity of HCN pacemaker channels. 2003. *Nature 425:200-205.*

Zheng, J., M.C. Trudeau and W.N. Zagotta. 2002. Rod cyclic nucleotide-gated channels have a stoichiometry of three CNGA1 subunits and one CNGB1 subunit. *Neuron* 36(5):891-896.

Zhuo, M., A.S. Scott, R.R. Kandel and R.D. Hawkins. 1993. Nitric oxide and carbon monoxide produce activity-dependent long-term synaptic enhancement in hippocampus. *Science* 260:1946-1950.

Zimmerman, A.L. and D.A. Baylor. 1986. Cyclic GMP-sensitive conductance of retinal rods consists of aqueous pores. *Nature* 321:70-72.

Zimmerman, A.L. and D.A. Baylor. 1992. Cation interactions within the cyclic GMP-activated channel of retinal rods from the tiger salamander. *J. Physiol.* 449:759-783.

Zimmerman, A. L. 1995. Cyclic nucleotide-gated channels. *Curr. Opin. Neurobiol.* 5:296-303.

Zong, X, H. Zucker, F. Hofmann, and M. Biel. 1998. Three amino acids in the C-linker are major determinants of gating in cyclic nucleotide-gated channels. *EMBO J.* 17:353-62.

Zufall, F. and S. Firestein. 1993. Divalent cations block the cyclic nucleotide-gated channels of olfactory receptor neurons. *J. Neurophys.* 69:1758-1768.

Zufall, F., H. Hatt, and S. Firestein. 1993. Rapid application and removal of second messengers to cyclic nucleotide-gated channels from olfactory epithellium. *Proc. Natl. Acad. Sci. USA.* 90:9335-9339.

Zufall, F., S. Firestein and G.M. Shepherd. 1994. Cyclic nucleotide-gated ion channels and sensory transduction in olfactory receptor neurons. *Annu. Rev. Biophys. Biomol. Struct.* 23:577-607.

Zufall, F. and T. Leinders-Zufall. 1997. Identification of a long-lasting form of odor adaptation that depends on the carbon monoxide/cGMP second messenger system. *J. Neurosci.* 17:2703-2712.

ACKNOWLEDGEMENTS

"NON BISOGNA SOGNARE LA PROPRIA VITA MA ESSERE COMPLETAMENTE IN TUTTO CIO CHE SI FA" (Tratto da Zen e arti marziali)

Ho deciso di scrivere quesi ringraziamenti in italiano, perchè solo in questo modo credo di poter esprimere quello che sento nel profondo del cuore.

Innanzi tutto sento il dovere di ringraziare le persone che mi hanno guidato in questo cammino sicuramente affascinante ed entusiasmante ma anche molto impegnativo: il carissimo professore Vincent Torre che mi ha permesso di ampliare ed approfondire le mie conoscenze in campo scientifico dandomi molte opportunità ed insegnandomi molto in merito. Ringrazio poi la carissima dottoressa Carla Marchetti, la prima "guida" in questo mio percorso di studi e professionale, persona che mi ha fatto innamorare del mio lavoro in laboratorio, grazie al suo esempio ed ai suoi insegnamenti. Non posso poi dimenticare la mia "maestra", nonchè amica Katia Gamel che in una settimana di intenso lavoro mi ha avvicinato a quello che era per me l'oscuro mondo della biologia molecolare.

Un altro maestro che desidero ringraziare dal profondo del cuore è il mio caro "sensei" Giorgio Farace, persona che con i suoi, sempre interessanti ed impegnativi allenamenti di Karate-do, mi ha insegnato rigore, disciplina, capacità di lottare e non arrendersi di fronte alle difficoltà e alla fatica e quindi mi ha aiutata non soltanto ad imparare questa bellissima arte marziale, ma mi ha dato anche buoni spunti ed insegnamenti da mettere in pratica nella vita quotidiana.

Non posso fare a meno di ringraziare mia madre, persona alla quale è dedicata questa tesi, perchè grazie al suo esempio, ai suoi insegnamenti, ai suoi consigli ed al suo infinito amore sono divenata la persona che sono oggi. La ringrazio anche per avermi sempre appoggiata nelle mie scelte e nelle mie decisoni.

Grazie a voi nonna Tina e nonno Aldo che mi avete sempre voluto bene e siete sempre stati fieri di me, e tu nonno, anche se non sei più quì so che in questo momento mi stai sorridendo e so anche che ovunque tu sia adesso sei orgoglioso di me e di quello che ho fatto fino ad ora.

Grazie poi a una persona speciale che con la sua amicizia e il suo sostegno mi ha aiutata, supportata e confortata nei momenti difficili, mi ha fatto ridere e gioire e con la quale ho trascorso e trascorro momenti sereni e felici: grazie Corrado!

Grazie anche a due carissimi amici, Caterina e Stefano che non potrò mai dimenticare anche se i nostri destini ci stanno separando, siete e sarete sempre nel mio cuore e nei miei pensieri.

Un particolare pensiero è dedicato a Laura, genovese come me, che conosco da molti anni ma che, solo da quando sono qui a Trieste, ho incominciato a conoscere meglio ed a considerare una cara amica.

Grazie a tutti gli amici del "teatro Verdi" di Trieste, Giulia, Valentina, Diego G, Simone, Oreste, Max, Sonia P, Andrea, Laura e Diego con i quali mi sono divertita tantissimo in questo ultimo anno e mezzo qui a Trieste. Grazie per le spensierate e sempre pazze serate trascorse insieme.

Grazie poi a tutti i componenti del "dojo Sakurakay" di Trieste.

Grazie ai "Soup of the day" (Giada, Sergio, Carlo, Davide, Ras e Elisa) gruppo con il quale ho trascorso divertenti serate e con il quale ho provato il brivido del palcoscenico...

Grazie poi a tutti i colleghi del "Galileo" e dell'area di ricerca; grazie per le discussioni scientifiche ma anche grazie per i momenti in amicizia che abbiamo trascorso insieme: Laura, Jelena, Sofija, Elizabeth, Dylan, Paolo, Paolino, Andrea, Giada, Sergio, Davide, Gabriella, Sandra, Sonia, Federica, Jessica, Tullio, Walter e Roberta, Pavel, Elisabetta, Alberto, Alejandro, Marco, Manuela, Chiara e il sig. Becciani. Grazie a tutti!

Ci sono poi altri cari amici che non posso fare a meno di non citare qui: Samuela, Manu, Luigi, Barbara, Betta e Sandro, Magda e Mauro, Chiara, Floriana, Mark, Claudio, Andrea, Gianluca, il Baschi, Mamo, Giuseppe, Barbara, Alice, Roberto e Federica, Grazie a tutti ragazzi!

Un particolare pensiero è rivolto al mio caro "cavaliere" Federico. Grazie!!!!

Grazie a te mio caro Jody!!!!

Grazie infine a tutte le persone che ho incontrato fino a questo momento e che, nel bene e nel male, mi hanno aiutata a crescere, a migliorarmi e a diventare la persona che ora sono.

Non posso esentarmi dal ringraziare il mio gatto Artù, che mi ha fatto compagnia in tutti questi quattro anni di mia permanenza qui a Trieste, il Karate, la mia bicicletta, la mia musica e i miei libri. Tutte queste cose sono e fanno parte di me e della mia vita.

ANCORA UN GRAZIE

DAL PROFONDO DEL MIO CUORE E DELLA MIA ANIMA.

Monica (Trieste, settembre 2003).